# Beneficiation of an ilmenite waste stream containing undesirable levels of chromite

by

Joalet Dalene Steenkamp

Submitted in partial fulfilment of the requirements of the degree Master of Engineering
in the Faculty of Engineering, Built Environment and Information Technology,
University of Pretoria, Pretoria

April 2003

**Role and responsibility of the author**

Because this thesis relies on inputs of testwork done by others, the role and responsibilities of the author are discussed in detail below.

This work started when one of the managers from IHM Heavy Minerals asked me to compare the roasting behaviour of LSR with that of crude ilmenite (which was the material which IHM were familiar with). I conducted a brief literature survey and designed the test programme based on work conducted by Nell and Den Hoed on behalf of IHM Heavy Minerals in 1996 (as presented at the 1997 Heavy Minerals Conference). As the IHM Heavy Minerals plant was in the detail design phase and the industry was extremely secretive sourcing of material for test work was difficult. I had to share the small amount of material that was available with other projects that utilised the material for detail plant design test work.

Since I worked for IHM Heavy Minerals and was based in Pretoria the equipment available to me at Kumba R&D included the fluidised bed roaster (that could roast ilmenite samples of 40g or less); the Linn-type furnace that could roast larger samples; the Frantz barrier magnetic separator; a Readings laboratory scale magnetic separator and a Carpco laboratory scale magnetic separator. To familiarise myself with the operation of the fluidised bed reactor and the Frantz separator I conducted tests on crude ilmenite myself (under the conditions reported). I physically preheated the reactor, placed samples in the glass tube, put the glass tube in the reactor, introduced the fluidising gas, observed during roasting, timed the process, removed the reactor from the furnace, cooled the sample, weighed it before and after roasting, logged the data into a log sheet, bagged, labelled and numbered the samples. I did not operate the Linn furnace myself but use of the furnace was demonstrated to me. I used the Frantz separator myself, splitting samples into fractions at different amperages.

Kumba R&D employed a technician (Jonathan Skosana) who was well trained on the operation of the equipment and he conducted the bulk of the remaining test work on the fluidised bed reactor and the Frantz. Although I was working on the Heavy Minerals Project at that stage (working on the detail design and pre-commissioning activities) I also had an office at the pilot plant where I spent several days a week whilst Jonathan did the test work. Jonathan borrowed the magnetic susceptibility meter from Geotron for the LSR test work. I did not use this specific meter myself but used the meter that was purchased by Kumba R&D at a later stage whilst conducting shift work (engineer on shift) during a roasting pilot plant campaign at Mintek at a later stage (not part of this thesis).

To conduct XRF, XRD and QEMSEM analyses specialised equipment were utilised and although I am familiar with XRF machines (as utilised by laboratories providing a service to steel and heavy minerals plants) I only interpreted the results from the datasets received from the various laboratories.

I wrote the paper and presented the results of this study at the Heavy Minerals Conference in 2001 (Gouws and Van Dyk 2001). At that stage I still assumed that nothing happened to the chromite during roasting. One of the conference attendees commented on the graph for roasted LSR and challenged that assumption. That was the origin of the second hypothesis. I contacted the University of Pretoria and discussed the matter with Prof Pistorius who was quite keen to investigate the matter with me. Both the professor and I investigated possible sources for clean chromite. The best option would have been to separate the chromite in the LSR from the ilmenite. Due to the low chromite concentrations in the LSR this option was impractical. I discussed the matter with the refractory supplier as well as the geologist on site. Prof Pistorius discussed the matter with the Geology Department at the University and they sourced the chromite rock from the UG1 deposit.

The roasting and magnetic separation test work was once again conducted by Jonathan Skosana. By this time it was easy to manage the execution of the test work even from a distance as I had established a relationship with the personnel at Kumba R&D. I updated the literature review over the whole period with an extensive survey in the last 12 months of the project while I was writing the thesis and trying to make sense of the test results. I performed all of the data analysis and interpretation. The conclusions and recommendations were my own.

From the above statements it is clear that I not only contributed to the work but was fully responsible for the research idea, development and execution of the experimental plan, data analysis and interpretation and recommendations made for application of the results and further studies.

**Role and responsibility of the author**

Because this thesis relies on inputs of testwork done by others, the role and responsibilities of the author are discussed in detail below.

This work started when one of the managers from IHM Heavy Minerals asked me to compare the roasting behaviour of LSR with that of crude ilmenite (which was the material which IHM were familiar with). I conducted a brief literature survey and designed the test programme based on work conducted by Nell and Den Hoed on behalf of IHM Heavy Minerals in 1996 (as presented at the 1997 Heavy Minerals Conference). As the IHM Heavy Minerals plant was in the detail design phase and the industry was extremely secretive sourcing of material for test work was difficult. I had to share the small amount of material that was available with other projects that utilised the material for detail plant design test work.

Since I worked for IHM Heavy Minerals and was based in Pretoria the equipment available to me at Kumba R&D included the fluidised bed roaster (that could roast ilmenite samples of 40g or less); the Linn-type furnace that could roast larger samples; the Frantz barrier magnetic separator; a Readings laboratory scale magnetic separator and a Carpco laboratory scale magnetic separator. To familiarise myself with the operation of the fluidised bed reactor and the Frantz separator I conducted tests on crude ilmenite myself (under the conditions reported). I physically preheated the reactor, placed samples in the glass tube, put the glass tube in the reactor, introduced the fluidising gas, observed during roasting, timed the process, removed the reactor from the furnace, cooled the sample, weighed it before and after roasting, logged the data into a log sheet, bagged, labelled and numbered the samples. I did not operate the Linn furnace myself but use of the furnace was demonstrated to me. I used the Frantz separator myself, splitting samples into fractions at different amperages.

Kumba R&D employed a technician (Jonathan Skosana) who was well trained on the operation of the equipment and he conducted the bulk of the remaining test work on the fluidised bed reactor and the Frantz. Although I was working on the Heavy Minerals Project at that stage (working on the detail design and pre-commissioning activities) I also had an office at the pilot plant where I spent several days a week whilst Jonathan did the test work. Jonathan borrowed the magnetic susceptibility meter from Geotron for the LSR test work. I did not use this specific meter myself but used the meter that was purchased by Kumba R&D at a later stage whilst conducting shift work (engineer on shift) during a roasting pilot plant campaign at Mintek at a later stage (not part of this thesis).

To conduct XRF, XRD and QEMSEM analyses specialised equipment were utilised and although I am familiar with XRF machines (as utilised by laboratories providing a service to steel and heavy minerals plants) I only interpreted the results from the datasets received from the various laboratories.

I wrote the paper and presented the results of this study at the Heavy Minerals Conference in 2001 (Gouws and Van Dyk 2001). At that stage I still assumed that nothing happened to the chromite during roasting. One of the conference attendees commented on the graph for roasted LSR and challenged that assumption. That was the origin of the second hypothesis. I contacted the University of Pretoria and discussed the matter with Prof Pistorius who was quite keen to investigate the matter with me. Both the professor and I investigated possible sources for clean chromite. The best option would have been to separate the chromite in the LSR from the ilmenite. Due to the low chromite concentrations in the LSR this option was impractical. I discussed the matter with the refractory supplier as well as the geologist on site. Prof Pistorius discussed the matter with the Geology Department at the University and they sourced the chromite rock from the UG1 deposit.

The roasting and magnetic separation test work was once again conducted by Jonathan Skosana. By this time it was easy to manage the execution of the test work even from a distance as I had established a relationship with the personnel at Kumba R&D. I updated the literature review over the whole period with an extensive survey in the last 12 months of the project while I was writing the thesis and trying to make sense of the test results. I performed all of the data analysis and interpretation. The conclusions and recommendations were my own.

From the above statements it is clear that the I not only contributed to the work but was fully responsible for the research idea, development and execution of the experimental plan, data analysis and interpretation and recommendations made for application of the results and further studies.

Table of contents

**List of abbreviations**

| Abbreviation | Description |
|---|---|
| AC | Alternating current |
| CPC | Central processing complex |
| CSTR | Continuous stirred tank reactor |
| DC | Direct current |
| DIC | Dry ilmenite circuit |
| DMDS | Dry magnetic drum separation |
| EDX | Energy-dispersive X-ray analysis |
| HCP | Hexagonal closed packed |
| HGMS | High gauss magnetic separators |
| HIWMS | High intensity wet magnetic separators – also called WHIMS |
| HMC | Heavy mineral concentrate |
| HSR | High susceptibility fraction |
| IA | Image analyzer |
| LIMS | Low intensity magnetic separators |
| LIWMS | Low intensity wet magnetic separators |
| LSR | Low susceptibility fraction |
| PFR | Plug flow reactor |
| PWP | Primary wet plant |
| QEM*SEM | Quantitative Evaluation of Materials by Scanning Electron Microscopy |
| URIC | Unroasted ilmenite circuit |
| R&D | Research and Development |
| ROM | Run-of-mine product |
| SEM | Scanning electron microscope |
| VHM | Valuable heavy mineral |
| WDS | Wavelength dispersive spectrometry |
| WHIMS | Wet high intensity magnetic separators – also called HIWMS |
| XRD | X-ray diffraction |
| XRF | X-ray fluorescence |

# Chapter 1: Introduction

Several authors have studied the roasting of ilmenite concentrates for beneficiation purposes (Westcott and Parry 1968, Bergeron and Prest 1974, Nell and Den Hoed 1997 and many more). Furthermore oxidative roasting is applied on an industrial scale to beneficiate ilmenite concentrates from South African East Coast heavy minerals deposits (McPherson 1982). Why then another study on the impact of oxidative roasting on the magnetic properties of ilmenite? In this chapter I discuss the reasoning behind the study as well as the major hypothesis and the research program that followed. The outline of Chapters two to five of the thesis concludes this chapter. The order of discussion is:

1.1 Idea if the thesis and motivation for the study
1.2 The research topic and hypothesis
1.3 Research design and methodology in general
1.4 Outline of chapters two to five of thesis

## *1.1 Idea of the thesis and motivation for the study*

The Heavy minerals industry provides feed material for the production of $TiO_2$ pigment. $TiO_2$ pigment is used as an opacifier in paints, paper and fibres and has a variety of other end uses. Considered a 'quality of life' product, the overall level of economic activity on a national and international level governs the consumption of $TiO_2$ pigment. As the consumption of $TiO_2$ pigment rises the demand for $TiO_2$ feed materials for the pigment production plants increases. High $TiO_2$ slag is one of the raw materials supplied by the heavy minerals industry to $TiO_2$ pigment production plants (Fisher 1997). High $TiO_2$ slag is produced in smelting furnaces by reducing ilmenite with a carbonaceous reductant (Pistorius, 1999). Ilmenite (nominally $FeTiO_3$) is a natural occurring heavy mineral associated with the heavy minerals sands deposits. In heavy minerals sands operation, producing high $TiO_2$ slag from the mining to the smelting stage, different mineral properties are exploited by means of different types of equipment to produce specific types of mineral concentrates. Ilmenite is separated from other minerals in the heavy mineral concentrate, based on magnetic susceptibility properties (Balderson 1999). In high chrome heavy mineral deposits the magnetic susceptibility properties of the ilmenite and chromite in their natural states are very similar. A crude ilmenite concentrate produced from a Southern African East Coast deposit, contains typically 90 per cent ilmenite, 5 per cent Ti-hematite, 3 per cent spinel (including chromite, magnetite etc) and 2 per cent silicates by weight. The $Cr_2O_3$ content can be as much as 0.3 per cent (Nell and Den Hoed 1997). Only when the per cent $Cr_2O_3$ in ilmenite concentrate is less than 0.1 per cent is the ilmenite suitable for the production of high $TiO_2$ slag (Beukes and Van Niekerk 1999).

Several authors found that when roasting an ilmenite concentrate it is possible to increase the bulk magnetic susceptibility of ilmenite. Different roasting atmospheres were described ranging from oxidative (Westcott and Parry 1968; Bergeron and Prest 1974; Nell and Den Hoed 1997; and Nell 1999) to neutral (Grey and Li 2001) to reductive (Walpole 1991; Guzman et al. 1992; Merrit and Cranswick 1994; and Reaveley and Scanlon 2001). Nell and Den Hoed (1997) stated that when roasting crude ilmenite concentrates under oxidising conditions the magnetic susceptibility of the ilmenite increases, but the bulk magnetic susceptibility of the chromite does not increase. This induced difference in magnetic susceptibility properties is used to remove the $Cr_2O_3$-containing spinel from the ilmenite concentrate during secondary beneficiation by magnetic separation (Beukes and Van Niekerk 1999).

In their paper Beukes and Van Niekerk (1999) compared three secondary beneficiation processes for crude ilmenite produced from a Southern African East Coast deposit. Their aim was to produce ilmenite with $Cr_2O_3$-levels less than 0.1 per cent from an ilmenite concentrate with $Cr_2O_3$-levels in the order of 0.3 per cent. They claimed that the third process described by them has a lower operational cost than the conventional process patented by Bergeron and Prest (1974).

Bergeron and Prest patented the first process described by Beukes and Van Niekerk (1999) in 1974. The process consists of three steps:

- Step 1: Wet magnetic separation of the crude ilmenite concentrate at 2000-3000 Gauss. In this step chromite with a high magnetic susceptibility reports to the magnetic reject fraction.
- Step 2: Roasting the non-magnetic fraction in an oxidizing atmosphere.

- Step 3: Dry magnetic separation of the roasted material at 1000-2000 Gauss.

Beukes and Van Niekerk (1999) claimed that this process resulted in 80 per cent yield of smelter grade ilmenite with less than 0.1 per cent $Cr_2O_3$.

The second process described by Beukes and Van Niekerk (1999) consists of three steps as well but does not include roasting:

- Step 1: Drying of the crude ilmenite concentrate.
- Step 2: Dry magnetic separation of the dried crude ilmenite concentrate at 2350 Gauss.
- Step 3: Dry magnetic separation of the non-magnetic fraction at 6500 Gauss.

Beukes and Van Niekerk (1999) claimed that this process resulted in 70 per cent yield of smelter grade ilmenite with less than 0.1 per cent $Cr_2O_3$.

The third process described by Beukes and Van Niekerk (1999) consists of five steps:

- Step 1: Drying of the crude ilmenite concentrate.
- Step 2: Dry magnetic separation of the dried crude ilmenite concentrate at 2350 Gauss.
- Step 3: Dry magnetic separation of the non-magnetic fraction at 6500 Gauss – the non-magnetic fraction is called the low susceptible rejects (LSR).
- Step 4: Roasting of the non-magnetic fraction (LSR) in an oxidizing atmosphere.
- Step 5: Dry magnetic separation of the roasted material at 1000-2000 Gauss.

Beukes and Van Niekerk (1999) claimed that this step resulted in 80 per cent yield of ilmenite with less than 0.1 per cent $Cr_2O_3$. This recovery figure is similar to that obtained in Process #1 but with less material requiring roasting.

To remain competitive in industry one of the strategies a company can follow is to continuously investigate new methods to produce the same product at a lower cost (Porter 1988). Beukes and Van Niekerk did investigate alternative production routes but did not recommend process conditions for the roasting step in Process #3, which they claimed to be more cost effective.

Other authors, especially in mineralogy, studied the mechanism of magnetic susceptibility in ilmenite. Authors in this category include Ishikawa and Akimoto (1957a), Ishikawa Y and Akimoto S (1957b), O'Reilly W and Banerjee SK (1966 and 1967), Nord GL et al (1989), Banerjee SK (1991) and Nell and Den Hoed (1997).

### *1.2 The research topic & hypothesis*

Based on the statement made by Beukes and Van Niekerk (1999) that their 3rd process would result in lower production costs but without roasting conditions recommended for the stream to be roasted to support their statement, I decided to test the following hypothesis:

"It is possible to produce an ilmenite product suitable for ilmenite smelting by subjecting low susceptibility rejects (LSR) to roasting and subsequent magnetic separation, using the roasting conditions recommended for crude ilmenite by Nell and Den Hoed (1997) or Bergeron and Prest (1974)"

Based on the statement made by Nell and Den Hoed (1997) that oxidising roasting does not increase the magnetic susceptibility of chromite, I decided to test the following hypothesis:

"The magnetic susceptibility of chromite remains constant during magnetizing roasting of an ilmenite concentrate under the oxidizing conditions reported by Nell and Den Hoed (1997)."

### *1.3 Research design and methodology in general*

From the preliminary reading I decided to:

- Source or prepare samples of crude ilmenite, the waste stream (LSR) described by Beukes and Van Niekerk (1999) and chromite in this waste stream (LSR);
- Characterise all three samples prior to roasting and magnetic separation;
- To conduct laboratory scale batch roast tests on all three types of material at the temperatures reported by Nell and Den Hoed (1997);

- To measure the magnetic susceptibility of each roasted sample. The optimum roasting condition is defined as the condition at which the magnetic susceptibility of the roasted sample has the highest value relative to all other samples;
- To roast larger samples of all three types of material at the optimum roasting conditions determined by the small scale tests;
- To fractionate the larger sample at various intervals of magnetic susceptibility, subject each ilmenite containing sample to XRF analysis and determine the $Cr_2O_3$ and $TiO_2$ distributions thereof. This would be done to:
    - Confirm that an ilmenite product with less than 0.1 per cent $Cr_2O_3$ can be produced from the LSR or crude ilmenite at the ideal conditions;
    - To determine the yield of this product; and
    - To evaluate the distribution of chromite vs. ilmenite before and after roasting.

### *1.4 Outline of chapters two to five of thesis*

In chapter 2 the key concepts available in literature are reviewed and discussed. In chapter 3 the research design and methodology are discussed. Chapter 4 presents the results and the discussion of the results. Chapter 5 concludes the study with a summary of the important points, linking the results to literature and theory, and recommending further test work.

In short: the aim of chapter one was to clarify why another study on ilmenite roasting was required and what it entailed. An overview of the major hypothesis of the study, how the hypothesis was investigated and how the study would be reported on in the remainder of the thesis, was included. In chapter two I review the literature available on ilmenite roasting in more detail.

## Chapter 2: Literature review

As this is another study on ilmenite roasting I review the current body of knowledge in chapter 2. The scholarship review is organized according to:

2.1 $TiO_2$ pigment and titanium containing feed material industries
2.2 Exploitation of heavy minerals resources
2.3 Definition of crude ilmenite and its constituents
2.4 Beneficiation of crude ilmenite from Southern African East Coast deposits
2.5 Description of alternative flow lines to beneficiate crude ilmenite from Southern African East Coast deposits
2.6 Describing the principles of magnetic beneficiation
2.7 Descriptions of the principles of magnetization
2.8 Magnetic susceptibility of chromite
2.9 Mechanism of magnetic susceptibility changes in ilmenite
2.10 Defining roasting
2.11 Phase chemical changes during oxidative roasting
2.12 Equipment
2.13 Findings and conclusions

Magnetism, the mechanism of changes in magnetic susceptibility of ilmenite and the enhancement of magnetic susceptibility of ilmenite by roasting in an oxidative atmosphere are discussed in detail. The other scholarships ($TiO_2$ industry; exploitation of heavy minerals resources; definition of crude ilmenite and its constituents; beneficiation of Southern African East Cost deposits and equipment) are touched on either to clarify concepts or for comprehensiveness. The chapter is concluded with a discussion on how the test program followed in the study was derived from this scholarship review.

### *2.1 Discussion of the $TiO_2$ pigment and titanium containing feed material industries*

Fisher (1997) gave an excellent review on the history of titanium dioxide consumption, from discovering its use as a pigment in 1908 to its current status as the white pigment used as opacifier in paints, paper and fibres and a variety of other end uses. Being more environmental friendly it replaced competing white lead pigments in the 1950s and 1960s. Considered a 'quality of life' product, the overall level of economic activity on a national and international level governs the consumption of the $TiO_2$ pigment. Consumption has been rising since the 1950s (figure 2.1 after Fisher 1997).

Figure 2.2 is an overview of the link between the $TiO_2$ pigment industry and the titanium-containing feed materials industry. Two commercial processes are utilized to produce titanium dioxide pigments. These are the sulphate process and the chloride process – the former being the older of the two processes. The chloride process is replacing the sulphate process due to commercial and environmental improvements. In 1997 57 per cent of all $TiO_2$ pigment was produced via the chloride process (Fisher 1997).

The sulphate process is a batch process with the following sequential primary unit operations (Fisher 1997):
1. Digestion where the $TiO_2$ containing feed material reacts with sulphuric acid to produce titanyl sulphate.
2. Precipitation of titanium dioxide hydrate.
3. Separation and washing of the hydrate.
4. Calcination and thermal formation of the pure $TiO_2$ crystals.

The chloride process is a continuous process with the following sequential primary unit operations (Fisher 1997):
1. Chlorination where chlorine reacts with the titanium containing feed materials under reducing conditions, at elevated temperature.
2. Condensation and purification where the low, medium and high boiling point chlorides are separated by fractional distillation.
3. Oxidation of the titanium tetrachloride with oxygen at elevated temperatures to form titanium dioxide pigment particles.

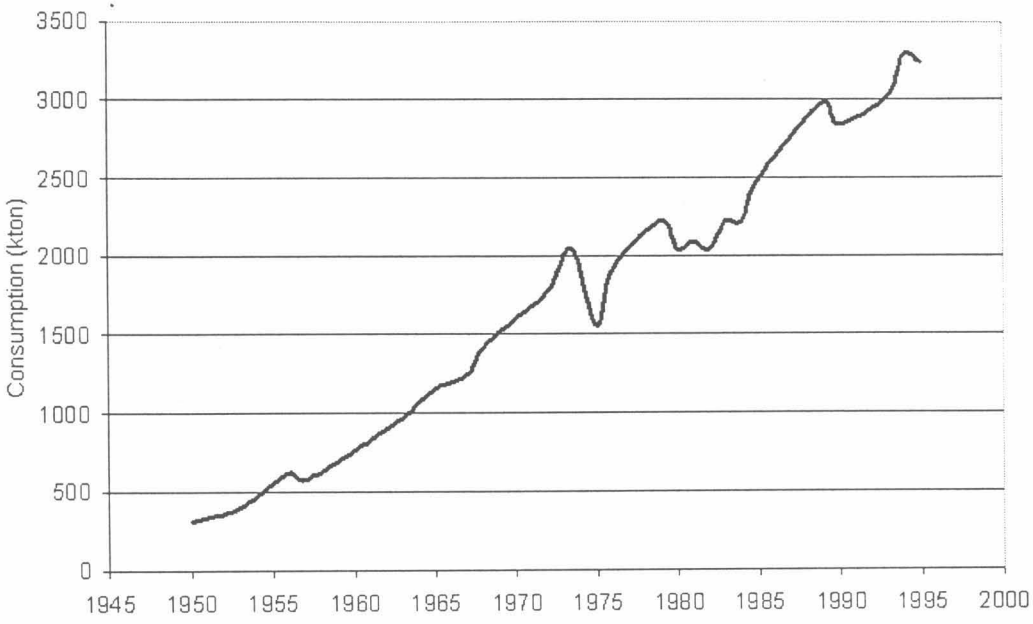


**Figure 2.1: Worldwide $TiO_2$ pigment consumption from 1950 to 1995 - after Fisher (1997).**

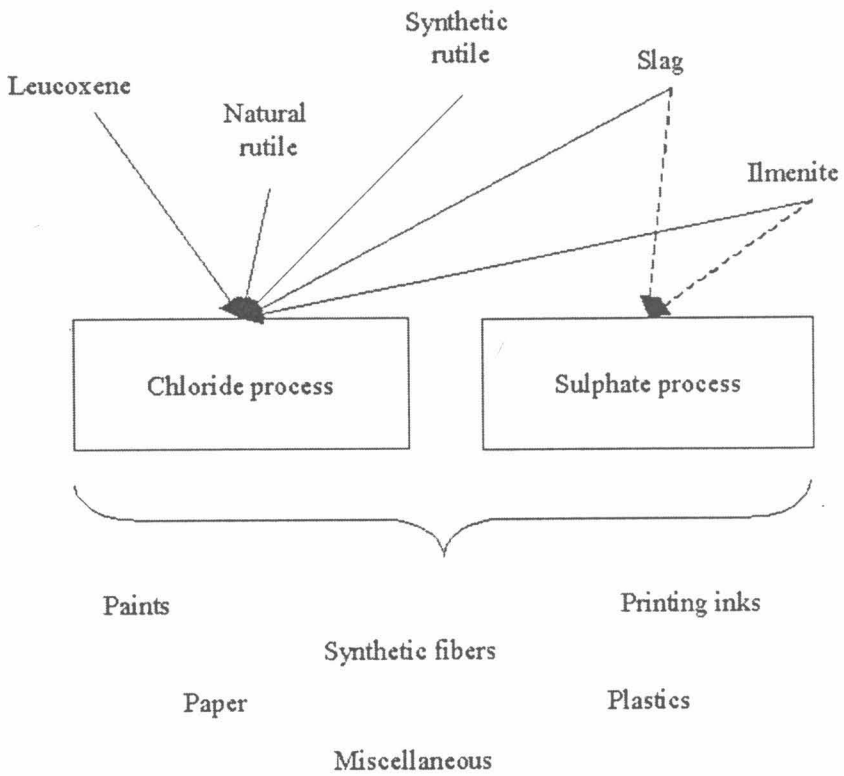


**Figure 2.2: Overview of the link between the $TiO_2$ pigment industry and the titanium containing feed materials industry (after Fisher 1997).**

The heavy minerals industry provides the titanium containing feed material for the production of $TiO_2$ pigment. As the consumption of $TiO_2$ pigment rises the demand for $TiO_2$ feed materials for the pigment production plants increases. High $TiO_2$ slag is one of the raw materials supplied by the heavy minerals industry to $TiO_2$ pigment production plants (Fisher 1997). High $TiO_2$ slag is produced in smelting furnaces by reducing ilmenite with a carbonaceous reductant (Pistorius, 1999). Other titanium containing feed materials include natural rutile, synthetic rutile, leucoxene and ilmenite (Fisher 1997).

The $TiO_2$ feed materials have to meet a number of chemical composition requirements set by the pigment producers and based on the impact the chemical components have on the operation or final pigment quality. The requirements for feed materials for the sulphate $TiO_2$ pigment production process are described below (Fisher 1997).

- *Heavy metals*: Most of them end up as contaminants in the final $TiO_2$ pigment product or waste acid. Chromium and vanadium can degrade the optical properties of the pigment and their presence in the waste acid makes it difficult to dispose of or to recycle into useful products. Phosphorus, manganese and niobium should also be avoided.
- *$Fe^{3+}$*: Will absorb on the $TiO_2$ pigment particle and discolour it. It is reduced in the sulphate process by adding iron scrap. Its presence in the feed materials therefore increases production costs, and lower is better.
- *$Ti^{3+}$*: In this process $Ti^{3+}$ forms $Ti_2O_3$, which reports to the waste stream resulting in losses of $Ti^{3+}$ units.
- *Clay*: Levels should be as low as possible to minimize digest cake dissolving times.

The requirements for feed materials for the chloride $TiO_2$ pigment production process are described below (Fisher 1997).

- *Silica*: Low silica levels are desirable, as silica is inert in the chlorinator and tends to accumulate, reducing the throughput of the chlorinator.
- *Alkaline earth oxides*: Low alkaline earth oxides levels are definite requirements as the chlorides of these oxides are liquid in the chlorinator, which will agglomerate the fluidizing particles into a viscous mass terminating all chlorination taking place.
- *Arsenic and tin*: Arsenic should be avoided as it ends up in the final $TiO_2$ pigment rendering it unsuitable for applications in the food and personal care industries. $SnCl_4$ tends to build up in the recycling stream with the same effect on chlorinator throughput as silica.

### *2.2 Exploitation of heavy minerals resources*

Titanium is the ninth most abundant element in the earth's crust. It is found in a number of minerals (table 2.1), of which only ilmenite ($FeTiO_3$), rutile ($TiO_2$) and leucoxene warrant economic exploitation. Ilmenite and rutile occur mainly in heavy minerals sand deposits but ilmenite is also associated with magnetite, or hematite in some minor instances, in magmatic deposits. For rock deposits to be commercially workable the $TiO_2$ content of the deposits should range between 17 and 35 per cent and the $TiO_2$ containing minerals should not be too intimately intergrown with other minerals. For sand deposits as little as 1 per cent $TiO_2$, when in the form of rutile, can render a deposit commercially workable (Hammerbeck 1992b).

**Table 2.1: The main titanium and associated iron oxide minerals (after www.ngu.no/prosjekter/Geode/titanium)**

| Mineral (end member composition) | % $TiO_2$ (theoretical) | Physical properties (H= hardness, D= specific gravity) | Occurrence |
|---|---|---|---|
| Ilmenite ($FeTiO_3$) | 52.7 | H 5.5-6, D 4.7, black, weakly magnetic, trigonal | Common in gabbros and anorthosites; in placers |
| Magneto-ilmenite | - | - | Ilmenite with intergrowths of magnetite |
| Hemo-ilmenite | - | - | Ilmenite with intergrowths of hematite |
| Rutile ($TiO_2$) | 100 | H 6-6.5, D 4.2, reddish brown, tetragonal | In eclogites, granites, pegmatites, gneisses and placers |
| Anatase ($TiO_2$) | 100 | H 5.5-6, D 3.9, brown, tetragonal | In altered titanium-bearing rocks and placers |
| Brookite ($TiO_2$) | 100 | H 5.5-6, D 4.1, yellowish brown, orthorombic | In veins and placers |
| Leucoxene/altered ilmenite | - | H 4-4.5, D 3.5-4.5 | Alteration product; mixture of rutile, hematite, titanite, etc. |
| Perovskite ($CaTiO_3$) | 58.9 | H 5.5, D 4.1, orthorombic | In some alkaline rocks |
| Pseudobrookite ($Fe_2TiO_5$) | - | H 6, D 4.4, brown to black, orthorombic | In various igneous rocks |
| Titanite ($CaTiSiO_5$) | 40.9 | H 5-5.5, D 3.5, brownish, monoclinic | Common accessory mineral in a variety of rocks |
| Hematite ($Fe_2O_3$) | - | H 5.5-6.5, D 5.3, reddish brown to black, trigonal | Common in a variety of rocks |
| Ilmenohematite | - | - | Hematite with intergrowths of ilmenite |
| Magnetite ($Fe_3O_4$) | - | H 6, D 5.2, black, strongly magnetic, cubic | Common in a variety of rocks |
| Titanomagnetite | - | - | Some Ti in solid solution in magnetite |
| Ilmenomagnetite | - | - | Magnetite with intergrowths of ilmenite |
| Ulvøspinel ($Fe_2TiO_4$) | 35.7 | Dark, magnetic, cubic | Exsolves from magnetite-ulvøspinel solid solutions and may be subsequently oxidised to ilmenite |

According to Hammerbeck (1992b) in South Africa ilmenite and rutile from magmatic origin occur in the Bushveld igneous complex, in small amounts in kimberlite and carbonite deposits and also as accessory minerals to granite and pegmatite deposits. As part of fossil beach deposits they occur in the Waterberg system and the Karoo system (Bothaville, Wolmaransstad, Delmas and Carolina). As quaternary beach deposits they occur as older red and brown coastal sands, younger dunes and beach sands or in coastal lagoons. The older red and brown coastal sand dunes of Zululand contain from 2 to 25 per cent heavy minerals (7 to 10 per cent on average). The size of the heavy minerals ranges from 75 to 150 micron diameter. The heavy minerals concentrate in the older red and brown coastal sand dunes usually consists of:

- 70 to 80 per cent ilmenite;
- 2 to 5 per cent leucoxene;
- 2 to 5 per cent rutile;
- 8 to 10 per cent zircon;

- 2 to 8 per cent magnetite;
- Trace to 0.3 per cent monazite;
- 1 to 5 per cent garnet, pyroxene etc.

The $Cr_2O_3$ content of the ilmenite from older red and brown coastal sand dunes of Zululand is comparable to that of the ilmenite found in the Karoo system (0.1 to 0.7 per cent). Other deposits in South Africa and elsewhere contain very low levels of $Cr_2O_3$. In table 2.2 the typical composition of ilmenite from South Africa and other heavy mineral sands are stated (Hammerbeck 1992b).

**Table 2.2: Composition of natural occurring ilmenite from all over the world – after Hammerbeck (1992b)**

| Per cent | $TiO_2$ | FeO | $Fe_2O_3$ | $Cr_2O_3$ | $V_2O_5$ |
|---|---|---|---|---|---|
| South Africa: St Lucia | 49.0 | 32.5 | 14.3 | 0.38 | - |
| South Africa: Richards Bay | 49.7 | 36.6 | 11.1 | 0.19 | 0.29 |
| South Africa: Isipingo | 46.6 | 39.5 | 9.1 | 0.10 | 2.76 |
| South Africa: Umgababa | 49.9 | 37.2 | 10.5 | 0.16 | 0.33 |
| South Africa: Sandy Point | 50.3 | 36.5 | 10.9 | 0.07 | - |
| South Africa: Morgan Bay | 50.0 | 38.0 | 13.1 | 0.05 | - |
| South Africa: West Coast | 41.6 | 34.1 | 19.7 | 0.0 | 0.92 |
| Florida | 57.5 | 12.3 | 24.6 | - | - |
| Quebec | 70.7 | 12.2 | 1.5 | 0.25 | 0.55 |
| Malaya | 53.1 | 33.6 | 8.7 | 0.005 | 0.02 |
| India | 60.6 | 9.3 | 24.2 | 0.12 | 0.15 |
| Australia | 55.4 | 22.5 | 11.1 | 0.03 | 0.13 |
| Brazil | 48.3 | 32.4 | 16.6 | 0.5 | 0.06 |

Figure 2.3 depicts, schematically, a generic flow sheet for a heavy minerals sands operation producing high $TiO_2$ slag, from mining the sand deposit to the smelting stage. The slag is then sold to the $TiO_2$ pigment producers as described in paragraph 2.1. In the flow sheet in figure 2.3 different mineral properties are exploited, by means of different types of equipment, to produce specific types of mineral concentrates. The sandy, run-of-mine material is produced by water or non-water based mining methods. A heavy mineral concentrate is produced from the run-of-mine material, utilizing size difference and specific gravity properties. Ilmenite is separated from other minerals in the heavy mineral concentrate, based on magnetic susceptibility properties (Balderson 1999). In high chrome heavy mineral deposits i.e. the older red and brown coastal sand dunes of Zululand, the magnetic susceptibility properties of the ilmenite in the crude ilmenite concentrate is enhanced in order to separate the ilmenite from the chromite minerals. The ilmenite is suitable for the production of high $TiO_2$ slag only when the $Cr_2O_3$ content of ilmenite concentrate is less than 0.1 per cent (Beukes and Van Niekerk 1999).

### *2.3 Definition of crude ilmenite and its constituents*

For the purpose of this study *crude ilmenite* is defined as an ilmenite-containing concentrate, produced with one or a combination of the methods indicated in figure 2.3, with a $Cr_2O_3$ content in excess of 0.1 per cent. Crude ilmenite is therefore unacceptable for $TiO_2$ slag production. Nell and Den Hoed (1997) stated that crude ilmenite, produced from a Southern African East Coast deposit, contains typically 90 per cent ilmenite, 5 per cent Ti-hematite, 3 per cent spinel and 2 per cent silicates by weight, as separate phases. Naturally occurring ilmenite particles can have $Fe_2O_3$ (hematite) in solid solution in the $FeTiO_3$ matrix (Nell and Den Hoed 1997). The importance of this solid solution will become clearer as the discussion proceeds.

The $Cr_2O_3$ content of crude ilmenite, produced from a Southern African East Coast deposit, can be as much as 0.3 per cent and is present in spinels of variable composition (Hammerbeck 1992b, Nell and Den Hoed 1997). Dana and Dana (1944) and Deer et al (1966) define the naturally occurring chromite spinel series as variations on the pure spinels magnesiochromite ($MgCr_2O_4$) and chromite ($FeCr_2O_4$). Deer et al (1966) stated that all natural magnesiochromites contain a considerable amount of $Fe^{2+}$ (which replaces $Mg^{2+}$) and $Al^{3+}$ or $Fe^{3+}$ (replacing $Cr^{3+}$). In natural chromites a considerable amount of $Mg^{2+}$ replaces $Fe^{2+}$ with generally appreciable replacement of $Cr^{3+}$ by $Al^{3+}$, but less so by $Fe^{3+}$. To produce smelter grade ilmenite the $Cr_2O_3$ containing spinel particles have to be separated from the

ilmenite particles. Various secondary beneficiation methods for crude ilmenite, to separate the chromite from the ilmenite in order to reduce the $Cr_2O_3$ content of the final ilmenite product, will be described as the discussion proceeds.

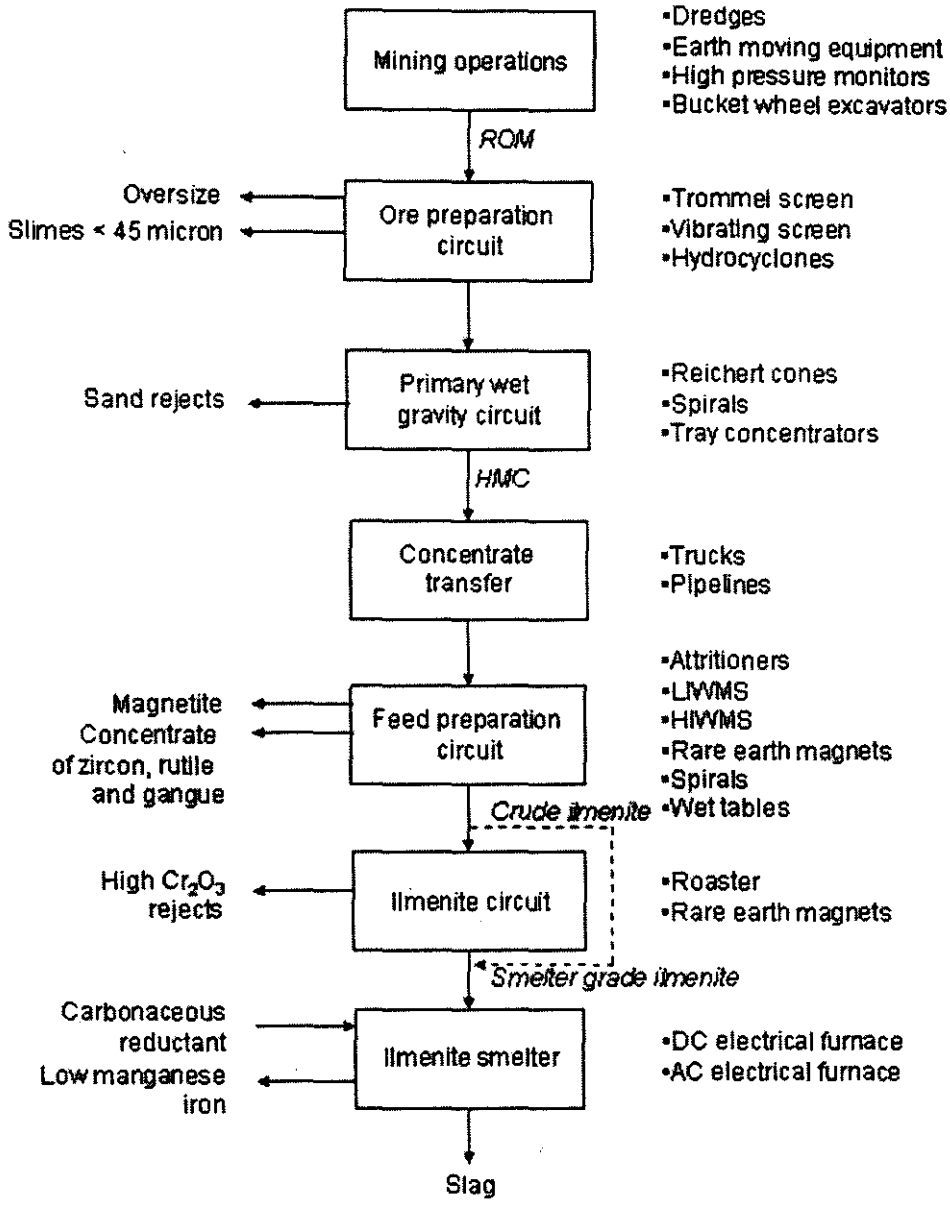


**Figure 2.3: Generic flow sheet for a heavy minerals operation producing high $TiO_2$ slag after Balderson (1999), Beukes and Van Niekerk (1999) and Pistorius (1999).**

### *2.4 Beneficiation of crude ilmenite from Southern African East Coast deposits*

According to Kelly and Spottiswood (1995) mineral separation is brought about by suspending particles in a medium and passing this suspension through a suitable piece of equipment named a separator. Liberation of particles is a prerequisite for perfect separation, i.e. all particles that require separation from each other should be discrete particles. In most cases particles are not completely liberated.

Furthermore Kelly and Spottiswood (1995) state that separation depends on three factors:

- The properties of the minerals of which ideally only one is exploited in order to separate particles form each other;

- The characteristics of the separator; and
- Production requirements of grade and recovery – the former determined by the client and the latter by the financial feasibility of the project.

According to Kelly and Spottiswood (1995) in a set of particles there is normally a range in the value of the property being exploited. This range of property values of a given set may be presented as a frequency curve, also known as a separability curve. In a separability curve the fraction of the set of particles with a specific value of property X is expressed as a function of the value of property X. It is important to remember that the separation predicted from separability curves represents the maximum separation that can be achieved, on the material as it exists, by exploiting that particular property. Engineering limitations mean that a separator never achieves the maximum separation indicated by the separability curves, but one may give a better performance than the other (Kelly and Spottiswood 1995).

This study is limited to a single property of the ilmenite and $Cr_2O_3$-containing spinel minerals, i.e. magnetic susceptibility, which is exploited and manipulated in order to separate the particles from each other. The specific gravity of ilmenite (4.1-5.1 $t/m^3$) and chromite (4.5-5.0 $t/m^3$) is very similar. They therefore report to the same stream when using separation methods based on gravity i.e. in the feed preparation circuit as described by Balderson (1999) in figure 2.3.

When a satisfactory displacement does not exist between separability curves, whether no displacement at all or too little displacement, two alternatives exist:

1. Change the distribution of values of X by some pre-treatment;
2. Exploit a different property.

Bergeron and Prest (1974), Nell and Den Hoed (1997) as well as Beukes and Van Niekerk (1999) constructed separability curves for crude ilmenite from Southern African East Coast deposits, represented by $TiO_2$, and chromite, represented by $Cr_2O_3$, based on magnetic susceptibility. When the displacement between ilmenite and chromite was not satisfactory the authors of all three papers decided to subject the material to an oxidising roast, i.e. change the distribution of the magnetic susceptibility of the ilmenite by some pre-treatment. All of them produced two sets of curves: one of the mineral concentrate before roasting and one of the mineral concentrate after roasting. Figure 2.4 is reproductions of the two curves from Nell and Den Hoed (1997).

In this study production requirements of grade, as defined by the client and described in paragraph 2.1 and 2.2, play an important role and recovery is referred to but not focussed on in detail.

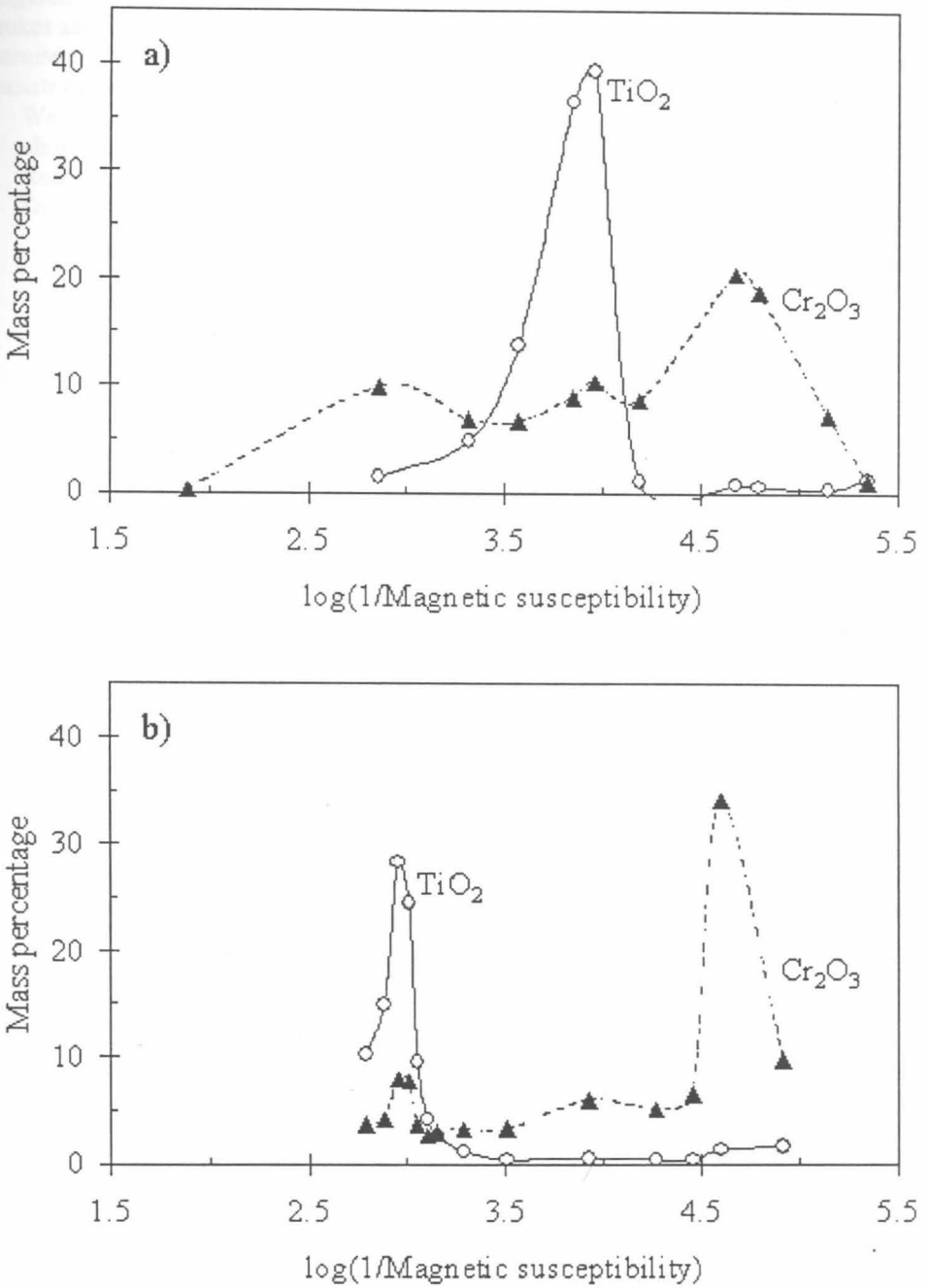


**Figure 2.4: $TiO_2$ and $Cr_2O_3$ distribution of a) unroasted ilmenite concentrate and b) ilmenite concentrate roasted at 750°C in a mixture of air and $CO_2$ reported by Nell and Den Hoed (1997). The retention time of the sample in the roasting atmosphere was not reported. Redrawn from the results of Nell and Den Hoed (1997). (Mass magnetic susceptibility in cgs units).**

### *2.5 Description of alternative flow sheets to beneficiate crude ilmenite from Southern African East Coast deposits*

In their paper Beukes and Van Niekerk (1999) compared three secondary beneficiation processes for crude ilmenite produced from a Southern African East Coast deposit. Their aim was to produce ilmenite with $Cr_2O_3$-levels less than 0.1 per cent, from an ilmenite concentrate with $Cr_2O_3$-levels of the

order of 0.3 per cent. They claimed that the third process described by them, has a lower operational cost than the conventional process patented by Bergeron and Prest (1974).

Bergeron and Prest patented the first process described by Beukes and Van Niekerk (1999) in 1974. Beukes and Van Niekerk (1999) claimed that this process resulted in 80 per cent yield of smelter grade ilmenite with less than 0.1 per cent $Cr_2O_3$. The process is presented schematically in figure 2.5 and consists of the following three steps:

1. Wet magnetic separation of the crude ilmenite concentrate at 2000-3000 Gauss. In this step chromite with a high magnetic susceptibility reports to the magnetic reject fraction.
2. Roasting the non-magnetic fraction in an oxidizing atmosphere.
3. Dry magnetic separation of the roasted material at 1000-2000 Gauss.

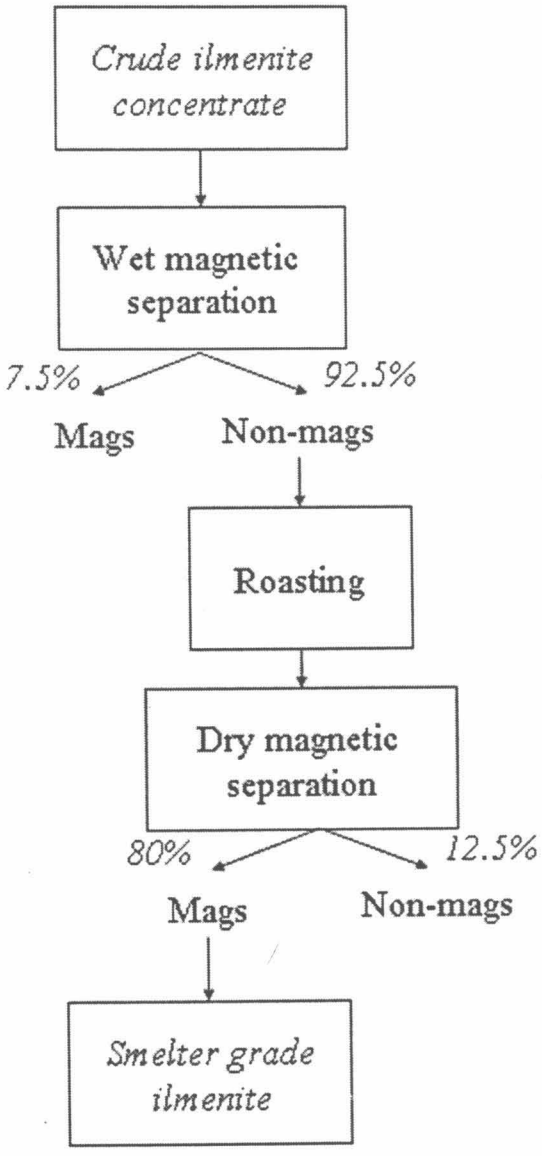


**Figure 2.5: Process #1 of the three secondary beneficiation processes for crude ilmenite described by Beukes and Van Niekerk (1999).**

The separability curve constructed by Nell and Den Hoed (1997) in figure 2.4b supports the statement made by Beukes and Van Niekerk (1999). In the crude ilmenite concentrate after roasting the $TiO_2$ is concentrated in a single population with a higher magnetic susceptibility than prior to roasting – refer figure 2.4a - and the $Cr_2O_3$ retains a bimodal population. A product with less than 0.1 per cent $Cr_2O_3$ can probably be produced from this concentrate by extracting the $TiO_2$-containing fraction to the high susceptible side as in the method described by Beukes and Van Niekerk (1999). Nell and Den Hoed (1997) claimed that 90 per cent by weight of the roasted crude ilmenite would report to the magnetic

fraction and the $TiO_2$ recovery would be 95 per cent. They stated that roasting did not change the magnetic susceptibility of the chromium-rich spinel. The recovery reported by Nell and Den Hoed (1997) is based on laboratory scale studies, which are closer to ideal conditions than the pilot studies conducted by Beukes and Van Niekerk (1999). The studies by Beukes and Van Niekerk are closer to the performance of industrial scale plants.

The second process described by Beukes and Van Niekerk (1999) is depicted in figure 2.6. Beukes and Van Niekerk (1999) claimed that this process resulted in 70 per cent yield of smelter grade ilmenite with less than 0.1 per cent $Cr_2O_3$. The process consists of the following three steps:

1. Drying of the crude ilmenite concentrate.
2. Dry magnetic separation of the dried crude ilmenite concentrate at 2350 Gauss.
3. Dry magnetic separation of the non-magnetic fraction at 6500 Gauss.

The main differences with the first process are hence that no roasting is performed and the 'cleaning' separation step is performed at a higher field strength.

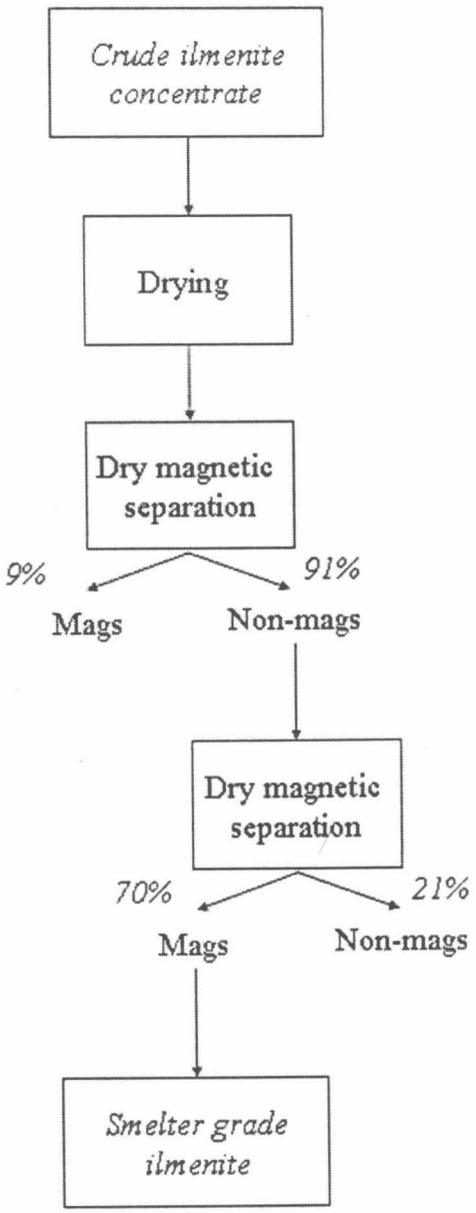


**Figure 2.6: Process #2 of the three secondary beneficiation processes for crude ilmenite described by Beukes and Van Niekerk (1999).**

The separability curve constructed by Nell and Den Hoed (1997) in figure 2.4a supports the statement made by Beukes and Van Niekerk (1999). In the crude ilmenite concentrate prior to roasting the $TiO_2$ is concentrated in a single population and the $Cr_2O_3$ in a bimodal population. A product with less than 0.1 per cent $Cr_2O_3$ can probably be produced from this concentrate by extracting the $TiO_2$-containing fraction which lies between the bimodal distributions of chromite, as in the method described by Beukes and Van Niekerk (1999). Nell and Den Hoed (1997) did not discuss this option and therefore no laboratory scale mass or $TiO_2$ recoveries for this option is available.

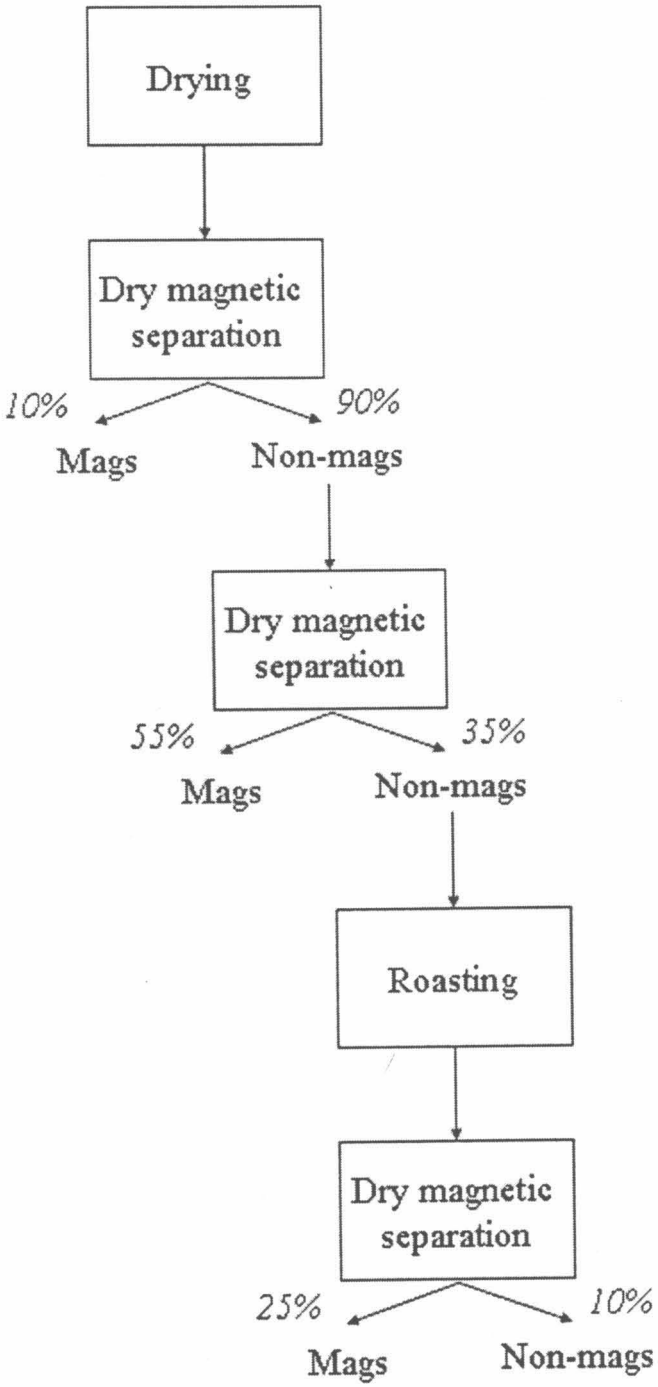


**Figure 2.7: Process #3 of the three secondary beneficiation processes for crude ilmenite described by Beukes and Van Niekerk (1999).**

The third process described by Beukes and Van Niekerk (1999) is depicted in figure 2.7. They claimed that this step resulted in 80 per cent yield of ilmenite with less than 0.1 per cent $Cr_2O_3$. This recovery

figure is similar to that obtained in Process #1 but with less material requiring roasting. The process consists of the following five steps:

1. Drying of the crude ilmenite concentrate.
2. Dry magnetic separation of the dried crude ilmenite concentrate at 2350 Gauss.
3. Dry magnetic separation of the non-magnetic fraction at 6500 Gauss.
4. Roasting of the non-magnetic fraction – for the purpose of this study referred to as LSR[1] - in an oxidizing atmosphere.
5. Dry magnetic separation of the roasted material at 1000-2000 Gauss.

The process is hence similar to Process #2, but with an additional roasting and magnetic separation step.

Beukes and Van Niekerk (1999) proposed that because the ilmenite distribution concentrated to the high-susceptibly side after roasting and the chromite distribution remained bi-modal and did not change during oxidizing roasting (as stated by Nell and Den Hoed 1997), the roasting of the LSR would render the ilmenite magnetic and the chromite non-magnetic. If that were the case it would be possible to separate the ilmenite from the chromite. The roasting conditions most probably would be similar to that for crude ilmenite published by Nell and Den Hoed (1997) or Bergeron and Prest (1974). This led to the decision to test the hypothesis in the work presented here:

"It is possible to produce an ilmenite product suitable for ilmenite smelting by subjecting LSR to roasting and subsequent magnetic separation, using the roasting conditions recommended for crude ilmenite by Nell and Den Hoed (1997) or Bergeron and Prest (1974)"

The following are quotes on the behaviour of chromite during oxidising roasting of chromite containing ilmenite concentrates:

"...roasting does not increase the magnetic susceptibility of the other minerals present in the concentrate and specifically that of chromium-bearing spinel..." - Nell and Den Hoed (1997).

and

"...At the same time the chromite phase, the major $Cr_2O_3$ contaminant in the ore, remains relatively unchanged..." - Bergeron and Prest (1974)

The statements in these quotes led to the decision to test the second hypothesis in the work presented here:

"The magnetic susceptibility of chromite remains constant during magnetizing roasting of an ilmenite concentrate under the oxidizing conditions reported by Nell and Den Hoed (1997)."

### *2.6 Description of the principles of magnetic beneficiation*

The dominant external force on a particle in a magnetic separator is the magnetic force. The separation of one mineral from another depends on the motion of the particle in response to this magnetic force vs. the motion of the particle in response to other competing forces. The competing forces include gravitational, hydrodynamic drag, inertial, friction and centrifugal (in the case of rotating drum separators) forces as well as interparticle forces of electromagnetic and electrostatic origin. The importance of each competing force is a function of the type of magnetic separator and the properties of the particles involved. To ensure separation between minerals with strong magnetic properties and minerals with less strongly magnetic properties, the magnetic force acting on the strong magnetic mineral ($F^m_{mag}$) must be greater than the sum of the competing forces ($\sum F^m_c$). Likewise for the mineral with less strongly magnetic properties the magnetic force acting on the strong magnetic mineral ($F^n_{mag}$) must be less than the sum of the competing forces ($\sum F^n_c$) – refer to equation 2.1.

**A)** $\mathbf{F^M_{MAG} \geq \sum F^M_C}$

**B)** $\mathbf{\sum F^N_C \geq F^N_{MAG}}$

[1] LSR is the abbreviation of Low Susceptibility rejects

**Equation 2.1: Conditions to be met in a magnetic separator to ensure efficient separation of the magnetic minerals from non-magnetic minerals (Svoboda, 1987)**

Hayes (1993) divided magnetic separation processes into high (>100 $Am^{-1}$) and low (<10 $Am^{-1}$) intensity processes. Hayes (1993) stated that low intensity processes are used to separate materials with high magnetic susceptibilities from materials with low susceptibilities (e.g. $Fe_3O_4$ from $SiO_2$). Likewise high intensity processes are used to separate materials with weak magnetic susceptibilities from process streams.

When feeding slurry into a magnetic separator, two streams should exit it: one consisting of magnetic minerals and the other of non-magnetic minerals (Kelly and Spottiswood 1995; Svoboda 1987). In real separation not only are there three streams – magnetic, middlings and non-magnetic – but both magnetic and non-magnetic minerals also report to all three streams. Separation is complete in very limited cases (Svoboda 1987). Figure 2.8 is a schematic presentation of the ideal vs. real magnetic separator.

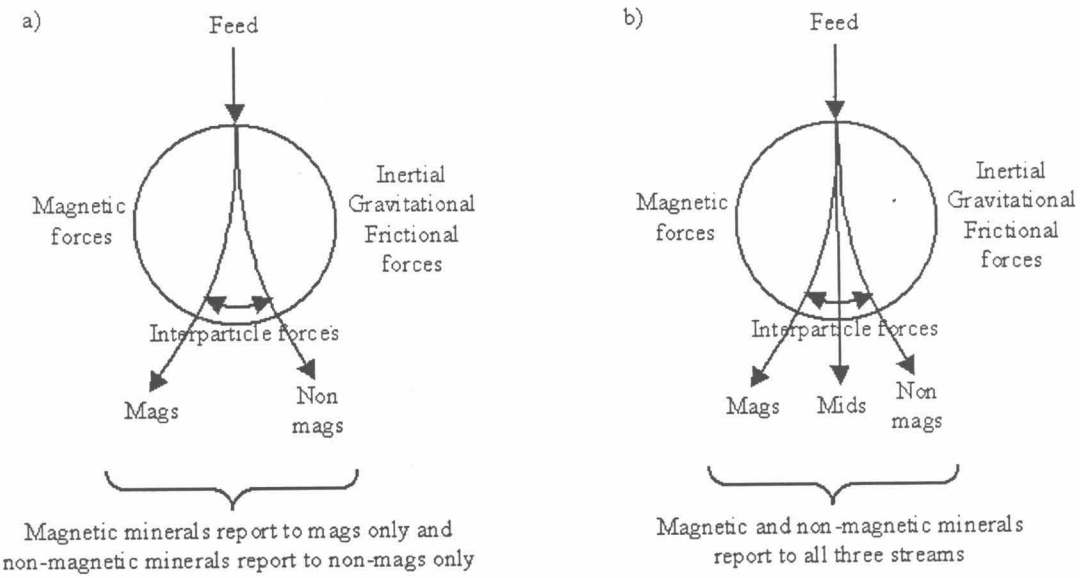


**Figure 2.8: Schematic representation of a) an ideal and b) a real magnetic separator after Svoboda (1987).**

## *2.7 Description of the principles in magnetization*

### 2.7.1 Magnetization, magnetic force and magnetic susceptibility

Hayes (1993) stated that the magnitude of the interaction of a material with a magnetic field is often described in terms of magnetic susceptibility, Svoboda (1987) defined both volume magnetic susceptibility ($\kappa$) and specific or mass magnetic susceptibility ($\chi$). In equation 2.2,

$$a)\ M=\kappa H$$

$$b)\ J = \mu_o \kappa H$$

**Equation 2.2: Definition of volume magnetic susceptibility (Svoboda 1987)**

$\kappa$ is the magnetization per unit field or the volume magnetic susceptibility of an isotropic material in equilibrium in a magnetic field strength H, with a magnetization M along the field direction. The unit of measurement of volume magnetic susceptibility is dimensionless. In equation 2.3,

a) $\kappa = \rho\chi$
therefore b) $\chi = \kappa/\rho$
and eq 3a) into b) $\chi = M/H * 1/\rho$

**Equation 2.3: Definition of mass or specific magnetic susceptibility (after Svoboda 1987 and Hayes 1993)**

$\chi$ is the mass or specific magnetic susceptibility with respect to the unit mass of material with a density $\rho$. The unit of measurement of specific magnetic susceptibility is $m^3kg^{-1}$.

Svoboda (1987) summarized the relationships between the different systems of units that magnetic susceptibility was expressed in literature. These relationships were stated in equation 2.4:

a) $\kappa(SI) = 4\pi\kappa(cgs)$
b) $\kappa(cgs) = \rho\chi(cgs)$
c) $\kappa(SI) = 4\pi\rho\chi(cgs)$
d) $\chi(SI) = 4\pi*10^{-3}*\chi(cgs)$

**Equation 2.4: Summary of the relationships between the different systems of units that magnetic susceptibility as expressed in literature (Svoboda 1987)**

In table 2.3 the conversion factors between volume and specific magnetic susceptibilities are stated in both SI and cgs systems (Svoboda, 1987).

**Table 2.3: Definitions and units of measurement used in the definition of magnetic susceptibility – Sears et al (1986); Kelly and Spottiswood (1995) and Svoboda (1987)**

| Symbol | Definition | SI unit | Cgs unit | Conversion factor $F^2$ |
|---|---|---|---|---|
| B | Magnetic induction | Tesla [T] | Gauss [G] | $10^{-4}$ |
| H | Magnetic field strength | $[A.m^{-1}]$ | Oersted [Oe] | $10^3/4\pi$ |
| J | Magnetic polarization | Tesla [T] | [emu $cm^{-3}$] | $4\pi * 10^{-4}$ |
| M | Magnetization | $[A.m^{-1}]$ | [emu $cm^3$] | $10^3$ |
| $\mu_0$ | Magnetic permeability of a vacuum/free space | $[Hm^{-1}]$ | 1 | $4\pi \times 10^{-7}$ |
| | Magnetic flux | Weber [Wb] | Maxwell [Mx] | $10^{-8}$ |
| $\kappa$ | Volume magnetic susceptibility | - | - | $1/4\pi$ |
| $\chi$ | Specific (mass) magnetic susceptibility | $[m^3\ kg^{-1}]$ | [$cm^3\ g^{-1}$ (or emu $g^{-1}$ or emu $g^{-1}cm^{-3}$)] | $1000/4\pi$ |
| $\mu_m$ | Magnetic moment | $[Tm^3]$ | [emu] | $4\pi10^{-10}$ |
| $\sigma_m$ | Specific polarization | $[Tm^3kg^{-1}]$ | [emu $g^{-1}$] | $10^{-7}$ |
| r | Distance between source point and field point | m | M | |
| v | Velocity vector of q | $ms^{-1}$ | $ms^{-1}$ | |
| $\theta$ | Angle between vector v and line qP | ° | ° | |
| k' | Proportionality constant | - | - | $\mu_0 4^{-1}\pi^{-1} = 10^{-7}$ |

Svoboda (1987) stated that most equations used volume magnetic susceptibility, but that experimentally it would be easier to determine mass or specific magnetic susceptibility. All experimental magnetic susceptibility measurements in this study were based on mass or specific magnetic susceptibility ($\chi$) and results were reported in cgs units as $cm^3\ g^{-1}$.

As the type of magnetic separator to be used in this study is a Frantz isodynamic separator, the only competing force would be gravitational. Svoboda (1987) mathematically described the gravitational force on a spherical particle with radius b of density $\rho_p$ as in equation 2.5.

[2] F is the number by which the quantity in cgs units must be multiplied to obtain the quantity in SI units, i.e. SI = cgs x F

$$F_g = {}^4/_3\pi(\rho_p - \rho_f)b^3g$$

**Equation 2.5: Mathematical definition of the magnitude of the competing gravitational force acting on a particle in a magnetic separator Svoboda (1987)**

Where $\rho_f$ is the density of the fluid medium and g the acceleration of gravity. When dry separation takes place the value of $\rho_f$ is zero. Svoboda (1987) also gave an equation for the hydrodynamic drag force, which would be a factor in any wet magnetic separation applications. Both the traction magnetic force and the competing gravitational force are functions of particle size. Therefore the larger the particle size the greater the influence of the gravitational force. Separation based on differences in magnetic susceptibility would only be possible for a narrow interval of particle size where separation conditions are optimum (Svoboda 1987).

### 2.7.2 Paramagnetic, diamagnetic and ferromagnetic materials

All matter responds to the presence of the external magnetic field, although the degree of the response varies considerably. The applied magnetic field interacts with the magnetic field of the atoms of the matter, which exists as a consequence of:

- The precessional motion of the charged nucleus;
- The orbital motion of the electrons around the nucleus and;
- The spin motion of electrons and nuclei (Svoboda 1987).

Svoboda (1987) stated that according to their properties minerals could be divided into three basic groups: ferromagnetic; paramagnetic and diamagnetic. Smith (1990) described two other groups: ferrimagnetic and antiferromagnetic. Hayes (1993) stated that for practical purposes ferro-, ferri- and antiferromagnetic material could be regarded as special cases of paramagnetic materials.

Prior to the development of HGMS (High Gauss Magnetic Separators) the technological classification for magnetic separation differed from the fundamental physical categorization (Svoboda 1987):

- *Strongly magnetic minerals*: minerals, such as magnetite, which could be recovered by a magnetic separator using a relatively weak magnetic induction of up to 1500 Gauss. The responding magnetic susceptibility of these minerals would be greater than $5*10^{-5}$ $m^3kg^{-1}$ ($4*10^{-3}$ $cm^3g^{-1}$);
- *Weakly magnetic minerals*: minerals, such as iron and manganese oxides and carbonates as well as ilmenite, which could be recovered by a magnetic separator using a relatively weak magnetic induction of up to 8000 Gauss. The responding magnetic susceptibility of these minerals ranged from $5*10^{-6}$ down to $1*10^{-7}$ $m^3kg^{-1}$ ($4*10^{-4}$ down to $8*10^{-6}$ $cm^3g^{-1}$). This broad group of minerals included ferrimagnetic and paramagnetic minerals and paramagnetic minerals with parasitic ferromagnetism;
- *Nonmagnetic minerals*: all minerals that could not be recovered by conventional magnetic separators, but which could be recovered by HGMS's. This group of minerals included diamagnetic minerals, which have a negative magnetic susceptibility. The responding magnetic susceptibility of these minerals was less than $1*10^{-7}$ $m^3kg^{-1}$ ($8*10^{-6}$ $cm^3g^{-1}$).

Each electron spinning on its own axis behaves as a magnetic dipole (Smith 1990). In most cases electrons in atoms are paired and therefore the positive and negative magnetic moments cancel. In *diamagnetic* materials the presence of an external magnetic field slightly unbalances the orbiting electrons and creates small magnetic dipoles within the atoms which are opposite in direction to the external magnetic field (Smith 1990). They therefore repel the external magnetic field, have relative permeability less than unity and negative magnetic susceptibilities - refer to table 2.4 (Kelly and Spottiswood 1995).

Svoboda (1987) explained diamagnetism differently and stated that the electrical charges partially shield the interior of the body from an applied magnetic field. The electron orbits the nucleus in the presence of the central electrostatic field in the atom. When an external magnetic field is applied, the induced current produces a magnetic field opposite to the applied field – according to Lenz's law stated in equation 2.6. According to Svoboda (1987) diamagnetism is present in all substances. It exists in substances that have neither spin nor orbital magnetic moments and diamagnetic susceptibilities are temperature-independent. Hayes (1993) simplified the definition to minerals which are repelled by a magnetic field and which move to positions of low field intensity.

$$\kappa = -\mu_0 N_a e^2 z \langle r^2 \rangle / (6m_0)$$

**Equation 2.6: The volume magnetic susceptibility for a mono-atomic molecule where $N_a$ is the number of atoms per unit volume, e the electronic charge, z the number of electrons in an atom, $m_0$ the rest mass of the electron and $\langle r^2 \rangle$ the mean square distance of electrons from the nucleus (Svoboda 1987).**

Svoboda (1987) stated that the magnetic atoms or ions in *paramagnetic* materials have permanent intrinsic magnetic moments and they occur in low concentrations in the material. Susceptibility arises from the competition between the aligning effect of the applied magnetic field and the randomizing effect of thermal vibrations. The magnetic effect disappears once the material is removed from the external magnetic field (Kelly and Spottiswood 1995). The material becomes magnetized when individual magnetic dipole moments align in the applied magnetic field. The individual magnetic dipole moments could be caused by unpaired electrons (total spin of system is not zero) in atoms or molecules or free atoms or ions with a partly filled inner electronic shell (Smith 1990, Svoboda 1987). The material de-magnetizes when the dipole moments de-align when the applied magnetic field is removed, the magnetic moments are randomly oriented and the overall magnetic moment is zero (Smith 1990, Svoboda 1987). According to the Curie law (equation 2.7) the magnetic susceptibility of a paramagnetic substance is inversely proportional to the temperature. Hayes (1993) simplified the definition to minerals attracted by a magnetic field and which move to positions of high field intensity.

$$\kappa = M/H = \mu_m^2 N_a/(3\mu_0 kT) = C/T$$

**Equation 2.7: Curie law with C as the Curie constant (Svoboda 1987)**

A *ferromagnetic* material is one in which the magnetic dipoles tend to line up parallel to each other even when no external magnetic field is present i.e. it magnetizes spontaneously. Individual magnetic dipole moments, of unpaired electrons in its atoms or molecules, tend to line up spontaneously (Smith 1990) against the disturbing force of thermal motion (Svoboda 1987). Thermal energy, i.e. heating, causes the magnetic dipoles in ferromagnetic material to deviate from perfect parallel alignment and finally a temperature is reached where the ferromagnetism in the material disappears and the material becomes paramagnetic (figure 2.9). This temperature is the Curie temperature of the material. Below the Curie temperature[3] the material is ferromagnetic and above paramagnetic, independent of whether heating or cooling is taking place (Smith 1990). Ferromagnetic materials have large relative permeability ($K_m$) values (refer to table 2.4). For ferromagnetic material $K_m$ is not constant. The value of $K_m$ increases as the value of the external magnetic field increases until saturation magnetization is reached. At saturation magnetization nearly all individual magnetic dipole moments have their axes parallel to the external magnetic field. Once saturation magnetization is reached the magnetization of the material, as well as the additional field caused by the material, remains constant irrespective of a further increase in the magnitude of the external magnetic field. Some ferromagnetic materials retain their magnetization once the external magnetic field is removed and can become permanent magnets. A ferromagnetic material is therefore characterized by hysteresis, or irreversibility of magnetization. A magnetized ferromagnetic material can be demagnetized by slow cooling from a temperature above its Curie temperature (Smith 1990).

Kelly and Spottiswood (1995) illustrated the linear relationship between magnetization (M) and the applied magnetic field (H) in paramagnetic and diamagnetic minerals and the non-linear relationship in ferromagnetic minerals in magnetization curves (figure 2.9 and figure 2.10). The linear relationship in paramagnetic and diamagnetic minerals indicates the constant magnetic susceptibility ($M.H^{-1}$) throughout the mineral and confirms that the permeability $K_m$ of the mineral is independent of the applied magnetic field. The non-linear relationship in ferromagnetic materials indicates that the permeability $K_m$ of the mineral, and therefore the magnetic susceptibility ($M.H^{-1}$) thereof, is independent of the applied magnetic field until saturation magnetization is reached.

Table 2.4 indicates examples of the different types of metals and minerals in each group with typical relative permeability values for the group and typical magnetic susceptibility for the material, where available. The minerals mentioned are related to this study.

[3] Also referred to as Curie point

**Table 2.4: Examples of the three groups of magnetic materials with typical values of their magnetic susceptibility**

| Group | Typical values of $K_m$ | Examples (Sears et al 1987) | Magnetic susceptibility @ T = 20°C [$cm^3\ g^{-1}$] | Reference |
|---|---|---|---|---|
| Diamagnetic | 0.99990 to 0.99999 | Copper | $-1.0 \times 10^{-5}$ | Sears et al (1987) |
| | | Quartz | $-0.45 \times 10^{-6}$ | Svoboda (1987) |
| Paramagnetic | 1.0001 to 1.0020 | Aluminium | $2.2 \times 10^{-5}$ | Sears et al (1987) |
| | | Hematite | $40 - 300 \times 10^{-6}$ | Svoboda (1987) |
| | | Ilmenite | $15 - 120 \times 10^{-6}$ | Svoboda (1987) |
| | | Chromite | $14 - 69 \times 10^{-6}$ | Andres (1976) |
| Ferromagnetic | 1000 to 10000 | Iron | Not applicable | Not applicable |
| | | Magnetite | Not applicable | Not applicable |

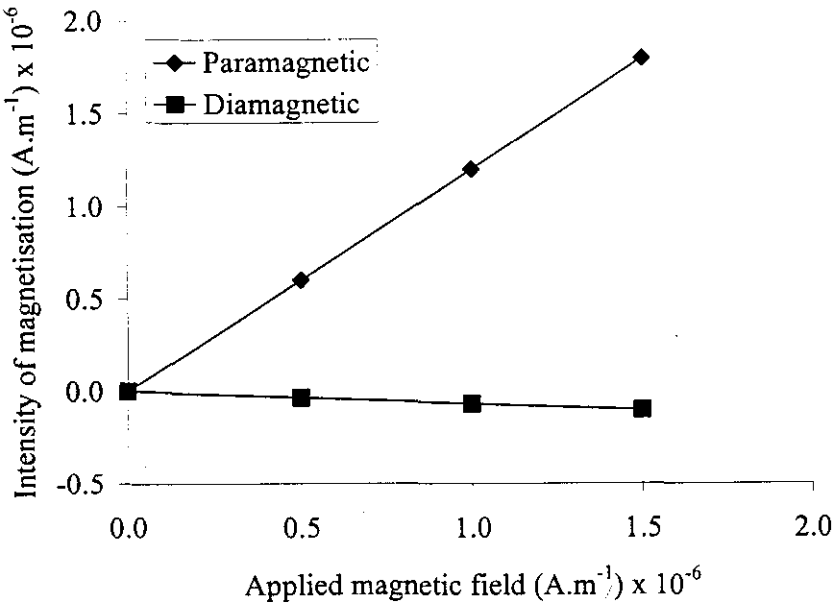


**Figure 2.9: Typical magnetisation curves for paramagnetic (hematite) and diamagnetic (quartz) minerals – after Kelly and Spottiswood (1995)**

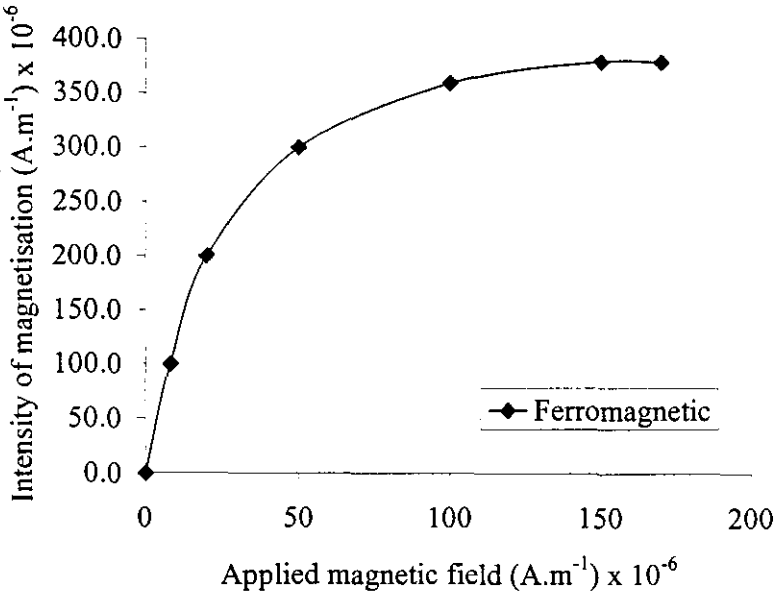


**Figure 2.10: Typical magnetisation curves for ferromagnetic minerals (magnetite) – after Kelly and Spottiswood (1995)**

### *2.8 Magnetic susceptibility of chromite*

De Waal and Copelowitz (1972) quoted Rait stating that in the system $MgAl_2O_4$-$MgCr_2O_4$-$MgFe_2O_4$ the straight line connecting the point, 30 mole percent $MgFe_2O_4$-70 mole percent $MgAl_2O_4$, with the point, 10 mole per cent $MgFe_2O_4$-90 mole per cent $MgCr_2O_4$, serves as the room temperature magnetic boundary. Therefore chrome spinels richer in $MgFe_2O_4$ than this boundary or rich in $Fe_3O_4$ are magnetic at room temperature – refer to figure 2.11.

Schwerer and Gundaker (1975) studied the mechanical and thermal effects on the magnetic properties of natural chromites – refer to table 2.5. They observed that mechanical working increased the saturation magnetisation of natural chromites. On crushing Transvaal hard-lumpy grade chromite they observed an increase in the saturation magnetisation on decreasing particle size, but observed that what they called 'high field susceptibility $\chi$' as relatively independent on particle size or therefore crushing treatment. On the other hand Schwerer and Gundaker (1975) observed that the high field susceptibility $\chi$ increased upon cooling and that the saturation magnetisation was independent of temperature when taking measurements at room temperature (300 K) and liquid-nitrogen temperature (78 K).

**Table 2.5: Composition of the spinel phase in the natural chromite samples studied by Schwerer and Gundaker (1975)**

| Component | Transvaal Hard Lumpy | Transvaal Low $SiO_2$ | MasInloc |
|---|---|---|---|
| $SiO_2$ | 0 | 0 | 0 |
| $Al_2O_3$ | 16.59 | 14.38 | 29.10 |
| CaO | 0 | 0.04 | 0.04 |
| MgO | 8.21 | 11.26 | 16.97 |
| $Cr_2O_3$ | 47.89 | 46.78 | 36.84 |
| FeO | 27.11 | 26.32 | 16.12 |
| $Fe_2O_3$ | - | - | 0 |
| $TiO_2$ | 1.42 | 0.57 | 0.27 |
| Total | 101.22 | 99.35 | 99.34 |

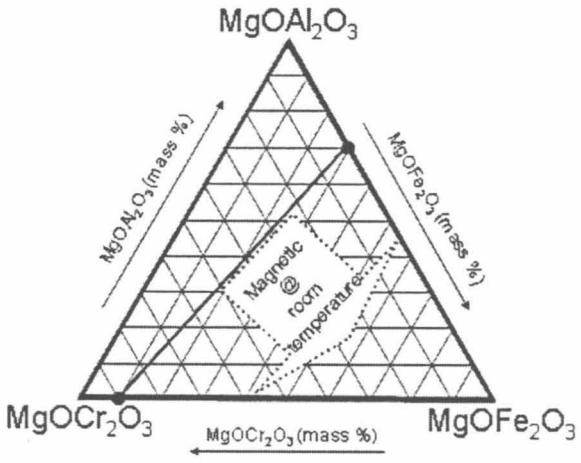


**Figure 2.11: The room temperature magnetic boundary of the $MgAl_2O_4$-$MgCr_2O_4$-$MgFe_2O_4$ system (after De Waal and Copelowitz 1972 and Ulmer 1970)**

Both the results of the mechanical working and the temperature study indicated the presence of a different phase or structure on the grain surface that differ from the bulk chromite matrix. Schwerer and Gundaker (1975) stated that the measured values of saturation magnetisation was due to a crushing-induced magnetic phase and the high field susceptibility measurements, that of the bulk of the chromite matrix. They attributed crushing-induced magnetisation to changes in surface structures rather than changes in the bulk of the chromite matrix. They stated that the interpretation is compatible with:

- Their observed increased sensitivity to furnace atmosphere at moderate temperatures (270 to 600°C) of crushed material in comparison with annealed material. This was observed when alternating furnace atmosphere between air or He-10 per cent$H_2$ gas mixtures;
- The general absence of chemical unmixing in chromites; and
- The observation of Fe-enriched phases on altered chromite grain surfaces.

Schwerer and Gundaker (1975) compared the changes in magnetic susceptibility of chromite, or lack thereof, with that of iron-titanium oxides. They attributed the changes in the iron-titanium oxides after heat treatments to chemical unmixing at high temperature, phases that are concentrated in magnetic ions with large saturation magnetisation values. This is similar to the mechanism of magnetisation proposed by Guzman, Taylor and Giroux (1992) discussed elsewhere. Schwerer and Gundaker (1975) quoted other authors who stated observations of microscopic veinlets of magnetite in magnetic natural chromite, but could not observe any of these with Mössbauer spectroscopy in the crushed natural chromites. They found that the ordering temperature for the surface structure is about 570°C and stated that it was close to that of magnetite ($Fe_3O_4$). They stated that the magnetic phase is associated either with Fe-enriched phases or with defect structures on the grain surface. They observed that annealing at temperatures in the range 500-600°C almost fully recovered the crushing induced phase and apparently increase the susceptibility of the chromite grains to gas-solid reactions at moderate temperatures – where the saturation magnetisation of the chromite particles decreased with exposure to an oxidising and increases with exposure to a reducing atmosphere at 430°C.

To summarise the statements made by De Waal and Copelowitz (1972) and the observations made by Schwerer and Gundaker (1975) that are relevant to this study:

- The bulk of the chromite matrix in the natural chromites studied by Schwerer and Gundaker (1975) was paramagnetic;
- Schwerer and Gundaker (1975) observed a mechanically induced surface structure was formed after crushing;
- The surface structure observed by Schwerer and Gundaker (1975) displayed ferromagnetic behaviour. This could have been $Fe_3O_4$, but this was not proven by the measurement techniques used in the study and the effect was removed during annealing i.e. it might well have been surface defect structures.
- The saturation magnetisation of the ferromagnetic phase, when heat-treated at 430°C (duration not stated), increased in a reducing atmosphere and decreased in an oxidising atmosphere, but no

observations on increase or decrease in bulk magnetic susceptibility when subjecting the chromite to oxidising roasting atmospheres were made (Schwerer and Gundaker 1975).

- Chrome spinel richer in $MgFe_2O_4$ than the boundary created by the straight line connecting the point, 30 mole percent $MgFe_2O_4$-70 mole percent $MgAl_2O_4$, with the point, 10 mole per cent $MgFe_2O_4$-90 mole per cent $MgCr_2O_4$, or rich in $Fe_3O_4$, are magnetic at room temperature (De Waal and Copelowitz 1972). It is therefore expected that an increase in the $Fe_2O_3$ or $Fe_3O_4$ content of a chromite mineral will lead to an increase in the magnetic susceptibility thereof.

## *2.9 Mechanism of magnetic susceptibility changes in ilmenite*

### 2.9.1 Ferrian ilmenite

According to Dunlop (1990) the most important terrestrial magnetic minerals are oxides of iron and titanium. Figure 2.12 is a ternary phase diagram of these oxides and their solid solution series.

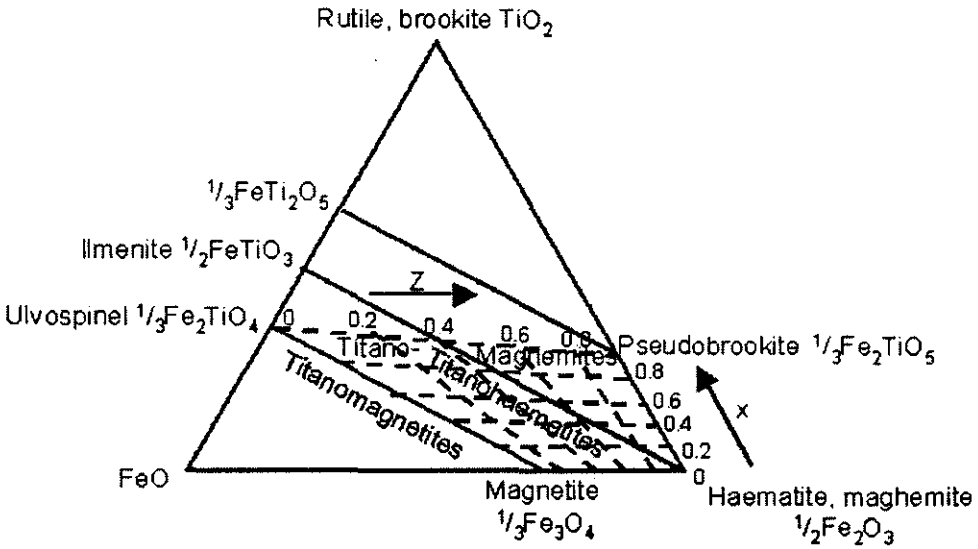


**Figure 2.12: Ternary phase diagram of iron-titanium oxides and their solid solution series, x is the Ti content in the titanomagnetites series and z is the oxidation parameter for titanomaghemites (derived from Dunlop 1990).**

The ferrian ilmenites ($Ti_yFe_{2-y}O_3$) have compositions between the end-members haematite ($\alpha Fe_2O_3$) and ilmenite ($FeTiO_3$) of which the solid solution is only complete at high temperatures. According to Nord (1989) solid solution between haematite ($\alpha Fe_2O_3$) and ilmenite ($FeTiO_3$) is complete (miscibility is reached) at temperatures above 700°C. Bozorth et al (1957) stated that the solid solution series of $FeTiO_3$-$Fe_2O_3$ have strong ferromagnetic properties although both end members ($FeTiO_3$ and $Fe_2O_3$) are paramagnetic or antiferromagnetic (Ishikawa and Akimoto, 1957). According to Dunlop (1990) single-phase ferrian ilmenites of intermediate composition can be preserved by rapid chilling from the solid-solution range. Unlike other ferromagnetic materials the single-phase ferrian ilmenites do not become demagnetised when they are cooled from their Curie temperatures but remain magnetised to some extent. Furthermore the direction of their magnetisation is opposite to that of the field applied during cooling.

### 2.9.2 Crystal structure of ferrian ilmenites

Dunlop (1990) states that ferrian ilmenites have a corundum structure (i.e. similar to $Al_2O_3$) with oxygen anions in the hexagonal close-packed lattice and Fe and Ti cations occupying two-thirds of the interstices – figure 2.13. Corundum ($Al_2O_3$), as ilmenite ($FeTiO_3$), is one of the minerals in the rhombohedral oxide mineral group. The structure of the rhombohedral oxide group consist of hexagonal close packed oxygen with two thirds of the octahedral interstices occupied to give the general formula: $A_2O_3$.

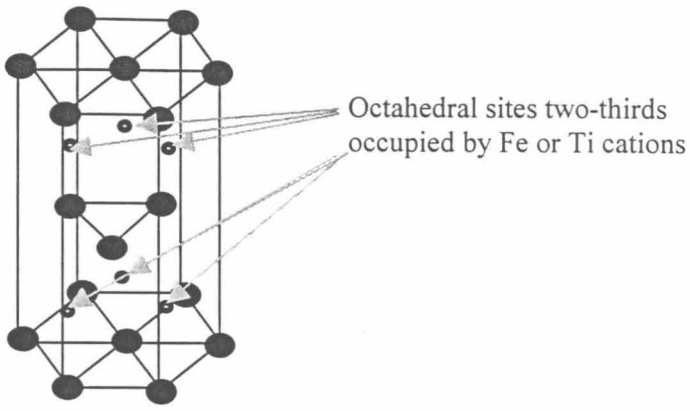


**Figure 2.13: Ferrian ilmenites have a corundum structure (similar to $Al_2O_3$) with O anions in the hexagonal close-packed lattice and Fe and Ti cations occupying only two-thirds of the octahedral interstices to maintain electrical neutrality (after Smith 1990 and Dunlop 1990).**

An isolated hexagonal closed packed unit cell has the equivalent of 6 atoms per unit cell (figure 2.14). Three atoms form a triangle in the middle layer; six $^1/_6$-atom sections and one ½-atom section are on both the bottom and top layer. In ferrian ilmenites these atoms are oxygen anions.

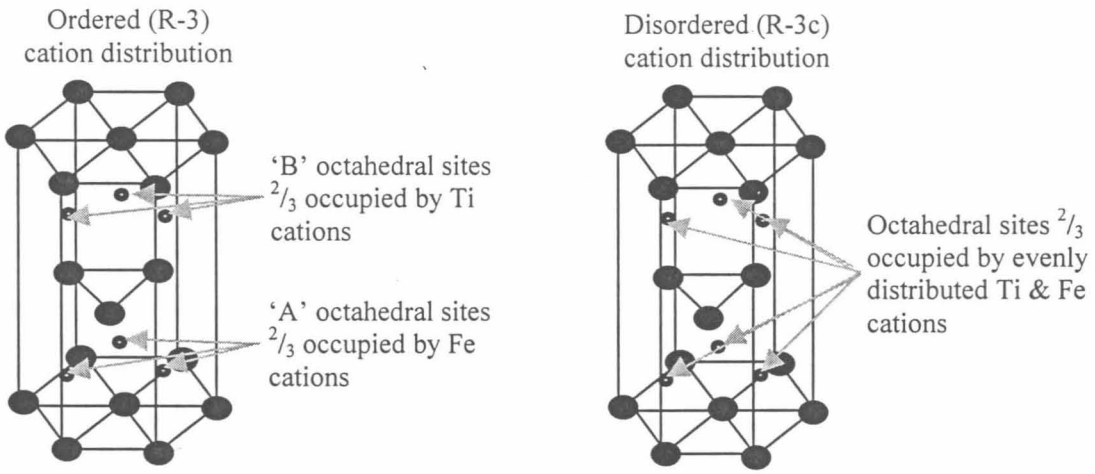


**Figure 2.14: The cation distribution of ferrian ilmenites is ordered (R-3) when the Fe and Ti cations are confined to alternate cation (basal) planes and disordered (R-3c) if they are evenly distributed (after Ishikawa and Akimoto 1957b; Dunlop 1990; Smith 1990).**

There are voids between the atoms or ions, which are packed into a crystal structure. These voids are interstitial sites where other atoms or ions can be fitted. In the hexagonal closed packed (HCP) structure there are two interstitial sites:

- The octahedral interstitial site, which is formed at the center where six atoms contact each other – indicated in figure 2.15 (Smith 1990);
- The tetrahedral interstitial site, which is formed at the center where four atoms contact each other – not indicated in figure 2.15.

In the HCP crystal structure there are as many octrahedral interstitial sites as there are oxygen atoms and twice as many tetrahedral sites as oxygen atoms (Smith 1990). In ferrian ilmenites the interstitial atoms are iron or titanium cations, which are confined to two-thirds of the octrahedral interstitial sites to maintain charge neutrality (Dunlop 1990). For charge neutrality in $A_2O_3$ two $A^{3+}$ cations balance three $O^{2-}$ anions and therefore $^2/_3A^{3+}$ balance one $O^{2-}$.

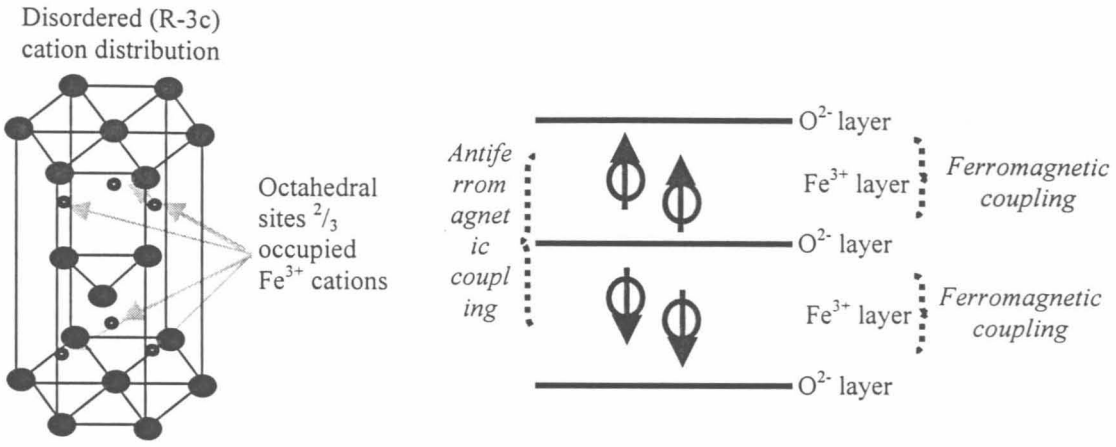


**Figure 2.15: The disordered (R-3c) crystal structure of hematite ($Fe_2O_3$) indicating the distribution of the $Fe^{3+}$ cations. The magnetic coupling due to the crystal structure indicate ferromagnetic coupling within layers and antiferromagnetic coupling between layers (after Ishikawa and Akimoto, 1957b; Bozorth et al 1957 and Banerjee 1991).**

### 2.9.3 Magnetic properties caused by the crystal structure of ferrian ilmenites

*a) Order/Disorder*

From Dunlop (1990) the cation distribution is ordered (R-3) when the Fe and Ti cations are confined to alternate cation (basal) planes without a center of symmetry. It is disordered (R-3c) if cations are evenly distributed with a center of symmetry – refer to figure 2.16.

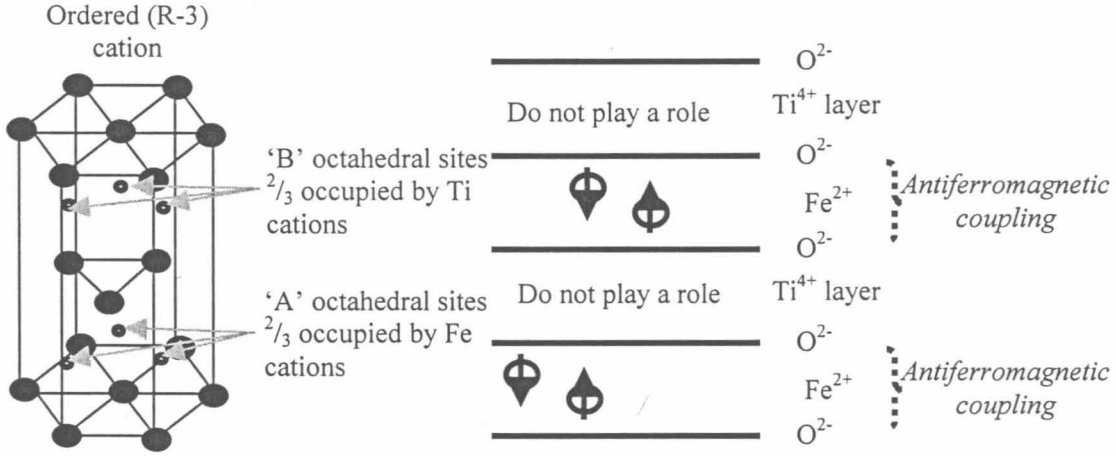


**Figure 2.16: The ordered (R-3) crystal structure of ilmenite ($FeTiO_3$) indicating the distribution of the $Ti^{4+}$ and the $Fe^{3+}$ cations. The magnetic coupling due to the crystal structure indicate antiferromagnetic coupling within layers (after Ishikawa and Akimoto, 1957b; Bozorth et al 1957 and Banerjee 1991).**

*b) Hematite ($Fe_2O_3$)*

Hematite ($Fe_2O_3$) crystallizes in the corundum (disordered R-3c) crystal structure (Banerjee, 1991) with only $Fe^{3+}$ cations filling $^2/_3$ of the interstitial sites (Bozorth et al, 1957). Bozorth (1957) stated that each $Fe^{3+}$ layer is ferromagnetic in itself and alternating layers antiferromagnetic to each other resulting in zero magnetization. Banerjee (1991) stated that hematite is in principle antiferromagnetic but because

the $Fe^{3+}$ spin moments are slightly canted towards each other, it results in a weak ferromagnetic[4] moment.

*c) Ilmenite ($FeTiO_3$)*

Ilmenite ($FeTiO_3$) crystallizes in the ordered R-3 hexagonal structure (Banerjee, 1991). $Fe^{3+}$ cations are replaced by $Ti^{4+}$ cations, accommodated in the 'B' planes, and $Fe^{2+}$ cations, accommodated in the 'A' planes as indicated in figure 2.16. This is to conserve charge balance: $2Fe^{3+} = Fe^{2+} + Ti^{4+}$(Banerjee, 1991). Ishikawa & Akimoto (1957) stated that titanium cations are always tetravalent in solid solution and that the $Ti^{4+}$ ions play no part in the magnetic coupling. Both Bozorth (1957) and Ishikawa and Akimoto (1957b) stated that the $Fe^{2+}$ cations are antiferromagnetically coupled *within* each layer. Therefore total magnetization in pure ilmenite is zero (Ishikawa and Akimoto; 1957b). But how then can the magnetic property of ilmenite be used, and improved, to separate it from minerals, which is less magnetic? Banerjee (1991) answered this question by stating that it can either be that one is dealing with titanohaematite solid solutions ($FeTiO_3$ to $Fe_{1.5}Ti_{0.5}O_3$ which is x=0.5 for $xTiFeO_3(1-x)Fe_2O_3$) or that fine-scale ferromagnetic magnetite is exsolved in the ilmenite.

*d) Ferrian ilmenites ($xTiFeO_3.(1-x)Fe_2O_3$)*

Dunlop (1990) stated that in ferrian ilmenites disordered structures (R-3c) occur for x<0.5 in $xTiFeO_3(1-x)Fe_2O_3$, although not explicitly stated it is assumed that this is at room temperature. Ishikawa and Akimoto (1957b) stated that when quenching ferrian ilmenites after 12 hours of heat treatment from 1200°C to room temperature, disordered structures (R-3c) occur at room temperatures for x<0.5 in $xTiFeO_3(1-x)Fe_2O_3$. Ordered structures (R-3) occur for x>0.5 (Dunlop, 1990; Ishikawa and Akimoto, 1957b). The disordered structures (R-3c) are antiferromagnetic (Dunlop 1990) or feebly ferromagnetic (Ishikawa and Akimoto 1957a). Ishikawa and Akimoto (1957a) observed magnetic induction of 1 to 2 gauss/gram in disordered structures (R-3c). The ordered structures (R-3) are ferrimagnetic (Dunlop 1990) or very strong ferromagnetic (Ishikawa and Akimoto 1957a). Ishikawa and Akimoto (1957a) observed magnetic induction of 30 to 70 gauss/gram in ordered structures (R-3).

Banerjee (1991) stated that the part of the titanohaematite solid solution that is magnetic at room temperature is the $Fe_{1.5}Ti_{0.5}O_3$ to $Fe_{1.27}Ti_{0.73}O_3$ solid solution. Banerjee (1991) stated that this solid solution range is ferrimagnetic and crystallographically ordered, where one cation layer contains iron cations only and the other iron and titanium cations. This layer configuration leads to a net magnetic moment in one direction. Other authors (Ishikawa and Akimoto, 1957b and Bozorth et al, 1957) report other cation configurations with $Ti^{4+}$ cations on both 'A' and 'B' layers, but for the purpose of this study the model proposed by Banerjee (1991) is accepted.

Banerjee (1991) stated that the 3d series (Fe, Mn, Ni, Co etc) are the main magnetic carriers in Fe-Ti oxides but that iron (Fe) is by far the most important source of magnetism. The spin moments for $Fe^{3+}$ and $Fe^{2+}$ are 5 and 4 respectively (Banerjee 1991). This implies that if Fe cations in an 'A' layer are coupled antiferromagnetically the net magnetic moment will not be zero but as in table 2.6. This is actually the definition of ferrimagnetism. The same is true for antiferromagnetic coupling between layers.

Each electron spinning on its own axis behaves as a magnetic dipole and has a dipole moment called the Bohr magneton $\mu_B$ (Smith 1990). Bozorth et al (1957) published data where they observed three regions (refer to figure 2.17) based on the Bohr magneton $\mu_B$ as a function of the mole fraction $Fe_2O_3$ (1-X) in the solid solution. Their data were collected for synthetic material, which was either slow cooled or quenched from 1200°C:

- X > 0.85: Little magnetization observed
- 0.5 < X < 0.85: Strong magnetization observed
- X < 0.5: Little magnetization observed

[4] Also referred to as parasitic ferromagnetism

**Table 2.6: Net magnetic moment for antiferromagnetic and ferromagnetic coupling between $Fe^{3+}$ and $Fe^{2+}$ cations**

| Ion | $Fe^{3+}$ | $Fe^{2+}$ |
|---|---|---|
| Spin moment (Bohr magneton per molecule) | 5 | 4 |
| Net magnetic moment – antiferromagnetic coupling | | 5 - 4 = 1 |
| Net magnetic moment – ferromagnetic coupling | | 5 + 4 = 9 |

Bozorth et al (1957) stated that although titanomagnetites have a ferrimagnetic order, a threshold amount of $Fe_2O_3$ must be added to $FeTiO_3$ before the weak antiferromagnetic coupling in the Fe layers of the $FeTiO_3$ is broken down by the stronger antiferromagnetic coupling between layers, as in $Fe_2O_3$. Bozorth et al (1957) found this threshold value to be 15 mole percent $Fe_2O_3$ and conducted their measurements from room temperature to 1.3K. Slow cooled samples followed the model proposed by Ishikawa and Akimoto (1957b) more closely than quenched samples, at $Fe_2O_3$ contents exceeding the threshold value of 15 per cent. The reason for the deviation in quenched samples was given as the preservation of the disordered cation structure (R-3c), which is present at higher temperatures. Nell and Den Hoed (1997) reported results, similar to the curve for slow cooled material reported by Bozorth (1957), for a natural ilmenite concentrate. Nell and Den Hoed (1997) did not describe the cooling method used.

Ishikawa and Akimoto (1957a) observed a similar deviation in the intensity of magnetisation when slow cooling and quenching $0.5TiFeO_3{\cdot}0.5Fe_2O_3$ samples heat treated in a vacuum at different temperatures for 5 hours – figure 2.18. They attributed it to a order-disorder transformation phenomenon, assumed to be R-3c to R-3. Ishikawa and Akimoto (1957a) stated that they suspected this transition temperature to be 600°C (for $0.5TiFeO_3{\cdot}0.5Fe_2O_3$). Nord et al (1989) determined the temperature and composition where the transition between the disordered (R-3c) and ordered (R-3) crystal structure take place as between 1000 and 1050°C for x = 0.7 in the $xTiFeO_3(1\text{-}x)Fe_2O_3$ solid solution.

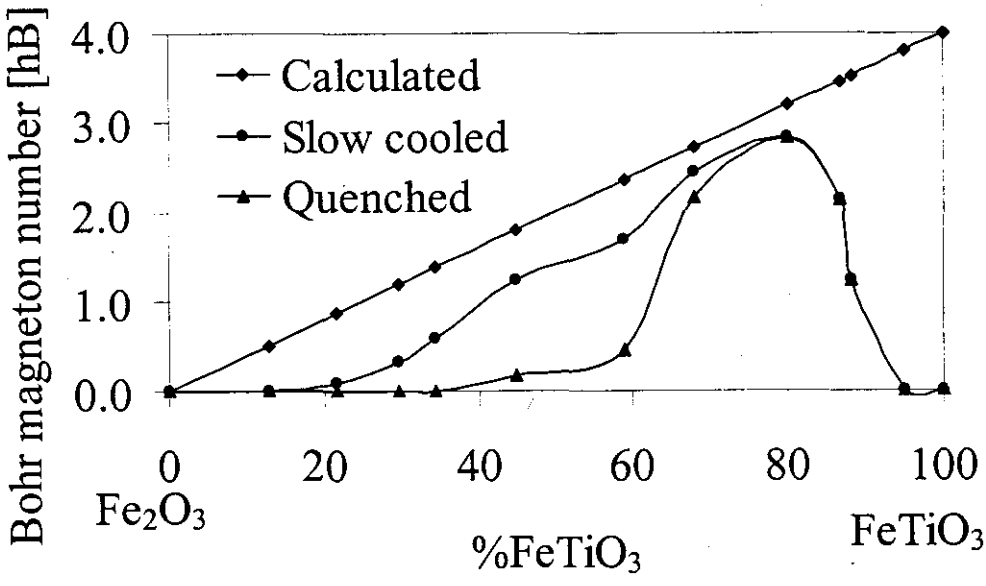


**Figure 2.17: Actual Bohr magneton numbers per mole percent $Fe_2O_3$ in $FeTiO_3$-$Fe_2O_3$ solid solutions vs. calculated – measured from 1.3°K to room temperature (from Bozorth et al 1957). Compositions plotted as mole percentages.**

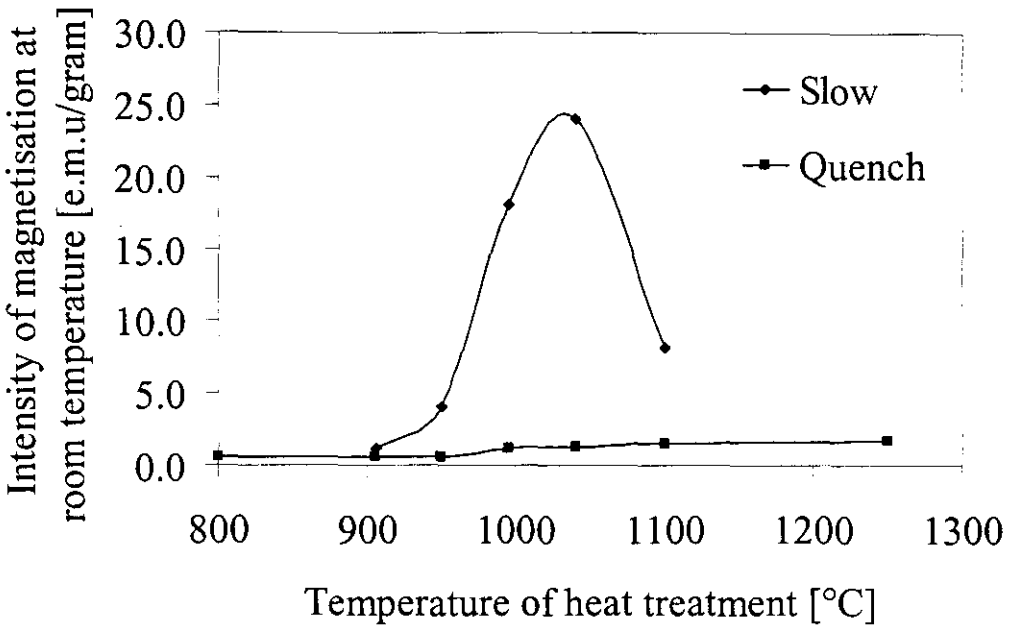


**Figure 2.18: Impact of slow cooling or quenching of $0.5TiFeO_3{\cdot}0.5Fe_2O_3$ samples at various temperatures in a vacuum (Ishikawa and Akimoto 1957a).**

Nell and Den Hoed (1997) quote Putnis (1992); Nord (1989) and Burton (1984) for a phase diagram for the $xTiFeO_3{\cdot}(1\text{-}x)Fe_2O_3$ solid solution that indicates both the cation crystallographic order/disorder (R-3c/R-3) and the magnetic order/disorder (Curie point) with compositional fields where self-reversing takes place – refer to figure 2.19.

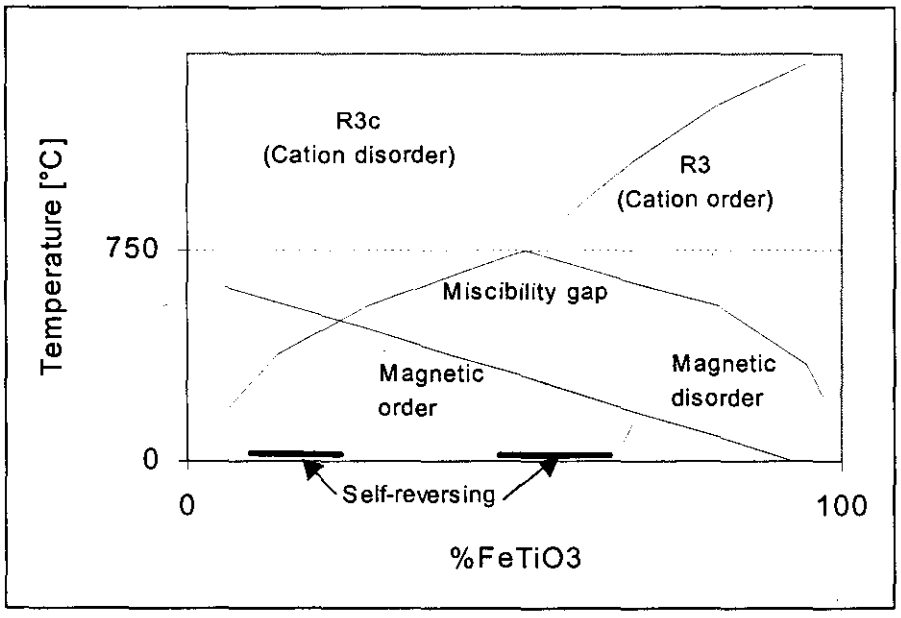


**Figure 2.19: Schematic ilmenite-hematite binary phase diagram indicating the R-3c to R-3 cation order-disorder transition, the magnetic order-disorder i.e. the Curie points and the fact that solid solutions in this range are self reversing (Nord et al. 1989).**

From this discussion it is concluded that to enhance the magnetic properties of ilmenite ($FeTiO_3$):

- A solid solution of ilmenite and hematite with a minimum of 15 per cent $Fe_2O_3$ is required, i.e. $x < 0.85$ for $xFeTiO_3(1\text{-}x)Fe_2O_3$ (Bozorth et al, 1957);
- Depending on the cooling rate the maximum amount of $Fe_2O_3$ in solid solution should be between 40 and 60 per cent, i.e. $x > 0.4$ to 0.6 for $xFeTiO_3(1\text{-}x)Fe_2O_3$, based on results reported by Bozorth et al (1957) and Nell & Den Hoed (1997);

- The crystal structure of the solid solution should be ordered (R-3) – in this instance limiting the maximum amount of $Fe_2O_3$ in solid solution to either 30 per cent (Nord, 1989) or 50 per cent (Nell & Den Hoed, 1997), i.e. $x = 0.7$ or $0.5$ for $x < 0.85$ for $xFeTiO_3(1-x)Fe_2O_3$;
- The solid solution should be below its Curie point to ensure magnetic order. This will be an issue if the Curie point of the solid solution is below operating (room) temperatures.

## *2.10 Definition of roasting*

### 2.10.1 Roasting in a reducing atmosphere

Walpole (1991) concluded from literature that in ilmenite the maximum magnetic enhancement is achieved when the mole ratio $Fe^{3+}$:$Fe^{2+}$ is within the range 1:1 - 1.57:1. This is for ferrian ilmenites with $0.56 < x < 0.67$ for $xFeTiO_3(1-x)Fe_2O_3$. For ilmenite with a low $Fe^{3+}$:$Fe^{2+}$ ratio oxidising conditions would be required to increase the percentage $Fe^{3+}$ in the solid solution and for ilmenite with a high $Fe^{3+}$:$Fe^{2+}$ ratio, reducing conditions to decrease the percentage $Fe^{3+}$ in solid solution. He claimed that his process of roasting, at 650-900°C for 30-90 minutes using excess carbon, stabilizes the roasting reaction in the zone where $Fe^{3+}$:$Fe^{2+}$ is within the range 1:1 - 1.57:1. This will be true if:

- The carbon defines the $pO_2$ in the atmosphere;
- The defined atmosphere is the equilibrium atmosphere for reaction 2.1 with 33-44 mole% $Fe_2O_3$; in solid solution and
- The following reactions are possible and at equilibrium:

a) $C + \frac{1}{2}O_2 = CO$ (controlling the $pO_2$ in the atmosphere)
b) $FeTiO_3 + O_2 = Fe_2O_3 + TiO_2$ (Oxidising reaction)
c) $Fe_2O_3 + TiO_2 + CO = FeTiO_3 + CO_2$ (Reducing reaction)

**Reaction 2.1: The reactions taking place during ilmenite roasting from Walpole (1991)**

(Refer to Appendix 1 at the end of this chapter for details on the calculations stated above).

Nell and Den Hoed (1997) also conducted their study on an ilmenite concentrate from Kwazulu-Natal and reported success when roasting at equilibrium conditions i.e. applying the equilibrium $pO_2$ at a specific temperature for as long as it requires to reach equilibrium. At 800°C the calculated $pO_2$ was $10^{-12}$ bar. The rate of oxidation is very low, though. More than 3 hours were needed at 800°C in 100 per cent $CO_2$ (measured $pO_2$ was $10^{-5}$ bar) to increase the magnetic susceptibility 5-fold. The sample composition was $(FeTiO_3)_{0.6}(Fe_2O_3)_{0.4}$.

Guzman, Taylor and Giroux (1992) patented a reductive roasting process in which magnetic susceptibility is enhanced by roasting at 400-700°C for 8-60 minutes in $CO_2$ or CO and $H_2$ gas mixtures. They claimed that the process is especially suitable for ilmenite that have a high $Fe_2O_3$:FeO ratio. They claimed that a possible explanation for the increase in magnetic susceptibility is the formation of highly magnetic magnetite, i.e. $FeO.Fe_2O_3$, in or on the ilmenite grains.

### 2.10.2 Roasting in a neutral atmosphere

Grey and Li (2001) reported that some ilmenite concentrates showed a large increase in magnetic susceptibility when roasted in a neutral atmosphere at temperatures higher than 600°C. This was true for altered ilmenite sand concentrates where $Fe^{2+}$-containing pseudorutile ($Fe_2Ti_3O_9$) was distributed uniformly as a major alteration phase in the ilmenite particle. Grey and Li (2001) postulated that the ferrous pseudorutile contained nanometer scale regions of disordered ilmenite-type structures, which could be transformed at low energy inputs to strongly magnetic ferrian ilmenite (ilmenite containing $Fe_2O_3$ in solid solution).

### 2.10.3 Roasting in an oxidative atmosphere

The roasting conditions of the process patented by Bergeron and Prest (1974) was for ilmenite concentrate from Kwazulu-Natal. Their feed material contained 47.5 per cent $TiO_2$, 36.5 per cent Fe and 0.4 per cent $Cr_2O_3$. They claimed to decrease the $Cr_2O_3$ content from 0.4 to 0.1 per cent at a mass recovery of 80 per cent. Their roasting process took place at 690-810°C for 10-45 minutes in the presence of 1-6 percent of excess oxygen over the stoichiometric amount of fuel required. The

preferable roasting conditions were at 750°C for 15 minutes in the presence of 3 per cent excess oxygen, (as mentioned in chapter 1, paragraph 1.2).

Nell and Den Hoed (1997) also conducted their study on an ilmenite concentrate from Kwazulu-Natal and reported excellent results when applying roasting conditions with excess oxygen and terminating roasting before the ilmenite reaches the equilibrium phase composition. In less than 2 hours even at temperatures as low as 700°C the magnetic susceptibility of the ilmenite increased 5- to 6-fold. They also observed a drop in magnetic susceptibility at extended reaction times (i.e. longer than 30 minutes at 800°C). They stated that the rate of oxidation seemed to be more influenced by temperature than by the gas composition in gas mixtures containing more than 1 per cent excess oxygen. As the present study is about oxidative ilmenite roasting I wanted to investigate it further.

## *2.11 Phase chemical changes during oxidative roasting*

### 2.11.1 Phase diagrams

During the oxidation of ilmenite oxygen atoms are added to the material – refer to reaction 2.1 (Van Dyk 1999). The ratio of titanium and iron remains constant. For theoretical ilmenite this is $N_{Ti}/(N_{Ti} + N_{Fe}) = 0.5$. This is represented schematically in figure 2.20. It is assumed that the ideal roasting conditions for ilmenite concentrate from Kwazulu-Natal is 750°C for 15 minutes in the presence of 3 per cent excess oxygen (Bergeron and Prest, 1974) or within a range of 700°C to 800°C with more than 1 per cent oxygen for 30 minutes or less (Nell and Den Hoed 1997). From the Fe-$Fe_2O_3$-$TiO_2$ phase diagrams at 700 & 800°C some conclusions on oxidative ilmenite roasting can be made. These diagrams were constructed from laboratory equilibrium test work. It is important to note that the conditions applied during laboratory scale and full-scale ilmenite roasting are such that equilibrium conditions are not reached. Thermodynamic information on a phase diagram is for equilibrium conditions. Therefore, only an indication of what could happen during ilmenite roasting is obtained from them. From these figures it is concluded that Fe2O3 solid solution in ilmenite is only feasible up to 15-16% $Fe_2O_3$. This narrows the range for magnetic enhancement down from the range of $Fe_2O_3$ solid solutions stated by Nell and Den Hoed (1997) and Nord et al (1989) quoted in paragraph 2.3.10.4.

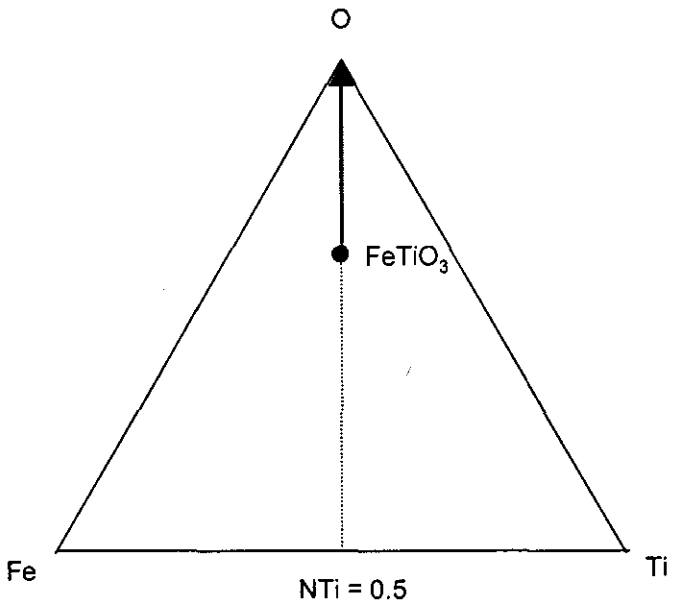


**Figure 2.20: Schematic Fe-O-Ti phase diagram indicating the oxidation of ilmenite (mole percentage).**

### 2.11.2 700°C

From the phase diagram at 700°C of Borowiec et al (1981) ilmenite ($FeTiO_3$) will change as follows during oxidation (figure 2.21):

1. TO a mixture containing rutile/anatase ($TiO_2$) and ilmenite-hematite solid solution ($M_2O_3$ - with increasing $Fe_2O_3$ content with increasing oxidation);

2. THEN a mixture containing rutile/anatase ($TiO_2$), magnetite-$Fe_2TiO_4$ solid solution ($M_3O_4$) and ilmenite-hematite solid solution ($M_2O_3$);
3. THEN a mixture containing rutile/anatase ($TiO_2$) and pseudobrookite solid solution ($FeTi_2O_5$-$Fe_2TiO_5$ - with increasing $Fe_2TiO_5$ content with increasing oxidation).

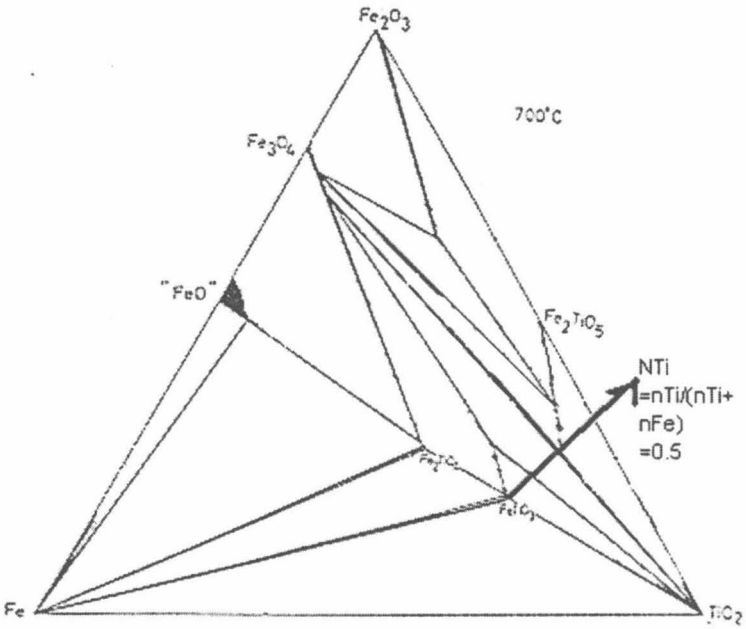


**Figure 2.21: Fe-$Fe_2O_3$-$TiO_2$ phase diagram at 700°C with components in mole percentages (Borowiec et al 1981). The arrow indicates the path followed during oxidation of $FeTiO_3$.**

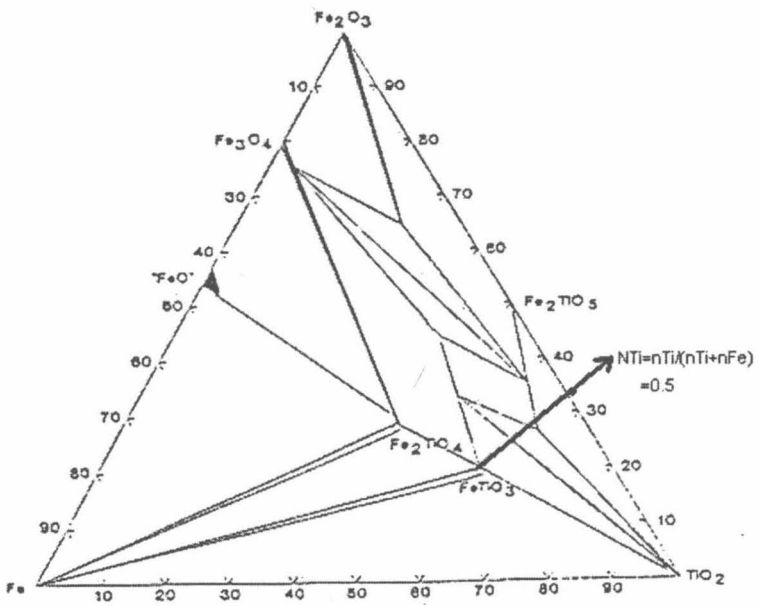


**Figure 2.22: Fe-$Fe_2O_3$-$TiO_2$ phase diagram at 700°C with components in mole percentages (Gupta et al 1989). The arrow indicates the path followed during oxidation of $FeTiO_3$.**

Gupta et al (1989) reviewed the phase diagrams proposed by Borowiec et al (1981). Their experiments confirmed the diagrams at 950°C, but differed considerably at 700°C. From their phase diagram at 700°C ilmenite ($FeTiO_3$) will change (figure 2.22):

4. TO a mixture containing rutile/anatase ($TiO_2$) and ilmenite-hematite solid solution ($M_2O_3$ - with increasing $Fe_2O_3$ content with increasing oxidation);

5. THEN a mixture containing rutile/anatase ($TiO_2$), pseudobrookite solid solution ($M_3O_5$ ) and ilmenite-hematite solid solution ($M_2O_3$ - fixed at $[Fe_2O_3]_{0.16}[FeTiO_3]_{0.84}$);
6. THEN a mixture containing ilmenite-hematite solid solution ($M_2O_3$ - with increasing $Fe_2O_3$ content with increasing oxidation) and pseudobrookite solid solution ($FeTi_2O_5$-$Fe_2TiO_5$ - with increasing $Fe_2TiO_5$ content with increasing oxidation) and;
7. THEN a mixture containing rutile/anatase ($TiO_2$) and pseudobrookite solid solution ($FeTi_2O_5$-$Fe_2TiO_5$ - with increasing $Fe_2TiO_5$ content with increasing oxidation).

### 2.11.3 800°C

Van Dyk (1999 p 77) described what happens at 800°C under equilibrium conditions (from Borowiec et al 1981). Material, with a phase composition close to theoretical ilmenite ($FeTiO_3$), will change during oxidation (figure 2.23):

1. TO a mixture containing rutile/anatase ($TiO_2$) and ilmenite-hematite solid solution ($M_2O_3$ - with increasing $Fe_2O_3$ content with increasing oxidation);
2. THEN a mixture containing rutile/anatase ($TiO_2$), pseudobrookite solid solution ($M_3O_5$ fixed at $[FeTi_2O_5]_x[Fe_2TiO_5]_y$) and ilmenite-hematite solid solution ($M_2O_3$ - fixed at $[Fe_2O_3]_{0.15}[FeTiO_3]_{0.85}$) and;
3. THEN a mixture containing rutile/anatase ($TiO_2$) and pseudobrookite solid solution ($FeTi_2O_5$-$Fe_2TiO_5$ - with increasing $Fe_2TiO_5$ content with increasing oxidation).
4. Evidently, full oxidation of ilmenite will eliminate the hematite-ilmenite solid solution with enhanced magnetic susceptibility. In the next section the equilibrium conditions for this solid solution are estimated.

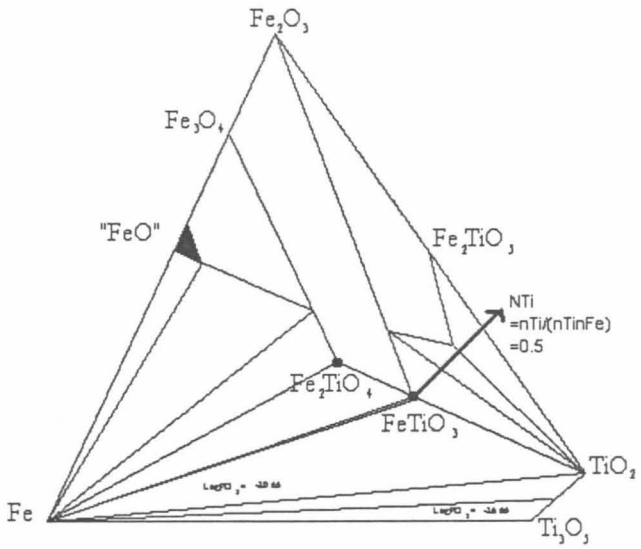


**Figure 2.23: Fe-$Fe_2O_3$-$TiO_2$ phase diagram at 800° with components as mole percentages (Van Dyk 1999, from Borowiec 1981). The arrow indicates the path followed during oxidation of $FeTiO_3$.**

### 2.11.4 The effect of $pO_2$ and temperature

The chemical reaction for the oxidation of ilmenite in the $TiO_2$–$M_2O_3$ phase field is given as reaction 2-1. With this reaction one can estimate the equilibrium roasting conditions (temperature and $pO_2$) to obtain 20 to 33 per cent ferric iron ($Fe^{3+}$) in solid solution in ilmenite. This, as well as the temperature at which the ilmenite is cooled, will result in an ordered R-3-crystal structure (Nell 1999).

When determining the relationship between $pO_2$ and $Fe_2O_3$ at a specific temperatures under equilibrium conditions, the following assumptions are made (Nell, 1999):

1. $a_{TiO2}^{Rutile} = 1$, because rutile is virtually pure $TiO_2$.
2. $X_{Fe2O3}^{ilmenite} + X_{FeTiO3}^{ilmenite} = 1$
3. $\gamma_{FeTiO3}^{ilmenite} = (\gamma_{Fe2O3}^{ilmenite})^{0.5}$ (assumed in the absence of equilibrium data)

The symbols used for the mole fractions and Raoultian activity coefficients are:

- $X_x^y$ = mol fraction x in y
- $\gamma_x^y$ = activity coefficient of x in y

The resulting relationship is:
$K = e^{-\Delta G^\circ/RT} = (X_{Fe2O3})^{0.5}/((1-X_{Fe2O3})(P_{O2})^{0.25})$

The results at various temperatures are given in the figure 2.24 (thermodynamic data from Kubaschewski et al, 1988-1994).

From the 800°C phase diagram the maximum amount of $Fe_2O_3$, which can go into solid solution in $FeTiO_3$, is 15-16 per cent. From figure 25 the associated $pO_2$ is $10^{-12.2}$ atm at 800°C. Borowiec et al (1981) did EMF measurements to determine the oxygen potential for all phase combinations, as a function of temperature. This was for the Fe- $Fe_2O_3$-$TiO_2$ system. The $pO_2$ value that they obtained for $M_2O_3$-$M_3O_5$-$TiO_2$ equilibrium above 780°C is $10^{-11.5}$atm.

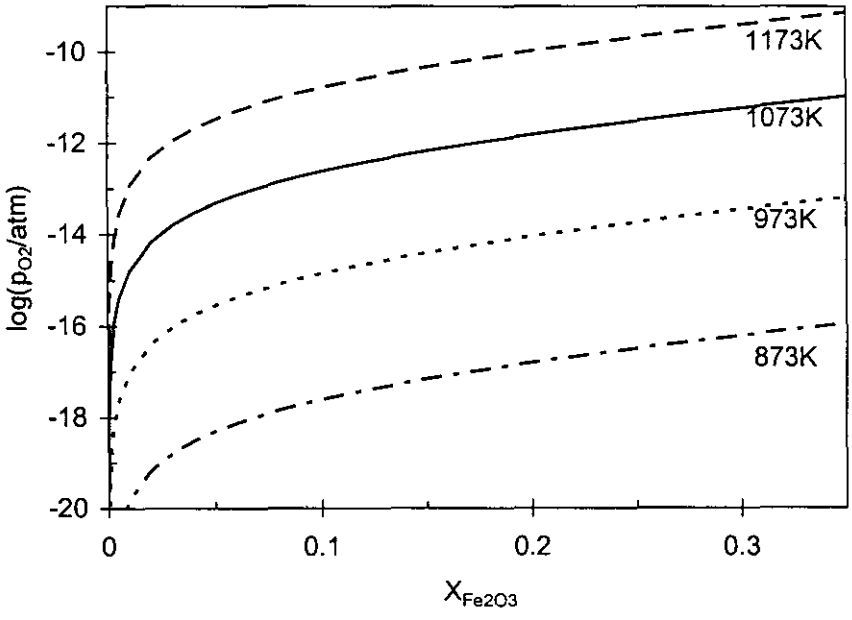


**Figure 2.24: Equilibrium oxygen potential as a function of the percentage hematite in solid solution in ilmenite, at various temperatures. Calculated from thermodynamic data from Kubaschewski et al (1988-1994).**

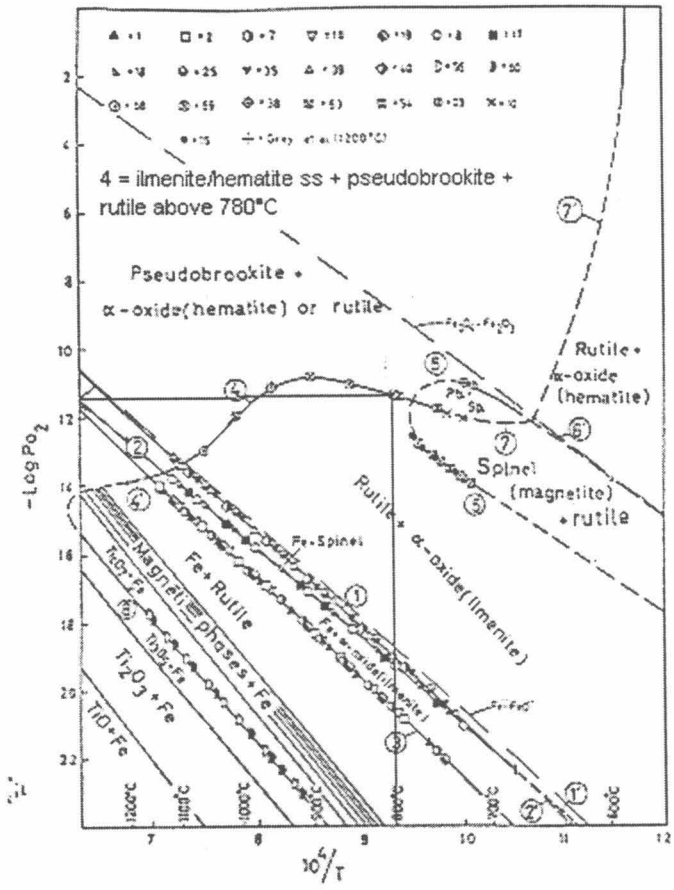


**Figure 2.25: Oxygen potential for various phase combinations as a function of temperature, determined from regressional analysis of EMF measurements (Borowiec et al, 1981).**

This result correlates fairly well with the results generated from thermodynamic data. It also indicates that at equilibrium conditions the roasting atmosphere need not be very oxidizing to obtain ilmenite with 15 to 16 per cent $Fe_2O_3$ in solution – figure 2.25.

## *2.12 Equipment*

### 2.12.1 Laboratory scale equipment

It is concluded from the discussion above that to decrease the $Cr_2O_3$ content of a crude ilmenite concentrate from 0.3 per cent to 0.1 per cent the following approach was used:

- Authors such as Nell and Den Hoed (1997) exploited the magnetic susceptibility property of both ilmenite and $Cr_2O_3$ containing spinels;
- They constructed a separability curve for an unroasted concentrate by dividing the concentrate into 10 fractions by adjusting the current settings on a Frantz isodynamic magnetic separator and subjecting each fraction to chemical analysis;
- They roasted samples of crude ilmenite at various roasting conditions and measured the magnetic susceptibility of the roasted material using an inductivity bridge using an alternating current technique;
- They constructed a separability curve for a roasted sample in a fashion similar to that for an unroasted sample.

Therefore the laboratory scale equipment they required were:

- Batch roasting equipment;
- A magnetic separator.

*a) Laboratory scale magnetic separators*

On laboratory scale equipment Kelly & Spottiswood (1995) mentioned that a Frantz isodynamic separator could be used to construct separability curves based on magnetic susceptibility properties of minerals. Nell and Den Hoed (1997) indeed reported the use thereof in their test work. A Frantz isodynamic separator was also the type of separator used in the present study due its availability at Kumba R&D, where the test work were conducted, and the minimization of forces (other than magnetic forces) applied to a particle in a Frantz separator. The competing forces on particles in any magnetic separator are (Kelly and Spottiswood 1995) gravity, hydrodynamic drag, friction, inertia and centrifugal – in rotating drum separators. When using a Frantz isodynamic magnetic separator to construct separability curves:

- Hydrodynamic drag is negligible because material is tested dry;
- The effect of friction and inertia is minimized because the separator surface is made of polished steel, installed at a slight angle and vibrated;
- No centrifugal forces are present because a rotating drum is not used.

The only forces of importance acting on a particle in a Frantz isodynamic separator are therefore that caused by the applied magnetic field (H) and gravity. If the material is tested dry the magnitude of the gravitational force remains constant.

The Frantz isodynamic separator utilizes specially shaped pole-pieces to produce a force that is almost independent of the distance in a region between pole-pieces. A narrow chute is placed between the pole-pieces and the material to be separated passes down the inclined chute under the influence of gravity. The chute is inclined both parallel and perpendicular to its length so that a component of gravitational force may compete with the magnetic force. Under the influence of gravitational and magnetic forces the grains migrate to one side or the other of the chute, which at one part is divided into two passages by a splitting ridge, which directs the products into two separate containers – figure 2.26 (Svoboda 1987).

Inclination of the chute is measured by the transverse slope $\theta$ and the longitudinal slope $\varphi$. The pole design is such that changes in the magnetic field exactly balance changes in the field gradient to yield a constant product HdH/dx. In figure 2.26 particles enter the chute at point A. For a paramagnetic particle if the gravity (Fg) and the magnetic (Fm) forces are balanced to cause the paramagnetic particle to move along AB, the particle has a 50 per cent chance of reporting to the magnetic or non-magnetic fraction. The force balance is stated in equation 2.8.

$$Fg = Fm$$

Or

$$mg\sin\theta = \tfrac{1}{2}\mu_0 \kappa V(H)^2$$

**Equation 2.8: The force balance in a Frantz magnetic separator with m the particle mass, $\theta$ the transverse slope, g the gravitational constant, $\kappa$ the volume magnetic susceptibility and H the magnetic field strength (Svoboda 1987)**

When rewriting equation 2.8 as in equation 2.9, with HdH/dx constant due to the pole design, the action of the separator on a single particle is determined solely by the mass susceptibility of the particle and not on the size or mass of the particle.

$$\sin\theta = \mu_0 \chi H/g.\delta H/\delta x$$

**Equation 2.9: Rearranging equation 2.8 with $\chi$ the mass or specific magnetic susceptibility (Svoboda 1987)**

By calibrating the Frantz separator with chemical compounds with a known magnetic susceptibility, the Frantz can be used to determine the mass susceptibility of specific material fractions – for more details on this method refer to Svoboda (1987).

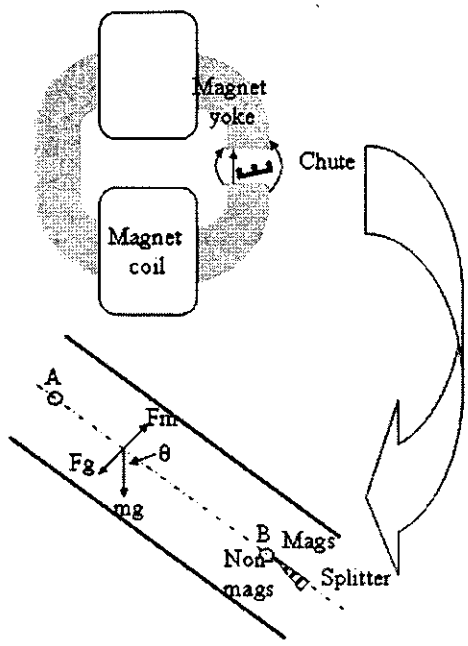


**Figure 2.26: Schematic drawing of the Frantz isodynamic separator and the forces acting on a particle in the separator (Svoboda 1987).**

Other magnetic separation equipment available on a laboratory scale, but which were not used in this study, include:

- Carpco induced roll magnet;
- Carpco permanent magnet ;
- Davis tube (Svoboda 1987) ;
- Laboratory high-gradient magnetic separators (Svoboda 1987).

*b) Laboratory scale roasting equipment*

Equipment available for batch roasting include:

- Muffle furnaces;
- Rotating reactors; and
- Fluidised bed reactors.

As I wanted to compare the results of my study to results published in literature (Bergeron and Prest 1974; Nell and Den Hoed 1997), and because of its availability at KUMBA R&D, I decided to utilise a batch fluidised bed reactor.

### 2.12.2 Full scale magnetic separators

This study does not include a study of the commercially available magnetic separators. What needs to be mentioned here is that two categories of commercially available magnetic separators exist (Kelly and Spottiswood 1995):

- *Low intensity* magnetic separators to be used for the separation of ferromagnetic and paramagnetic minerals with high magnetic susceptibility, from minerals with lower magnetic susceptibilities; and
- *High intensity* magnetic separators to be used for the separation of paramagnetic minerals with lower magnetic susceptibility, from minerals with lower magnetic susceptibilities.

Separation on both low and high intensity machines can be carried out wet or dry. Authors that published papers on the application of various types of magnetic separators include Hopstock (1975), Erasmus (1997), Balderson (1999), Arvidson and Rademeyer (1997), Van der Westhuisen (2001) and Arvidson (2001) to mention but a few.

### 2.12.3 Full scale roasting equipment

Equipment used for full-scale continuous roasting includes rotary kilns and fluidized bed reactors.

## *2.13 Findings and conclusions*

From this discussion it becomes clear that naturally occurring ilmenite concentrates from South African East Coast deposits contain as much as 0.3 per cent $Cr_2O_3$ which has to be upgraded to produce smelter grade ilmenite with less than 0.1 per cent $Cr_2O_3$. If the ilmenite and chromite particles are discrete particles as expected, i.e. no intergrowth between the ilmenite and chromite, the property exploited to achieve this is the difference in magnetic susceptibility of ilmenite and chromite containing minerals. Pure ilmenite is antiferromagnetic, i.e. has a low magnetic susceptibility, but the magnetic susceptibility thereof can be enhanced by obtaining $Fe_2O_3$ in solid solution and ordering the crystal structure of the solid solution. To ensure that this condition is met the $Fe_2O_3$ in solid solution should be controlled between 15 per cent and 30 per cent and the material should be slow cooled after roasting. Depending on the state of oxidation of the naturally occurring ilmenite, enhancement of magnetic susceptibility can be obtained by roasting in reducing, in oxidizing or in neutral atmospheres. Roasting conditions to enhance the magnetic susceptibility of ilmenite in South African East Coast deposits are oxidizing roasting conditions. Likewise I expected the magnetic susceptibility of chromite to increase should the $Fe_2O_3$ content thereof increase. To be able to test the hypotheses I decided to follow a similar test procedure as published by Nell and Den Hoed (1997) and to conduct my roasting tests in conductions published by Bergeron and Prest (1974).

In short: the aim of chapter 2 was to review the current body of knowledge available on ilmenite roasting. The review was organized according to:

- The application of magnetic separation to beneficiate chromite containing ilmenite concentrates in industry;
- Magnetism and the mechanism of changes in magnetic susceptibility of ilmenite;
- The enhancement of the magnetic susceptibility of ilmenite by roasting in various atmospheres, with special emphasis on oxidative roasting; and
- Equipment used in ilmenite roasting and magnetic separation.

I concluded the chapter with a discussion on how I derived my test program from this scholarship review. In chapter 3 this test programme is discussed in more detail.

## *2.14 Appendix 1: Calculation of the chemical composition of roasted ilmenite based on the findings of Walpole (1991)*

From $xFeTiO_3.(1-x)Fe_2O_3$ and $Fe^{3+}$:$Fe^{2+}$ 1:1 to 1.57:1 (Walpole 1991)

For $Fe^{3+}$:$Fe^{2+}$ 1:1:
$Fe^{3+}/Fe^{2+} = 2(1-x)/x = (2-2x)x = 1$
Therefore:
$2-2x = x$
$2 = 3x$
$x = 2/3 = 0.67$.....(1)

For $Fe^{3+}$:$Fe^{2+}$ 1.57:1:
$Fe^{3+}/Fe^{2+} = 2(1-x)/x = (2-2x)x = 1.57$
Therefore:
$2-2x = 1.57x$
$2 = 3.57x$
$x = 2/3.57 = 0.56$.....(2)

To calculate the mole per cent $Fe_2O_3$ in (1): $0.67FeTiO_3.(0.33)\ Fe_2O_3$
Mole per cent $Fe_2O_3 = 0.33/(0.67+0.33)*100 = 33\%$

To calculate the mole per cent $Fe_2O_3$ in (2): $0.56FeTiO_3.(0.44)\ Fe_2O_3$
Mole per cent $Fe_2O_3 = 0.44/(0.56+0.44)*100 = 44\%$

## Chapter 3: Research design & methodology

In chapter 2 I reviewed the current body of knowledge on ilmenite roasting and concluded the chapter with a discussion on how I derived my test program from this scholarship review. In chapter 3 I discuss the design and methodology of this test program in more detail by first identifying the key concepts and variables, then stating how these key variables were measured. Sample preparation and data collection are discussed. The chapter concludes with statements on data capturing methods. Tasks in chapter 3 were as follows:

3.1 Formulate hypotheses and overall experimental plan
3.2 Source and prepare crude ilmenite and LSR
3.3 Characterize crude ilmenite, LSR and chromite in LSR
3.4 Determine optimum roasting conditions for LSR and compare with crude ilmenite
3.5 Prepare fractionation curves for crude ilmenite and LSR before and after roasting at optimum roasting conditions
3.6 Source and prepare chromite
3.7 Characterize chromite
3.8 Data capturing

### *3.1 Formulation of hypotheses and overall experimental plan*

In chapter 2 I decided to test the following hypotheses based on the current body of knowledge on ilmenite roasting for chromite removal:

"It is possible to produce an ilmenite product suitable for ilmenite smelting by subjecting LSR to roasting and subsequent magnetic separation, using the roasting conditions recommended for crude ilmenite by Nell and Den Hoed (1997) or Bergeron and Prest (1974)"

and

"The magnetic susceptibility of chromite remains constant during magnetizing roasting of an ilmenite concentrate under the oxidizing conditions reported by Nell and Den Hoed (1997)."

To test the first hypothesis the key concepts are that once a sample of the LSR[5] described by Beukes and Van Niekerk (1999) was prepared this sample would have to be characterized and the results compared with that of the material described in literature. I would then determine the optimum roasting conditions for the LSR by conducting small-scale batch tests under conditions similar to those published by Nell and Den Hoed (1997) and Bergeron and Prest (1974). 'Optimum roasting conditions' were defined as the conditions where the maximum increase in magnetic susceptibility occurs in the roasted sample. Once the optimum roasting conditions have been determined a larger sample would be roasted at these conditions and a separability curve constructed to determine to which extent the separation of ilmenite from chromite would be possible. These results would also be compared with those published in literature for Southern African East Coast Deposits.

To test the second hypothesis the key concepts are to determine the chemical composition of the chromite in the LSR in order to be able to source a natural chromite with a similar composition. Then the sourced chromite would have to be prepared, characterized, roasted under the conditions used for the LSR, and fractionated at unroasted and optimum roasting condition.

From the literature survey in chapter 2 the key variables in the study were the oxidizing roasting conditions - temperature and $pO_2$ of the roasting atmosphere - and the resultant change in the magnetic susceptibility of the ilmenite, due to crystal chemical changes in the ilmenite particles themselves. To characterize the LSR before, and in some cases after, roasting:

- The chemical composition of the LSR was important because the client specified the chemical composition for the final product.
- The mineralogical composition of the LSR was important to determine what mineral components were included in the LSR and how these components would influence the roasting or magnetic separation process.

[5] Low susceptibility rejects

- The crystal chemical composition of the ilmenite in the LSR was important because it would influence the choice of $pO_2$ of the roasting atmosphere.

For the chromite only the chemical composition was determined.

To measure and/or control the key variables a test program was developed that consisted of the major steps defined in figure 3.1.

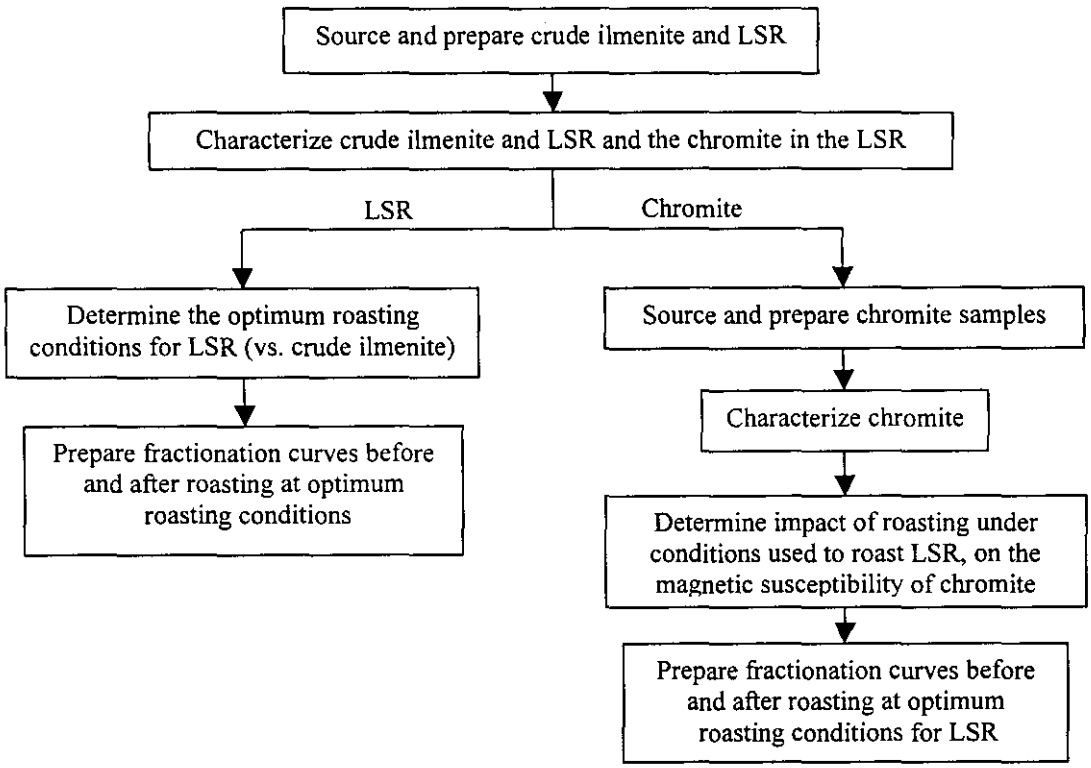


**Figure 3.1: Overall experimental plan for this study.**

Firstly gross samples of crude ilmenite and LSR were prepared. Then these gross samples were characterized. The optimum oxidizing roasting conditions for LSR were determined and lastly larger samples of LSR and crude ilmenite were roasted at the optimum roasting conditions to compare their results with each other. The chromite in the LSR was characterized and then the natural chromite sample sourced, prepared and characterized. Then the impact of roasting on the magnetic susceptibility of the chromite, when roasted under the conditions used for LSR, was determined. Lastly fractionation curves were prepared for both unroasted and roasted chromite primarily to determine whether or not the bimodality in the chromite observed in crude ilmenite was also observed in this chromite sample.

Details of these major steps follow in the rest of this chapter.

All test work were conducted at Kumba R&D in Pretoria West, South Africa except for magnetic susceptibility measurements, QEMSEM and QEMscan, some of the WHIMS test work and preparation of the natural chromite sample. Magnetic susceptibility measurements were conducted at Geotron in Potchefstroom, QEMSEM and QEMscan at Mintek in Randburg, WHIMS tests at Readings, Australia and chromite sample preparation at the University of Pretoria.

## *3.2 Sourcing and preparation of crude ilmenite and LSR*

Heavy Minerals Concentrate (HMC) for the determination of optimum roasting conditions for LSR was produced during a pilot plant trial in South Africa on a typical Southern African East Coast Heavy Minerals Deposit. Crude ilmenite was produced in Australia from the HMC with WHIMS machines[6].

[6] Details of settings not available

Back in South Africa a 380-mm diameter commercially available full-scale DMDS was used to remove HSR at 2600 Gauss. The feed rate was 4.5 tons per hour per meter (tph/m) and the rotation speed 65 rpm for the first pass and 55 rpm for the second and third. A 610-mm diameter commercially available full-scale DMDS was used to remove LSR at 6500 Gauss. The feed rate was 8.85 tph/m and the rotation speed 70 rpm for the first pass and 85 rpm for the second. All three fractions were riffled to produce two representative samples each. All of this work was conducted by others for detail flow sheet design (not part of the scope of this thesis). After the abovementioned test work the crude ilmenite was reconstituted for *this* study by blending the one product and one LSR fraction in the ratios that they were produced. Both the crude ilmenite and the LSR samples were then split with a rotary splitter into representative 40g samples. Preparation of these samples is illustrated in figure 3.2.

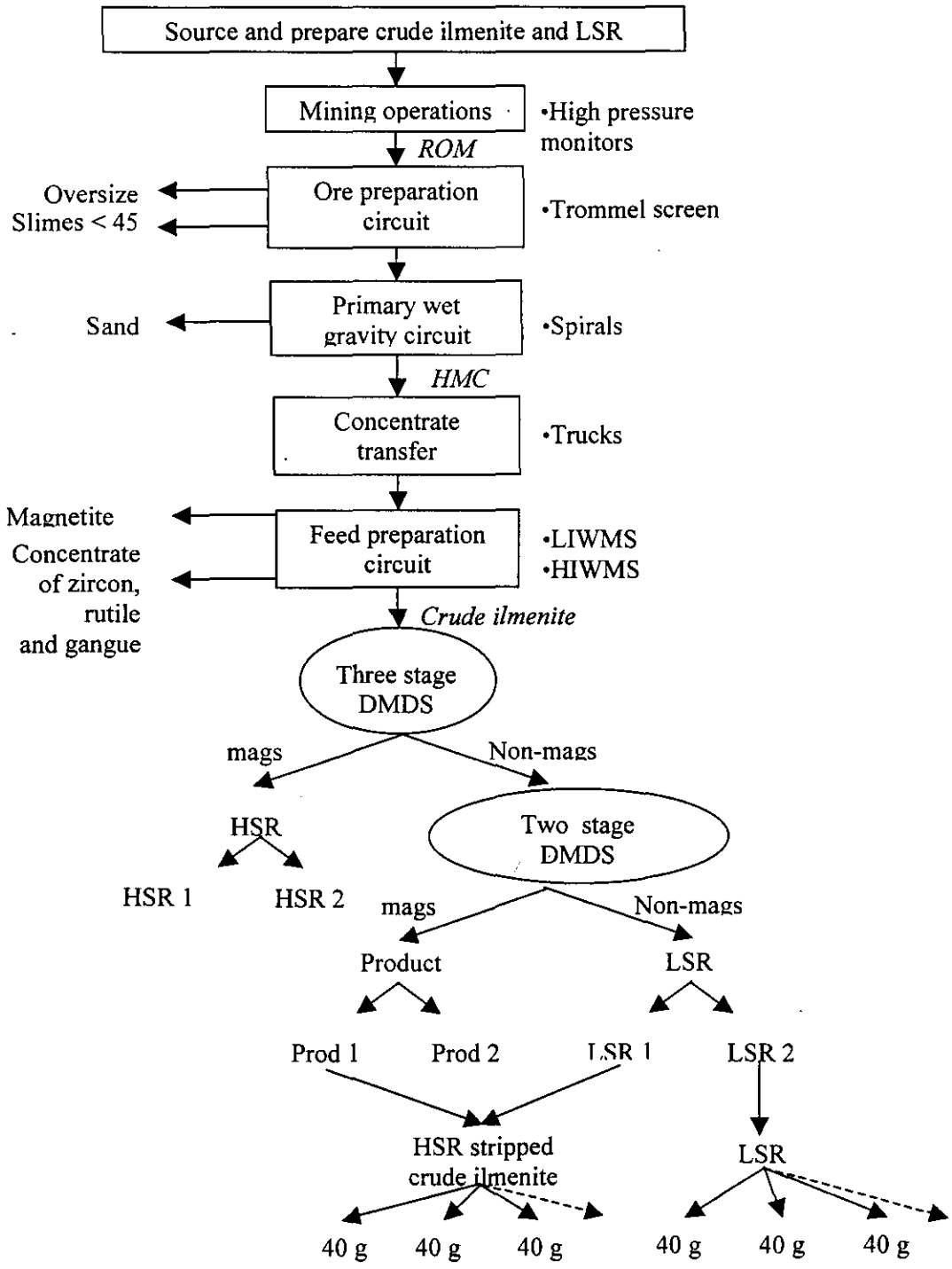


**Figure 3.2: Flow sheet for the sourcing and preparation of crude ilmenite and LSR for this study.**

One of the difficulties experienced at the stage was to obtain suitable samples to conduct the roasting tests on. The size of the 40g samples was therefore determined by the amount of material available on the one hand, and the minimum size sample that can be roasted in the batch fluidized bed reactor (in which these studies were to be conducted) on the other.

HMC for fractionation after optimum roasting was produced during another pilot plant trial on a typical Southern African East Coast Heavy Minerals Deposit. The crude ilmenite was prepared on commercially available full-scale WHIMS[7] equipment. The LSR was prepared in a similar fashion as described above, with 250-g samples instead of 40-g samples as final result. Although the samples used in the fractionation at optimum roasting conditions were prepared according to the same flow sheet as the material used in the tests to determine the optimum roasting conditions, the results of the two types of experiments were not directly comparable. The reasons are that the locations within the heavy minerals deposit, from which these samples were prepared, differed, as did the WHIMS equipment used.

Personnel from a heavy minerals producer on the Southern African East Coast prepared the two HMC concentrates, one in 1995 and the other in 1999. All the sample preparation work to determine the optimum roasting conditions, from receiving the HMC onwards, was conducted by research personnel at the pilot plant of ISCOR R&D[8] in Pretoria West in 1999. Sample masses were determined with laboratory type scales and recorded manually onto a log sheet.

Crude ilmenite, to fractionate after roasting at optimum roasting conditions, was produced by personnel from a heavy minerals producer on the Southern African East Coast at Readings in Australia in 2000. The rest of the sample preparation work, from receiving the crude ilmenite onwards, was conducted by research personnel at the pilot plant of ISCOR R&D[9] in Pretoria West in 2001.

### *3.3 Characterization of crude ilmenite, LSR and chromite in LSR*

The following chemical analyses were conducted on crude ilmenite and LSR:

- XRF-analysis with an ARL9400 sequential XRF analyzer to determine the chemical composition *quantitatively* - refer to figure 3.3;
- Titration to determine the $Fe^{2+}$ and $Fe^{3+}$ content *quantitatively*.

The following chemical analyses were conducted on the chromite in the LSR:

- Energy dispersive X-ray analyses (EDX) with a JEOL Low Vacuum 58100 Scanning Electron Microscope.
- Wavelength dispersive spectrometry (WDS) with a JEOL super probe 733.

The following mineralogical analyses were conducted on crude ilmenite and LSR:

- XRD to determine the mineralogical composition *qualitatively*;
- Reflected light microscopy to describe mineralogical properties of the samples with special reference to textural and weathering properties of the ilmenite *qualitatively*;
- Micro-analyses to investigate the chemical composition of unaltered mineral grains and alteration products *qualitatively*;
- Particle counting (using optical microscope images) to determine the textural properties of the minerals *semi-quantitatively*.
- QEMSEM, using a Leica Q 600 image analyser (IA) integrated with a LEO S440 scanning-electron microscope (SEM) and an ISIS energy-dispersive X-ray analysis system (EDX), to determine the modal[10] composition of each sample *qualitatively*.
- QEMscan, using a Leica Q 600 image analyser (IA) integrated with a LEO S440 scanning-electron microscope (SEM) and an ISIS energy-dispersive X-ray analysis system (EDX), to determine the degree of liberation in which iron oxides occur in the samples *qualitatively*.

[7] Details of settings not available
[8] Also referred to as ITEC or Kumba Technology
[9] Also referred to as ITEC or Kumba Technology
[10] Composition of a rock or mineral stream in terms of the relative amounts of minerals present

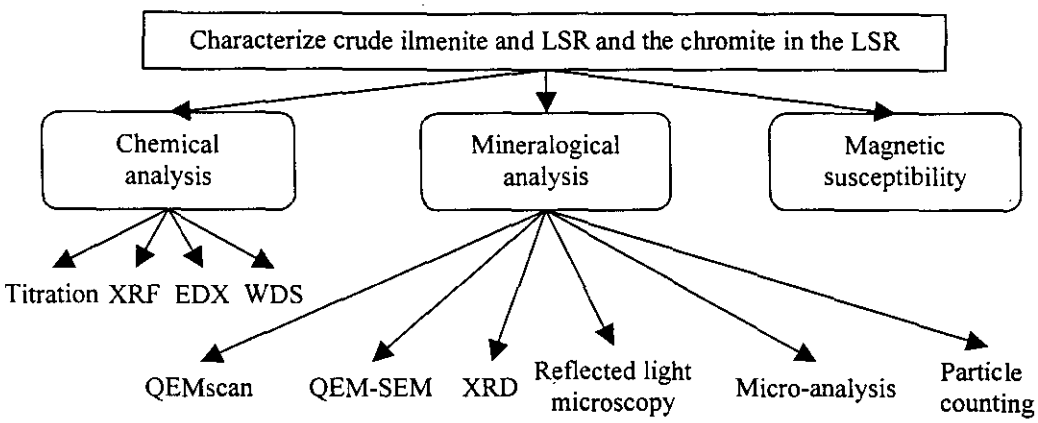


**Figure 3.3: Flow sheet for the characterization of crude ilmenite and LSR for this study.**

When conducting QEMSEM analysis on mineral samples these samples were divided into size fractions to minimize segregation during preparation and to improve mixing with the graphite matrix. Size fractions for screening were selected on the basis of the particle size distribution of the sample. 106 microns would be typical for beach sands, which have a very narrow particle size distribution between about 75 microns and 300 microns (Nell 2002). The as received samples of crude ilmenite and LSR were screened into two size fractions: +106μm and -106μm. Polished sections of each sample were prepared. Over four thousand grains in each sample - 2000 per size fraction - were classified according to their mineral composition. Their mineral composition was based on their chemical composition determined during QEMSEM analysis by raw EDX counts. The definitions used for each phase were indicated in table 3.1. Research personnel at Mintek in Randburg conducted the QEMSEM analysis in 1999.

**Table 3.1: Definitions used to classify different grains as different minerals based on the occurrence of elements in raw EDX counts, or QEMscan* results, on a polished sample of crude ilmenite or LSR.**

| Phase | Definition |
|---|---|
| Ilmenite* | EDX spectrum indicates Fe and Ti |
| Fe-oxide* | EDX spectrum indicates Fe only |
| Chromite | Classified on major elements present i.e. Cr and Fe (Coertze and Coetzee 1992) |
| Zircon | Classified on major elements present i.e. Zr and Si |
| Rutile* | EDX spectrum indicates Ti only |
| Siliceous Leucoxene* | EDX spectrum indicates Fe, Ti and Si |
| Quartz* | Classified on major elements present i.e. Si only (Coetzee and De Villiers 1992) |
| Other silicates* | Classified on major elements present i.e. Si and other elements (Coetzee and De Villiers 1992) |
| Monazite | Classified on major elements present i.e. Ce and Th (Von Backström 1992) |
| Sulphide | Classified on major elements present i.e. S (Hammerbeck 1992a) |

To obtain more information on the degree of liberation within grains each sample was subjected to QEMscan analysis where EDX analysis was conducted along a grid pattern with a spacing of 4μm. A very short counting time, in the order of 13 milliseconds (Nell, 2002), was used and therefore only the major elements present were detected. Light elements such as O and C were not considered. Definitions for minerals were as in table 3.1. Over one thousand grains in each sample - 500 per size fraction - were analysed. Research personnel at Mintek in Randburg conducted the QEMSEM analysis in 1999.

The magnetic susceptibility of all samples was determined with a KLY-2 Kappabridge (Agico, Brno in the Czech Republic). Results were reported as specific magnetic susceptibility ($cm^3/g$) – refer to

chapter 2 – utilizing a bulk density of 2.4 g/cm$^3$. Nell and Den Hoed (1997) reported their results in a similar fashion. Research personnel from the pilot plant of Kumba R&D conducted the analysis at Geotron in Potchefstroom in 2000.

### *3.4 Determination of the optimum roasting conditions for LSR and comparison with crude ilmenite*

To determine the optimum roasting conditions for LSR tests were conducted on 40g samples as per figure 3.4.

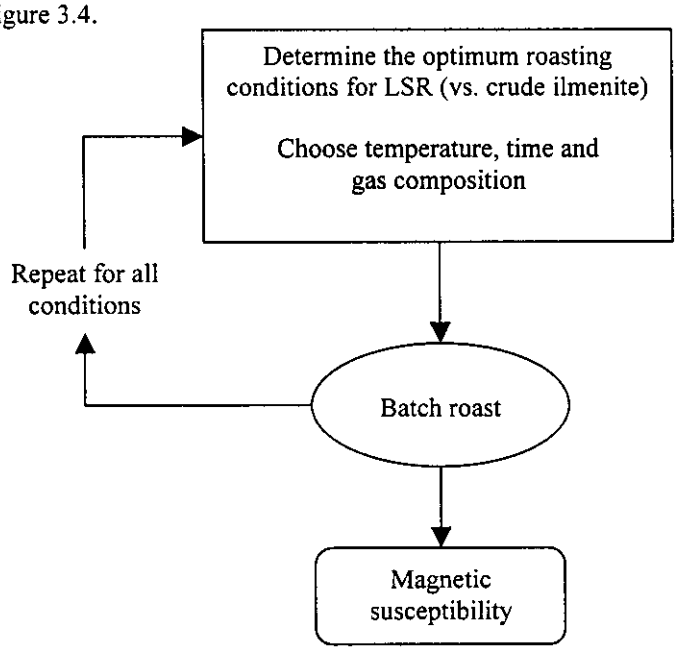


**Figure 3.4: Flow sheet for the determination of optimum roasting conditions for LSR.**

Batch-roasting tests were conducted in a custom made experimental set-up (refer to figure 3.5 for details). The set-up consisted of a quartz glass tube with a diameter of 30 mm and a length of 400 mm inside a tube furnace. An inner tube with a diameter of 25 mm was placed inside the outer tube. The bottom of the inner tube consisted of porous sintered glass disc. The sample was placed in the inner tube on the sintered disc.

a)

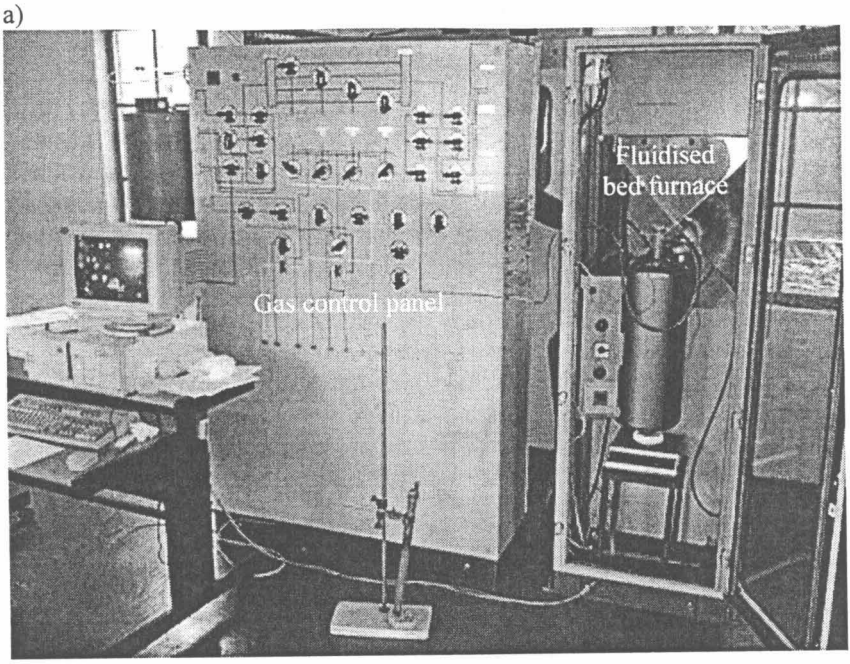


b)

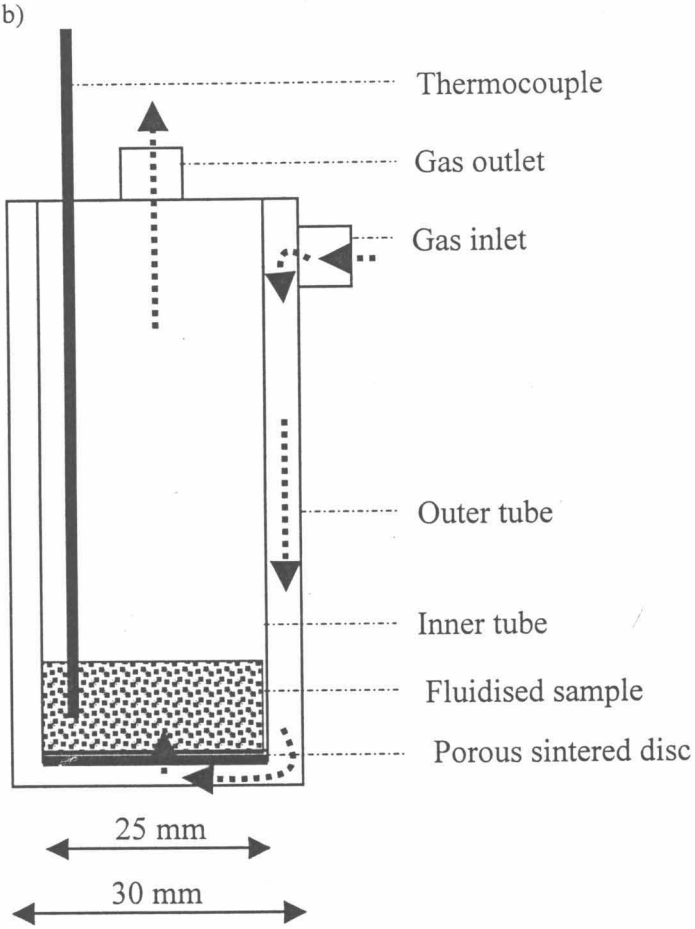


**Figure 3.5: a) Experimental set-up for the fluidised bed roaster b) schematic layout of the quarts glass inner and outer tube arrangement for the fluidised bed roaster.**

The 40g sample was place in the reaction tube and the reaction tube was then placed in a pre-heated furnace. The required atmosphere was then introduced from gas cylinders to the outer tube from where it passed through the sintered disc into the inner tube. This allowed the sample to be fluidised. A thermocouple in a silica sheath was also placed in the inner tube to measure the sample temperature

during the experiment. The furnace temperature was initially set to ~100°C below the required temperature.

Argon at a flow rate of 1 litre per minute was passed through the reactor once it was placed in the furnace. The sample was then heated to the reaction temperature over a period of 30 mininutes. Once the required temperature was reached, the experiment was started through the introduction of the required atmosphere. The sample temperature was continuously monitored for the duration of the experiment. After the required reaction time argon was once again introduced to the reactor and the sample was then removed from the furnace and allowed to cool down. The roasted samples were subjected to various analytical procedures. The magnetic susceptibility, the Fe(II) and Fe(III) content of the samples and the complete chemical analyses of the samples were determined by XRF analysis.

Roasting tests were conducted at temperatures ranging from 700-850°C for residence times of 5-40 minutes primarily in air but also in a mixture of 50 per cent air and 50 per cent $CO_2$ gas. For comparison purposes tests were also conducted on crude ilmenite at 750°C and 800°C for periods ranging from 5 minutes to 40 minutes in air. Details of the roasting experimental plan are shown in table 3.2.

**Table 3.2: Roasting conditions utilized for the determination of optimum roasting conditions for LSR.**

| | |
|---|---|
| **Time intervals [min]** | 0; 5; 10; 20; 30; 40 |
| **Temperatures [°C]** | 700; 750; 800; 850 |
| **Atmosphere** | Air; 50:50 Air: $CO_2$ |

At least two experiments were conducted for each condition. The difference between similar experiments was within 5 per cent, based on the observed increase in magnetic susceptibility. Research personnel from ISCOR R&D conducted the tests at the pilot plant in Pretoria West in 2000.

### *3.5 Preparation of fractionation curves for crude ilmenite and LSR before and after roasting at optimum roasting conditions*

To prepare separability curves for roasted LSR and roasted crude ilmenite tests were conducted on 250g samples as per figure 3.6. For comparison purposes separability diagrams for unroasted LSR and crude ilmenite were prepared in a similar fashion, excluding the roasting step.

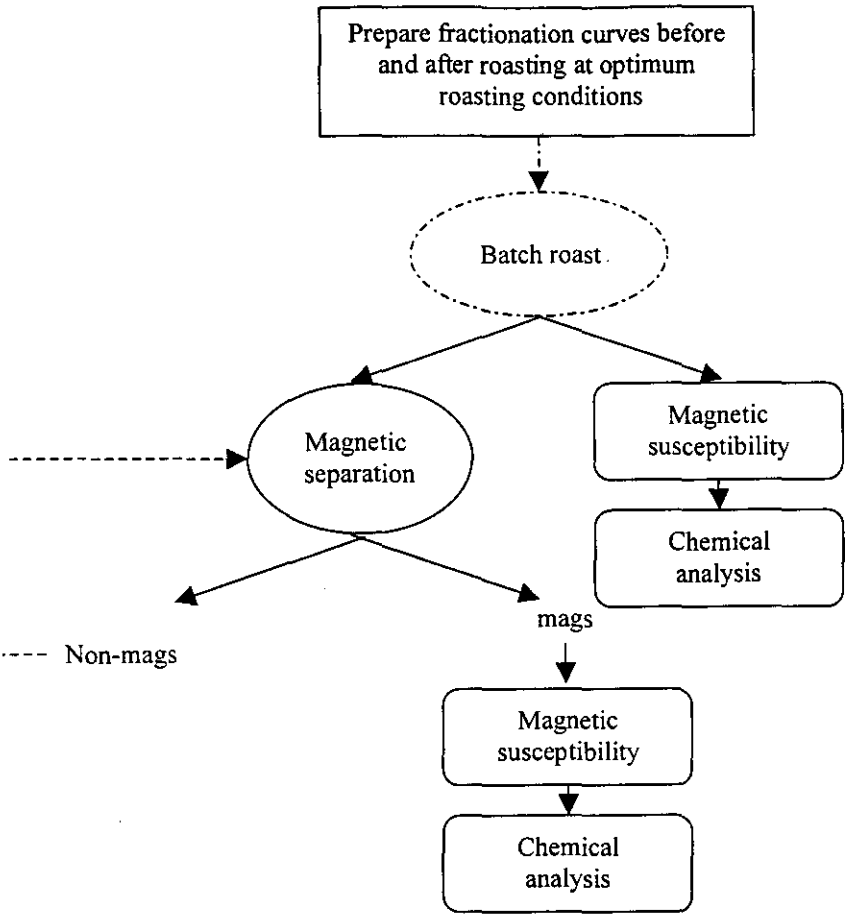


**Figure 3.6: Flow sheet for the preparation of fractionation curves for crude ilmenite and LSR before and after roasting**

After the optimum roasting conditions for LSR were determined, bulk samples of LSR and crude ilmenite was roasted in a custom made, Linn-type rotary furnace (internal diameter 150 mm and length 540 mm) at 800°C for 10 minutes; the furnace was rotated at 3 rpm. The externally heated furnace reactor was preheated to an operating temperature of 800°C whilst being rotated. On reaching the temperature, an oxidising gas was introduced at 6 liters per minute. The sample was loaded into the furnace reactor and roasted for 10 minutes. After 10 min the sample was cooled under rapidly flowing air and then discharged from the reactor. The roasted 250g sample was then split into two samples of 200g and 50g. The 50g sample was used for analysis of the roasted material (the magnetic susceptibility and the complete chemical analyses by XRF). The 200g sample was used for magnetic separation at various magnetic field strengths, and subsequent characterization of each fraction.

A Frantz barrier magnetic separator was used for fractionation. A vibrator feeder was used to feed a single layer of particles past the magnet. The angle of feed lane was kept at 25°. Nell & den Hoed (1997) used the same instrument settings during their study. For both material types splitting was conducted from a lower setting up to a higher setting. During fractionation a multimeter was connected in series to correlate the magnetic field strength – measured with a Gauss Meter - with the current (Ampere) settings. The following current settings were used:- 10mA, 20mA, 30mA, 40mA, 50mA, 100mA, 150mA, 200mA, 250mA, 300mA, 350mA, 400mA and 450mA. The correlation table between the field strength and current can be seen in table 3.3.

**Table 3.3: Correlation table for current (mA) and magnetic field strength (Gauss) readings.**

| CURRENT (MA) | 10 | 20 | 30 | 40 | 50 | 100 | 150 | 200 | 250 | 300 | 350 | 400 | 450 |
|---|---|---|---|---|---|---|---|---|---|---|---|---|---|
| Magnetic field strength (Gauss) | 250 | 384 | 481 | 584 | 751 | 1375 | 2150 | 2735 | 3450 | 4050 | 4650 | 5550 | 6210 |

Each fraction was analysed to determine the distribution of chemical components and the magnetic susceptibility. The magnetic susceptibility was determined as described elsewhere and the chemical analyses of the samples were determined by XRF.

To confirm the results of roasting at 800°C for 10 minutes samples of crude ilmenite and LSR were roasted in a similar fashion at another optimum roasting condition: 750°C for 20 minutes. Once again both samples were fractionated in a similar fashion at various magnetic field strengths and each fraction was chemically analysed in a similar fashion to determine the distribution of the components in each fraction. Research personnel from ISCOR R&D conducted the tests at the pilot plant in Pretoria West in 2000.

### *3.6 Souring and preparation of chromite*

A natural chromite sample was sourced from rock in the UG1 layer in the western limb of the Bushveld Igneous Complex, South Africa. The gross sample was prepared from this rock by crushing it (by, in sequence a jaw crusher, a gyratory crusher, and a laboratory rod mill) to a top size of 850 µm, screening with a laboratory sieve at 106 µm, and finally by performing magnetic separation with a Readings magnetic separator (set to reject the non-chromite gangue). The magnetic fraction was used as the gross sample for this study. In figure 3.7 the flow sheet for this part of the study was indicated. The sample was sourced by academic staff and preparation work conducted by a post graduate student at the University of Pretoria in 2001.

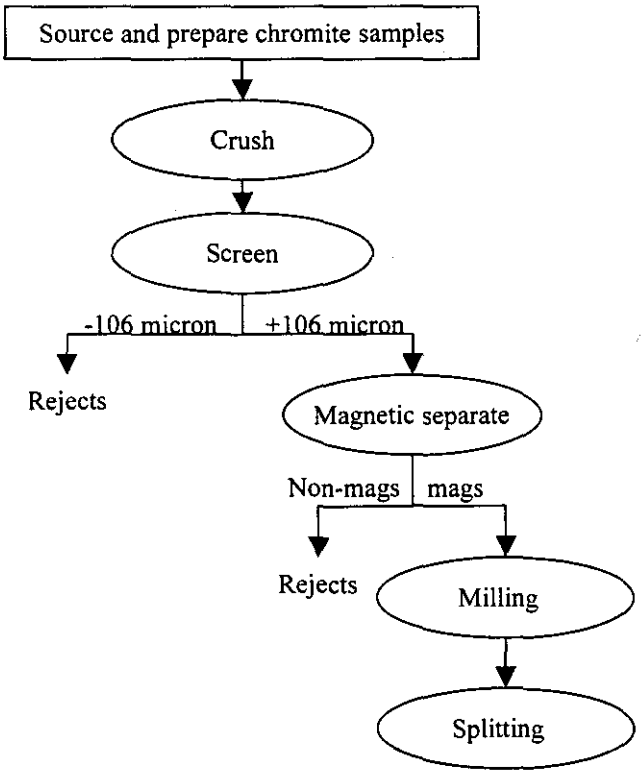


**Figure 3.7: Flow sheet for the sourcing and preparation of chromite for this study.**

### *3.7 Characterization of chromite*

As indicated in figure 3.8 the gross sample was characterized by determining its chemical composition, magnetic susceptibility and size distribution. The chemical composition was determined with WDS analysis utilizing an ARL SEMQ microprobe. The magnetic susceptibility was determined with a Barrington MS2 magnetic susceptibility meter. The size distribution was determined with a Malvern size analyzer. Secondary samples of the chromite were prepared by milling with a Bond ball mill, determining the size distribution with a Malvern size analyzer and splitting with a rotary splitter.

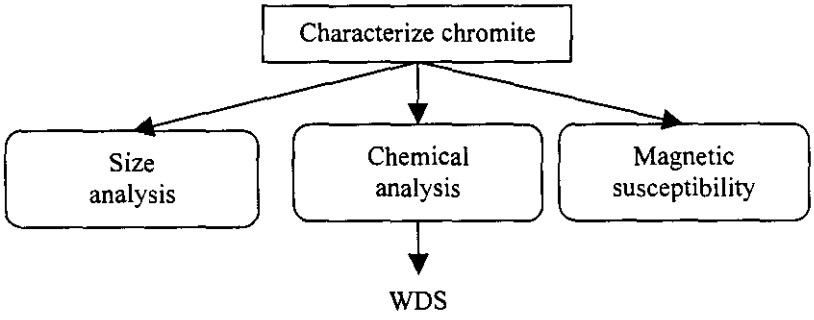


**Figure 3.8: Flow sheet for the characterisation of chromite for this study.**

### *3.8 Determination of the impact of roasting, at conditions used to determine optimum roasting conditions for LSR, on the magnetic susceptibility of chromite*

As summarized in figure 3.9 the individual secondary samples were roasted in batches under the different roasting conditions, stated in table 3.4, utilizing a custom-made fluidized bed roaster as described in paragraph 3.2.3. The roasted samples were characterized by determining the magnetic susceptibility thereof with a Barrington MS2 magnetic susceptibility meter, by SEM optical investigation and WDS and EDX chemical analyses.

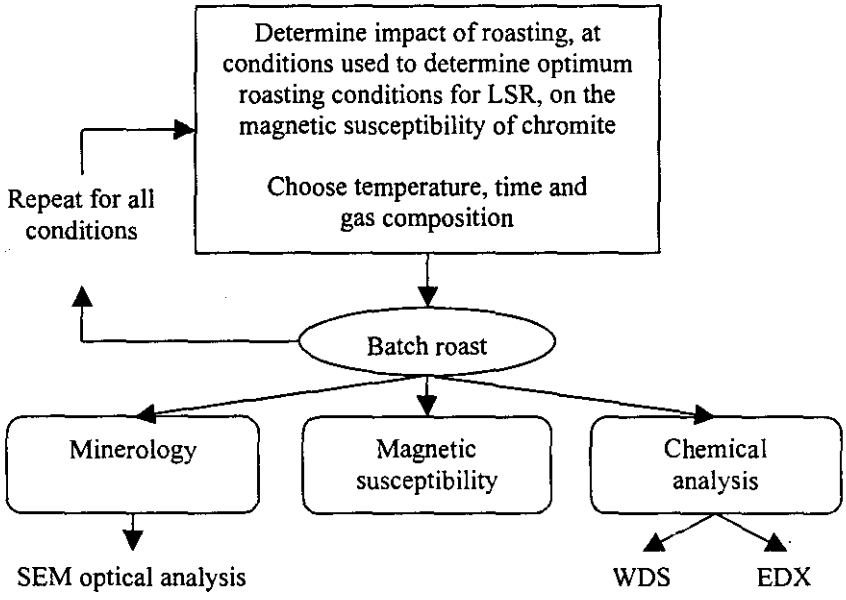


**Figure 3.9: Flow sheet to determine the impact of roasting of chromite at the roasting conditions utilized to determine the optimum roasting conditions for LSR.**

**Table 3.4: Roasting conditions to determine the impact of roasting of chromite.**

| | |
|---|---|
| **Time intervals [min]** | 0; 5; 10; 20; 30; 40 |
| **Temperatures [°C]** | 700; 750; 800; 850 |
| **Atmosphere** | Air |

### *3.9 Preparation of fractionation curves for chromite before and after roasting at optimum roasting conditions for LSR*

As shown in figure 3.10 fractionation curves for the UG1 chromite were constructed for unroasted chromite and for chromite roasted at 750°C for 20 minutes. The method used to construct these is described in paragraph 3.2.4.

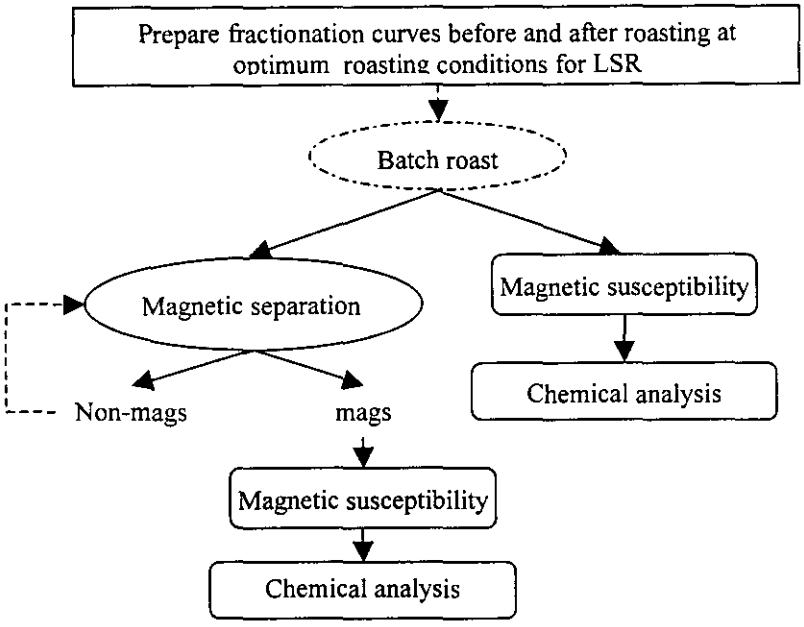


**Figure 3.10: Flow sheet for the preparation of fractionation curves for chromite before and after roasting at optimum conditions for LSR.**

### *3.10 Data capturing*

Data was captured either electronically or manually as indicated in table 3.5. Table 3.5 also indicates where the data was interpreted by others and submitted as a written report.

**Table 3.5: Details on how data was captured**

| Analysis | Electronic (e) or manual (m) | Interpreted by others |
|---|---|---|
| XRF | e | No |
| Titration | m | No |
| XRD | e | Yes |
| Reflected light microscopy | m | Yes |
| Micro-analysis | m | Yes |
| Particle counting | m | Yes |
| QEMSEM | e | Yes |
| QEMscan | e | Yes |
| Magnetic susceptibility | m | No |

In short: the aim of chapter 3 was to describe the design as well as the execution of the research program to test the hypotheses defined in Chapter 2. Firstly the key concepts and variables in this study were highlighted. The various test procedures used in this study were discussed in detail. A short comment was made on data capturing methods. In chapter 4 the results are presented and discussed.

## Chapter 4: Results – presentation and discussion

In chapter 3 I discussed the design and methodology of the test program in more detail. In chapter 4 the results from this test program are presented and discussed. The discussion is broken down into four parts. In all four parts the results are represented and discussed in one paragraph and the concluding remarks made in another. The four parts are:

4.1 Characterise crude ilmenite, LSR, chromite in LSR and UG 1 chromite before roasting
4.2 Characterise crude ilmenite, LSR, chromite in LSR and UG 1 chromite after roasting
4.3 Fractionate crude ilmenite, LSR and UG 1 chromite before roasting
4.4 Fractionate crude ilmenite, LSR and UG 1 chromite before roasting

### *4.1 Characterize crude ilmenite, LSR, chromite in LSR and UG 1 chromite before roasting*

### 4.1.1 Presentation and discussion of results

#### *4.1.1.1 Chemical analyses*

The average chemical compositions of the unroasted crude ilmenite, LSR[11], chromite in LSR and UG1 chromite are presented in table 4.1. During sample preparation thirty-two per cent of the crude ilmenite feed sample reported as LSR. When comparing the chemical analyses in table 4.1 with the mineralogical analyses in table 4.3 one notices that even though one third of the ilmenite and the majority of the rutile from the crude ilmenite reported in the LSR (table 4.3), the $TiO_2$ content of LSR at 39 per cent was significantly lower than that of crude ilmenite at 45 per cent (table 4.1 for the optimization material). This could be attributed to the high concentration of other non-magnetic material in the LSR (table 4.3). Hammerbeck (1976) published the $TiO_2$ content of ilmenite in KwaZulu-Natal, South Africa, as 49.0-49.7 per cent.

**Table 4.1: Chemical composition, in mass per cent, of the unroasted crude ilmenite and the LSR (XRF results), the chromite in the LSR with a) the EDX results and b) the WDS results and the unroasted UG 1 chromite WDS results.**

| Sample | $TiO_2$ | $Fe_{tot}$ | FeO | $Fe_2O_3$ | MgO | $Al_2O_3$ | CaO | $V_2O_5$ | $Cr_2O_3$ | MnO | $SiO_2$ | $K_2O$ | $P_2O_5$ | $ZrO_2$ | $Fe^{2+}$ | $Fe^{3+}$ |
|---|---|---|---|---|---|---|---|---|---|---|---|---|---|---|---|---|
| Crude [12] | 45.3 | - | - | - | 0.6 | 0.7 | 0.3 | 0.3 | 0.2 | 1.1 | 3.4 | 0.0 | 0.1 | 0.9 | 25.7 | 9.8 |
| LSR[13] | 39.2 | - | - | - | 0.7 | 1.6 | 0.7 | 0.2 | 0.6 | 1.1 | 7.8 | 0.1 | 0.3 | 3.2 | 25.7 | 17.1 |
| Crude [14] | 47.1 | 36.8 | - | - | 0.4 | 0.3 | 0.0 | 0.3 | 0.2 | 1.1 | 0.3 | ND | 0.0 | 0.1 | - | - |
| LSR[15] | 41.5 | 38.7 | - | - | 0.4 | 0.7 | 0.0 | 0.2 | 0.6 | 1.1 | 1.2 | 0.0 | 0.1 | 0.4 | - | - |
| Chromite in LSR[a] | - | - | 25 | 4 | 7 | 22 | - | - | 42 | - | - | - | - | - | - | - |
| Chromite in LSR[b] | - | - | 26 | 12 | 6 | 17 | - | - | 39 | - | - | - | - | - | - | - |
| UG 1 Chromite | - | - | 19 | 12 | 10 | 16 | - | - | 43 | - | - | - | - | - | - | - |

The $Cr_2O_3$ content of the crude ilmenite sample in table 4.1 is 0.21 per cent, far less than the typical value of 0.3 per cent published by Nell and Den Hoed (1997). At 0.56 per cent the $Cr_2O_3$ content of LSR was high.

Two types of behaviour were observed when analyzing the other components (table 4.1):

- The concentration of the component remained relatively constant when comparing the LSR with crude ilmenite; or
- The component was concentrated in the LSR fraction when comparing the LSR with crude ilmenite.

[11] Low susceptibility rejects
[12] Optimisation tests
[13] Optimisation tests
[14] Fractionation tests
[15] Fractionation tests

MgO, MnO and $V_2O_5$ were components that followed the first behaviour pattern. One explanation for this was that these components were in solid solution in ilmenite, as stated by Nell and Den Hoed (1997). CaO, $SiO_2$ and $Al_2O_3$ were examples of components that followed the second behaviour pattern. These components were part of discrete particles with low magnetic susceptibility. The CaO content of the LSR was 2.1 times more than that of crude ilmenite. This can only be attributed to contamination of the sample by Ca-containing material, such as cement, during preparation of the LSR sample. Both the $ZrO_2$ and the $P_2O_5$ levels were more than 3 times higher than that of the crude ilmenite. The discrepancy on the $P_2O_5$ was attributed to the very low $P_2O_5$ content of the mineral leading to inaccurate determination of the $P_2O_5$ content by XRF. The difference in $ZrO_2$ analysis was due to the concentration of zircon in the LSR – refer to table 4.3. For the purpose of the study the $K_2O$ content of both streams was negligible.

As stated in chapter 2 all natural magnesiochromites contain a considerable amount of $Fe^{2+}$ (which replaces $Mg^{2+}$) and $Al^{3+}$ or $Fe^{3+}$ (replacing $Cr^{3+}$). In natural chromites a considerable amount of $Mg^{2+}$ replaces $Fe^{2+}$ with generally appreciable replacement of $Cr^{3+}$ by $Al^{3+}$, but less so by $Fe^{3+}$ (Deer et al 1966). Both the EDX and the WDS results in table 4.1 confirmed that the chromite in the LSR was of the magnesiochromite spinel series. From table 4.1 the chromite in the LSR contained a considerable amount of MgO. The results of the two analysis methods – EDX and WDS – can be seen to be similar.

The distribution of iron between the divalent and trivalent states was estimated, based on the assumption that all the chromium is trivalent and that the spinel is stoichiometric $M_3O_4$. The procedure for this estimation is given in Appendix 2 at the end of this chapter.

The results in table 4.1 indicate that the chromite in the UG1 sample was not only of the magnesiochromite spinel series, but also very close in composition to that of the chromite in the LSR with slightly less $Al_2O_3$ and more $Cr_2O_3$. However, the match was not perfect, since the average $Fe_2O_3$: FeO mass ratio of the chromite in the LSR was 0.50 whereas that of the chromite in the UG1 sample 0.64. It was therefore expected that oxidising roasting would have a greater effect on the magnetic susceptibility of the chromite in the LSR than the chromite in the UG1 sample (since trivalent iron enhances the magnetic susceptibility of chromite).

#### *4.1.1.2 Mineralogical analyses*

From the XRD results in table 4.2 both crude ilmenite and the LSR consisted of ilmenite and hematite, but the *quantities* of the minerals could not be identified with this method. As the diffraction patterns for pseudobrookite, rutile and quartz were not clear this method was also inefficient in determining the *differences* between the various fractions.

**Table 4.2: Phase-chemical composition of crude ilmenite and LSR (XRD results).**

| Description | Main phases | Minor phases | Trace phases |
|---|---|---|---|
| Crude | Ilmenite | - | Hematite, (Pseudobrookite?) |
| LSR | Ilmenite | - | Hematite, (Rutile?) |

***Legend:*** *Ilmenite – $FeTiO_3$; Hematite – $Fe_2O_3$; Pseudobrookite – $Fe_2TiO_5$; Quartz – $SiO_2$; Rutile – $TiO_2$.*

The results of a QEMSEM investigation in table 4.3 confirmed the XRD results as all fractions consisted of ilmenite and iron bearing minerals. *Crude ilmenite* contained 90.8 per cent ilmenite, 2.3 per cent other valuable heavy minerals (zircon and rutile), 0.4 per cent chromite and equal amounts (3.3 per cent) of iron oxides and other gangue minerals (primarily $SiO_2$ bearing). Zircon and rutile reported in the crude ilmenite due to inefficient separation in the WHIMS. The *LSR fraction* had high iron oxide (3.9 per cent), chromite (1.1 per cent), valuable heavy mineral (6.1 per cent) and gangue mineral (4.2 per cent) contents and had low ilmenite content (84.6 per cent). In table 4.3 ninety percent of the valuable heavy minerals (VHM) and chromite, two thirds of the iron oxide and other gangue minerals, and a third of the ilmenite concentrated in the LSR fraction. From these results it was clear that the LSR fraction contained the majority of the unwanted minerals contained in crude ilmenite.

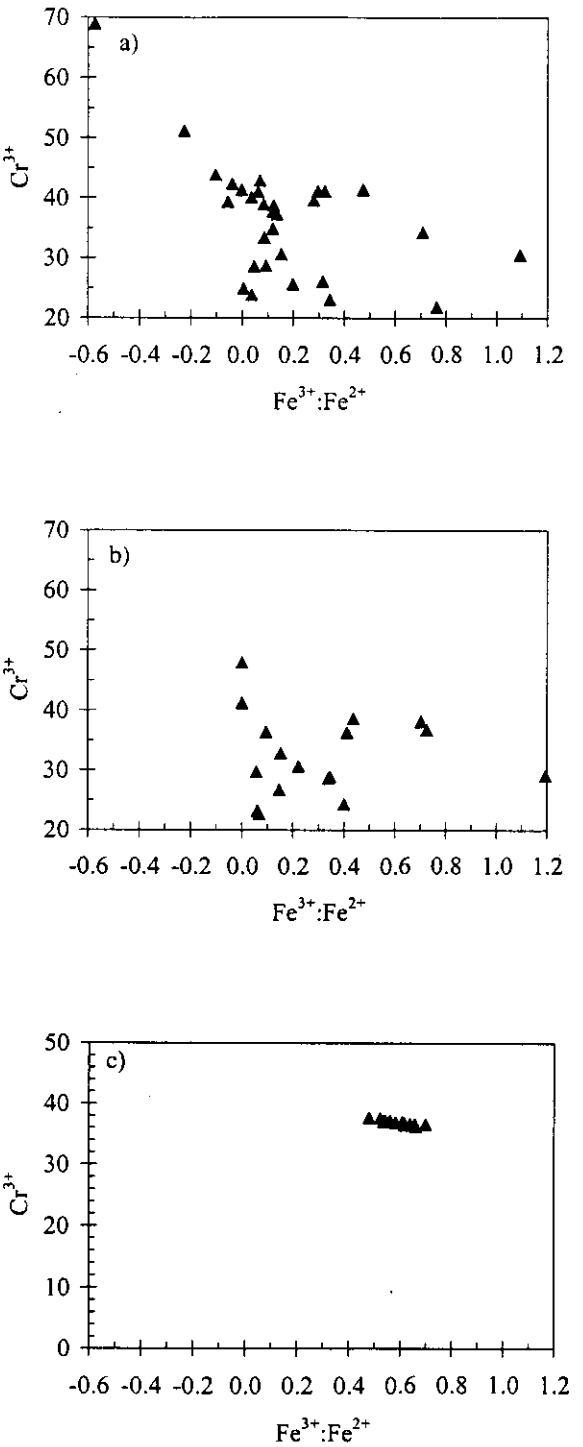


**Figure 4.1: The variation in chemical analysis of the chromite in unroasted LSR, indicated by the normalized mole percentage $Cr^{3+}$ and the $Fe^{3+}:Fe^{2+}$ ratio of the calculated mole percentage $Fe^{3+}$ and $Fe^{2+}$, based on a) the EDX analysis of 30 particles and b) the WDS analysis of 18 particles. c) Results for unroasted UG1 chromite (showing the WDS analysis of 15 particles).**

**Table 4.3: Modal analysis of the crude ilmenite and LSR (reported in mass per cent).**

| Phase | Crude | LSR | Phase | Crude | LSR |
|---|---|---|---|---|---|
| Ilmenite | 90.8 | 84.6 | Siliceous Leucoxene | 0.6 | 0.8 |
| Fe-oxide | 3.3 | 3.9 | Quartz | 0.9 | 0.6 |
| Chromite | 0.4 | 1.1 | Other silicates | 1.6 | 2.1 |
| Zircon | 1.5 | 4.7 | Monazite | 0.1 | 0.5 |
| Rutile | 0.8 | 1.4 | Sulphide | 0.1 | 0.2 |
| Total | | | | 100 | 100 |

The results of the QEMSEM analysis in table 4.4 present the results in table 4.3 in more detail. Crude ilmenite contained more unaltered ilmenite (66.0 per cent) than LSR (44.0 per cent). LSR contained more altered ilmenite (24.1 per cent) than crude ilmenite (20.2 per cent). The impact of the unaltered and altered ilmenite content on magnetic susceptibility and roasting was not clear. Being the fraction with lower magnetic susceptibility the LSR contained double the amount of hematite, five times as much rutile, 2.5 times as much zircon and monazite, 1.5 times as much chromite and 4 times as much gangue material, when compared to crude ilmenite. These minerals would not be affected by roasting.

**Table 4.4: Semi-quantitative phase distribution of the crude ilmenite and LSR (reported in mass per cent).**

| Particles | Crude | LSR |
|---|---|---|
| Homogenous, unaltered ilmenite | 66.0 | 44.0 |
| Slightly altered ilmenite // micro-fractures, grain boundaries, (0001) | 12.6 | 13.2 |
| Moderately altered ilmenite // micro-fractures, grain boundaries, (0001) | 1.2 | 2.0 |
| Alteration involving development of fine rutile lenses & titano-hematite | 0.6 | 0.4 |
| Partial heterogeneous alteration | 2.4 | 2.4 |
| Moderate heterogeneous alteration | 0.8 | 2.3 |
| Extensive heterogeneous alteration | 2.6 | 3.8 |
| Ilmenite with exsolved Hematite | 2.2 | 1.4 |
| Ilmenite-Hematite | 0.1 | 0.3 |
| Hematite with exsolved Ilmenite | 0.8 | 1.0 |
| Titano-hematite | 0.4 | 1.3 |
| Hematite | 5.0 | 9.4 |
| Porous aggregates of $TiO_2$-crystals & Secondary Rutile/Anatase | 0.4 | 1.0 |
| Primary Rutile | 0.3 | 1.5 |
| Zircon and Monazite | 1.8 | 5.0 |
| Chromite | 0.5 | 1.3 |
| Goethite | 0.3 | 1.8 |
| Gangue | 2.0 | 7.9 |
| Total | 100 | 100 |

From table 4.5 the Fe-oxide grains contained small inclusions of rutile and/or silicate minerals. For classifications purposes grains containing more than 80 per cent Fe-oxide were considered liberated. The data showed that about one third of the Fe-oxide grains in the crude ilmenite were liberated. The composite Fe-oxide-silicate grains were predominant in the LSR. Complex intergrowths of rutile, quartz and/or other silicates, ilmenite and hematite were present in both the crude ilmenite and the LSR.

**Table 4.5: Occurrence of Fe-oxide (reported as percent by volume).**

| | Crude | LSR |
|---|---|---|
| Total no. grains analyzed | >1000 | >1000 |
| No. Fe-oxide bearing grains | 53 | 87 |
| **Volume percent Fe-oxides in Fe-oxide bearing grains** | | |
| >80% Fe-oxides (liberated) | 33 | 28 |
| 60%<Fe-oxides<80% | 21 | 35 |
| 40%<Fe-oxides<60% | 21 | 7 |
| 20%<Fe-oxides<40% | 15 | 11 |
| <20% Fe-oxides | 10 | 9 |
| **Phase associations[16] of composite grains (<80% Fe-oxides)** | | |
| Fe-oxide associations | **Crude** | **LSF** |
| Ilmenite | 7 | 9 |
| Silicates | 13 | 25 |
| Ternary/Composite | 47 | 38 |

*4.1.1.3 Magnetic susceptibility*

Table 4.6 reports the magnetic susceptibility of unroasted crude ilmenite, LSR and UG1 chromite.

**Table 4.6: Measured magnetic susceptibility of unroasted crude ilmenite, LSR and UG 1 chromite and the magnetic susceptibility of the low susceptibility and high susceptibility peaks of the bimodal $Cr_2O_3$ peaks and the $TiO_2$ peak of unroasted crude ilmenite reported by Nell and Den Hoed (1997) reported in cgs units as $*10^{-6}$ $cm^3/g$.**

| Sample | Magnetic susceptibility |
|---|---|
| Unroasted crude ilmenite | 188 |
| Unroasted LSR | 113 |
| Unroasted UG 1 chromite | 149 |
| Low susceptibility peak of the bimodal $Cr_2O_3$ peaks of unroasted crude ilmenite | 20 (range was 20-65) |
| $TiO_2$ peak of unroasted crude ilmenite | 100 (range was 65-500) |
| High susceptibility peak of the bimodal $Cr_2O_3$ peaks of unroasted crude ilmenite | 1995 (range was 500-10000) |

*4.1.1.4 Size analyses*

The typical size analysis of the crude ilmenite and for the LSR was a $d_{50}$ of 140μm with fifty percent of the particles in the range 125-180μm and only 1.8 per cent below 75μm. The UG 1 chromite had a $d_{50}$ of 90μm.

### 4.1.2 Concluding interpretation

*4.1.2.1 Chemical analysis*

The $TiO_2$ content of both crude ilmenite and LSR was significantly less than that published by Hammerbeck (1976). This decrease was attributed to the presence of other minerals in both concentrate streams.

It was expected that due to its low $Cr_2O_3$ content the maximum requirement of 0.1 per cent $Cr_2O_3$ would easily be met when beneficiating the crude ilmenite by roasting and magnetic separation. On the

[16] Phase association data refer to composite grains (<80 per cent Fe-oxides present). For example, 33 per cent of the Fe-oxide in the crude ilmenite occurred as liberated grains. Of the remaining 67 per cent Fe-oxide in this sample 7 per cent occurred in particles consisting only of Fe-oxide and ilmenite, 13 per cent occurs in particles consisting only of Fe-oxide and silicates and 47 per cent occurs in complex grains.

other hand meeting the maximum requirement of 0.1 per cent $Cr_2O_3$ when beneficiating LSR would only be possible if roasting:

- Increased the magnetic properties of the ilmenite in the LSR dramatically;
- Did not increase the magnetic properties of $Cr_2O_3$ at all; and
- If $Cr_2O_3$ were only present in the LSR fraction as discrete non-ilmenite particles.

If one assumed that the titration results were an indication of what the ilmenite mineral composition was, the magnetic susceptibility of both the crude ilmenite and LSR would be enhanced by oxidative roasting. This is based on the assumption that in ilmenite the maximum magnetic enhancement is achieved when the mole ratio $Fe_2O_3$:FeO is within the range 1:1 - 1.57:1 (Walpole 1991). The $Fe_2O_3$:FeO ratio of crude ilmenite was 0.44 and that of LSR 0.78. Oxidation would increase the $Fe_2O_3$ content of the ilmenite and decrease the FeO content, as per reaction 4.1, and therefore the $Fe_2O_3$:FeO ratio.

$$FeO + \tfrac{1}{2}O_2 = \tfrac{1}{2}Fe_2O_3$$

**Reaction 4.1: Oxidation reaction taking place during the oxidation of ilmenite**

No amount of roasting and/or magnetic separation would decrease the content of MgO, MnO and $V_2O_5$ in the final ilmenite product, because these components are in solid solution in the ilmenite.

If only the magnetic susceptibility of the ilmenite in crude ilmenite or LSR was increased, the content of CaO, $SiO_2$ and $Al_2O_3$ in the final ilmenite product could be decreased by magnetic separation.

Despite the lower FeO: $Fe_2O_3$ mass in the UG 1 chromite, this natural chromite was considered to be sufficiently close in composition to that in the LSR to provide a test of the hypothesis that oxidising roasting leaves the magnetic susceptibility of the chromite unchanged.

#### *4.1.2.2 Mineralogical analysis*

XRD was not a very useful method for mineralogical analysis of the crude ilmenite nor that of the LSR. From the other mineralogical analysis methods in the order of 30 per cent of the ilmenite in crude ilmenite reported to LSR. Of this 65 per cent were unaltered ilmenite and 35 per cent altered ilmenite vs. 75 per cent unaltered ilmenite and 25 per cent altered ilmenite in crude ilmenite. When preparing LSR from crude ilmenite the majority of the iron oxides, chromite, other valuable heavy minerals and gangue minerals reported in the LSR.

#### *4.1.2.3 Magnetic susceptibility*

As expected the magnetic susceptibility of crude ilmenite was higher than that of LSR. The magnetic susceptibility of the LSR was similar to and that of the crude ilmenite 1.8 times that of the peak magnetic susceptibility in the fractionation curve reported by Nell and Den Hoed (1997). The magnetic susceptibility of the UG 1 samples was in between – higher than that of the LSR and lower than that of the crude ilmenite. The magnetic susceptibility of the UG 1 chromite was higher than that of the low susceptibility peak of the bimodal $Cr_2O_3$ distribution reported by Nell and Den Hoed (1997), but considerably less than that of the high susceptibility peak. This could be attributed to the higher $Fe_2O_3$: FeO mass ratio in the unroasted UG 1 chromite compared to that of the chromite in the LSR (De Waal and Copelowitz 1972). Typically, the magnetic susceptibility of UG 1 chromite is some 90 x $10^{-6}$ $cm^3/g$ (De Waal and Copelowitz 1972).

#### *4.1.2.4 Size analyses*

As reported from literature (Svoboda 1987) the only forces on a particle in a Frantz isodynamic separator are the applied magnetic field (H) and gravity. From chapter 2 (Svoboda 1987) the gravity force on a particle in a Frantz isodynamic separator is neglible and therefore size distribution could therefore be neglected as part of this study. .

## *4.2 Characterization of crude ilmenite, LSR, chromite in LSR and UG 1 chromite after roasting*

### 4.2.1 Presentation and discussion of results

To investigate the effect of roasting atmosphere on the magnetic susceptibility, LSR was roasted in air and in 50:50 air-$CO_2$ gas mixtures. The results are presented in table 4.7 and graphically presented in figure 4.2. The resulting increase in magnetic susceptibility was calculated as per equation 4.1. The results were presented in table 4.7.

$$a = c/b$$

**Equation 4.1: Equation to calculate the increase in magnetic susceptibility**

Legend for equation 4.1:
a = Relative increase in magnetic susceptibility
b = Magnetic susceptibility of unroasted sample
c = Magnetic susceptibility of sample roasted at specific conditions

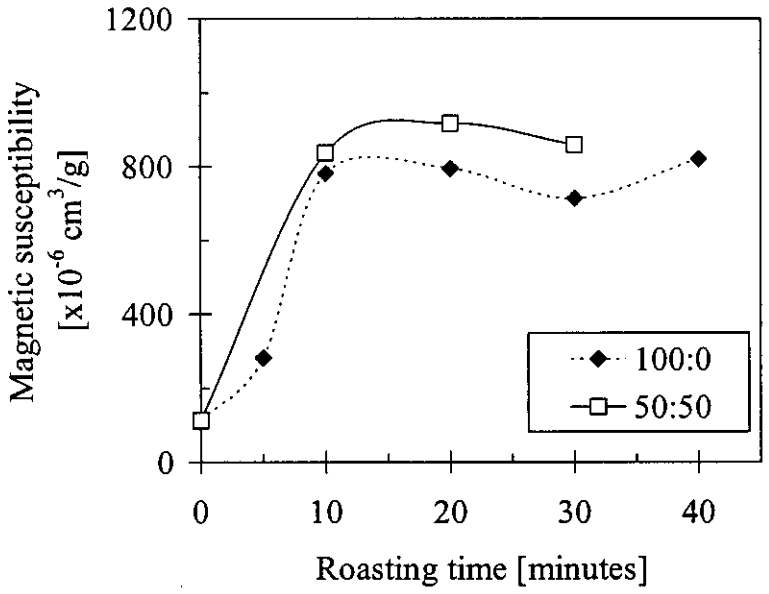


**Figure 4.2: Effect of roasting atmosphere on the magnetic susceptibility of LSR.**

**Table 4.7: The magnetic susceptibility (reported as $*10^{-6}$ $cm^3/g$) of LSR roasted in air at 750°C in different atmospheres and resulting increase in magnetic susceptibility when roasting LSR at 750°C in different atmospheres**

| Time [Minutes] | Magnetic susceptibility | | Increase in magnetic susceptibility | |
|---|---|---|---|---|
| | Atmosphere [air: $CO_2$] | | Atmosphere [air: $CO_2$] | |
| | 100:0 | 50:50 | 100:0 | 50:50 |
| 0 | 113 | 113 | 0 | 0 |
| 5 | 282 | - | 169 | - |
| 10 | 781 | 836 | 668 | 723 |
| 20 | 794 | 917 | 681 | 804 |
| 30 | 713 | 858 | 600 | 745 |
| 40 | 820 | - | 707 | - |

To investigate the effect of roasting temperature on the magnetic susceptibility, LSR was roasted in air at different temperatures. The results are presented in table 2.8 and graphically presented in figure 4.3. The resulting increase in magnetic susceptibility was also calculated with equation 1. The results are presented in table 4.8.

**Table 4.8: The magnetic susceptibility (reported as $*10^{-6}$ $cm^3/g$) of LSR roasted in air at different temperatures and resulting increase in magnetic susceptibility when roasting LSR in air at different temperatures**

| Time [Minutes] | Magnetic susceptibility Temperature [°C] | | | | Increase in magnetic susceptibility Temperature [°C] | | | |
|---|---|---|---|---|---|---|---|---|
| | 700 | 750 | 8000 | 850 | 700 | 750 | 800 | 850 |
| 0 | 113 | 113 | 113 | 113 | 0 | 0 | 0 | 0 |
| 5 | 310 | 282 | 1081 | 1110 | 197 | 169 | 968 | 997 |
| 10 | 394 | 781 | 1018 | 440 | 281 | 668 | 905 | 327 |
| 20 | 415 | 794 | 493 | 215 | 302 | 681 | 380 | 102 |
| 30 | 602 | 713 | 302 | 139 | 489 | 600 | 189 | 26 |
| 40 | 454 | 820 | 215 | 99 | 341 | 707 | 102 | -14 |

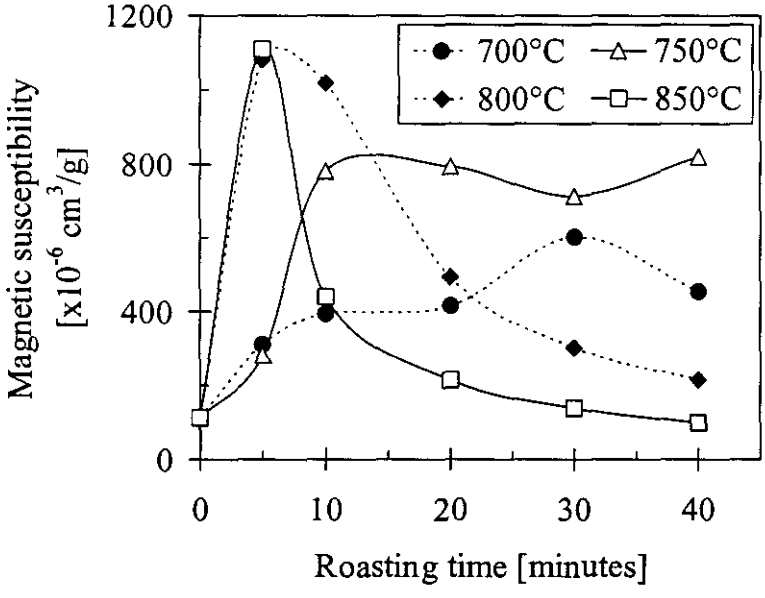


**Figure 4.3: Effect of roasting temperature on the magnetic susceptibility of LSR.**

From figure 4.2 and figure 4.3 the effect of a factor two change in the oxygen content of the roasting atmosphere on the increase in magnetic susceptibility of LSR was negligible compared to the effect of temperature. Figure 4.3 also indicates that there is no single, ideal set of roasting conditions for LSR. The largest increase in magnetic susceptibility was observed when roasting samples at high temperatures. The magnetic susceptibility increased ten-fold after 5 minutes of roasting at 800°C and 850°C. At 850°C the magnetic susceptibility decreased rapidly with further roasting. At 800°C very good results were obtained after 10 minutes. Even after 20 minutes the benchmark five- to six-fold increase, used by Nell and Den Hoed (1997), was still reached. Longer reaction times resulted in unacceptably low magnetic susceptibility values. Nell and Den Hoed (1997) also observed this phenomenon and stated that it was due to excessive $Fe^{3+}$ formation with the formation of small amounts of pseudobrookite in the most oxidised samples.

Samples of crude ilmenite were also roasted to confirm the roasting conditions determined by Nell and Den Hoed (1997) and to compare the roasting behaviour of LSR with that of the crude ilmenite from which it was beneficiated. The results are presented in table 2.9 and graphically presented in figure 4.4. The resulting increase in magnetic susceptibility was also calculated with equation 4.1. The results were presented in table 2.9.

**Table 4.9: The magnetic susceptibility (reported as $*10^{-6}$ $cm^3/g$) of LSR and crude ilmenite roasted in air at different temperatures and resulting increase in magnetic susceptibility when roasting LSR and crude ilmenite in air at different temperatures**

| Time [Minutes] | Magnetic susceptibility | | | | Increase in magnetic susceptibility | | | |
|---|---|---|---|---|---|---|---|---|
| | Temperature [°C] | | | | Temperature [°C] | | | |
| | 750 | | 800 | | 750 | | 800 | |
| | Crude ilmenite | LSR | Crude ilmenite | LSR | Crude ilmenite | LSR | Crude ilmenite | LSR |
| 0 | 188 | 113 | 188 | 113 | 0 | 0 | 0 | 0 |
| 5 | 1149 | 282 | 1168 | 1081 | 961 | 169 | 980 | 968 |
| 10 | 1159 | 781 | 847 | 1018 | 971 | 668 | 659 | 905 |
| 20 | 1022 | 794 | 401 | 493 | 834 | 681 | 213 | 380 |
| 30 | 1039 | 713 | 259 | 302 | 851 | 600 | 71 | 189 |
| 40 | 929 | 820 | 182 | 215 | 741 | 707 | -6 | 102 |

In figure 4.5 the effect of temperature on the magnetic susceptibility of crude ilmenite and that of LSR is compared. At 750°C crude ilmenite had a 12-75 per cent higher increase in magnetic susceptibility compared to LSR. At 800°C the increases in susceptibility for crude ilmenite and LSR were similar, but with differences in rate.

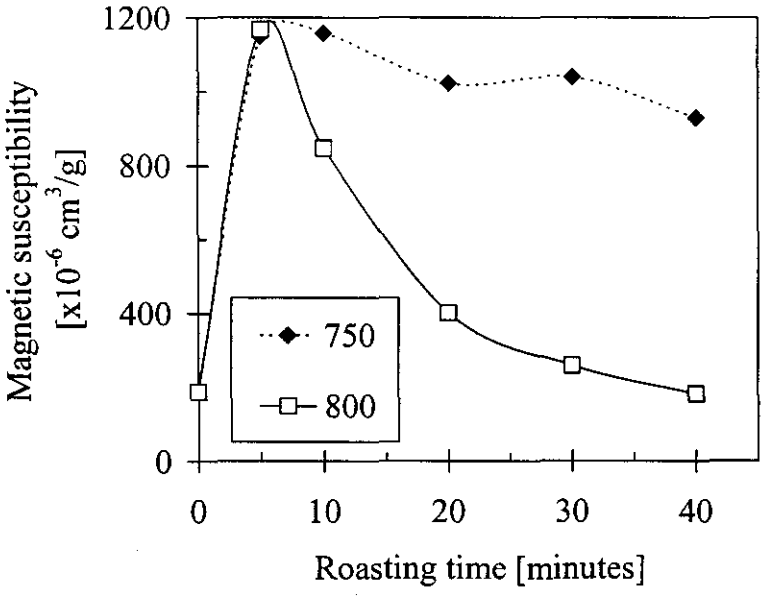


**Figure 4.4: Effect of roasting temperature (in °C) on the magnetic susceptibility of crude ilmenite.**

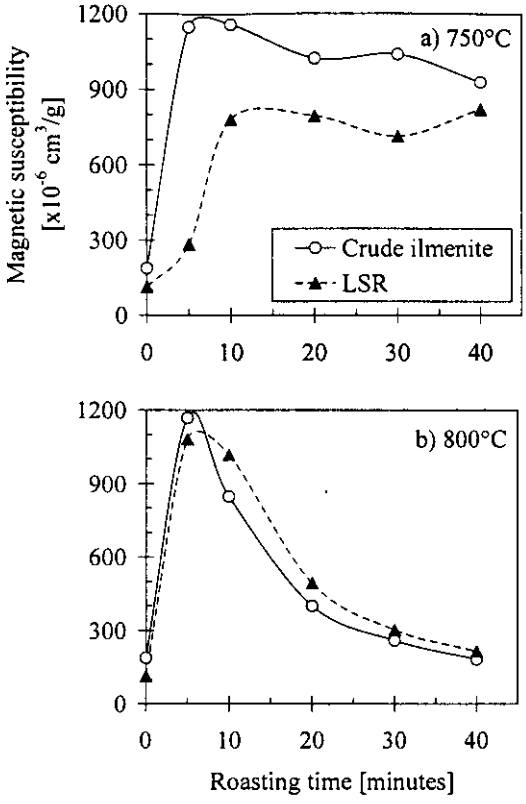


**Figure 4.5: The effect of roasting temperature on the magnetic susceptibility of LSR vs. that of crude ilmenite.**

The effect of oxidizing roasting at different temperatures and for different time intervals, on the magnetic susceptibility of the UG1 chromite samples, is summarized in Table 4.10. The results in Table 4.10 are plotted in Figure 4.6. The results in Figure 4.6 illustrate that oxidizing roasting did indeed affect the (average) magnetic susceptibility of the UG1 chromite. At all the roasting conditions evaluated the magnetic susceptibility of the roasted samples increased, by factors ranging from 1.4 to 2.6.

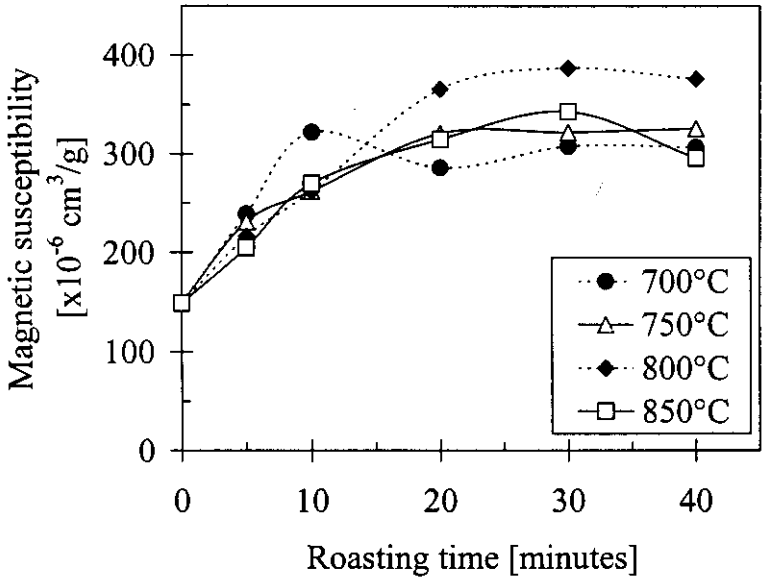


**Figure 4.6: Effect of roasting temperature on the magnetic susceptibility of UG1 chromite.**

**Table 4.10: The magnetic susceptibility (reported as $*10^{-6}$ $cm^3/g$) of UG 1 chromite roasted in air at different temperatures and resulting increase in magnetic susceptibility when roasting UG 1 chromite in air at different temperatures**

| Time [Minutes] | Magnetic susceptibility | | | | Increase in magnetic susceptibility | | | |
|---|---|---|---|---|---|---|---|---|
| | Temperature [°C] | | | | Temperature [°C] | | | |
| | 700 | 750 | 800 | 850 | 700 | 750 | 800 | 850 |
| 0 | 149 | 149 | 149 | 149 | 0 | 0 | 0 | 0 |
| 5 | 239 | 231 | 216 | 205 | 90 | 82 | 67 | 56 |
| 10 | 322 | 262 | 262 | 270 | 173 | 113 | 113 | 121 |
| 20 | 286 | 321 | 366 | 315 | 137 | 172 | 217 | 166 |
| 30 | 308 | 322 | 387 | 343 | 159 | 173 | 238 | 194 |
| 40 | 307 | 326 | 376 | 296 | 158 | 177 | 227 | 147 |

From table 4.11 the composition of the unroasted and the roasted UG 1 chromite virtually remained the same only with a slight increase in the $Fe_2O_3$ content..

**Table 4.11: Average chemical composition (WDS), in mass per cent, of the UG 1 chromite roasted at 750°C for 20 minutes in air as well as unroasted UG 1 chromite.**

| Sample | Number of particles analysed | FeO | $Fe_2O_3$ | MgO | $Al_2O_3$ | $Cr_2O_3$ |
|---|---|---|---|---|---|---|
| UG 1 chromite roasted in fluidised bed roaster | 16 | 22 | 8 | 8 | 16 | 46 |
| UG 1 chromite roasted in Linn furnace | 16 | 22 | 9 | 8 | 16 | 45 |
| Unroasted UG 1 chromite | 15 | 19 | 12 | 10 | 16 | 43 |

In figure 4.7a) and figure 4.7b) the lack of variation in chemical composition of unroasted and roasted UG1 chromite is illustrated.

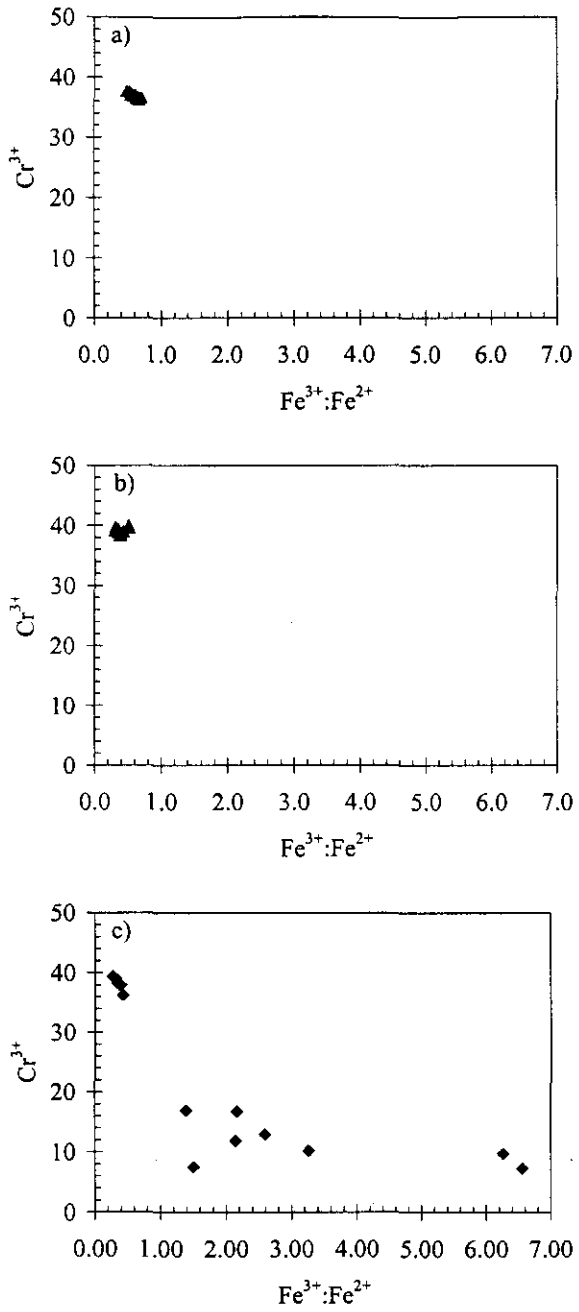


**Figure 4.7: The variation in chemical analysis of the UG1 chromite, indicated by the normalized mole percentage $Cr^{3+}$ and the $Fe^{3+}:Fe^{2+}$ ratio of the calculated mole percentage $Fe^{3+}$ and $Fe^{2+}$, based on a) the WDS analysis of 15 unroasted particles and b) the WDS analysis of 16 particles roasted at 750°C in air for 20 minutes. c) Results for the iron rich layer as well as the chromite rich matrix of the roasted UG1 chromite (showing the EDX analysis of 16 points).**

The roasting conditions used in this test program do not seem to oxidize the $Fe^{2+}$ in the chromite as in the ilmenite. If this is the case then the increase in the magnetic susceptibility of the chromite observed in figure 4.6 is due to a mechanism other than a change in the solid solution composition of the chromite caused by reaction 1. The behaviour (increase in magnetic susceptibility after roasting) is the opposite of that observed by Schwerer and Gundaker (1975). The surface structure observed by Schwerer and Gundaker (1975) displayed ferromagnetic behaviour and was *recovered* during annealing i.e. might well have been surface defect structures. EDX analysis of different areas of roasted UG1 chromite particles revealed a different picture all together – figure 4.7c). Investigating the sample, utilizing a scanning electron microscope (SEM), revealed the presence of iron rich exsolutions on the particle surface not present in the unroasted particles - refer to figure 4.8 and table 4.12.

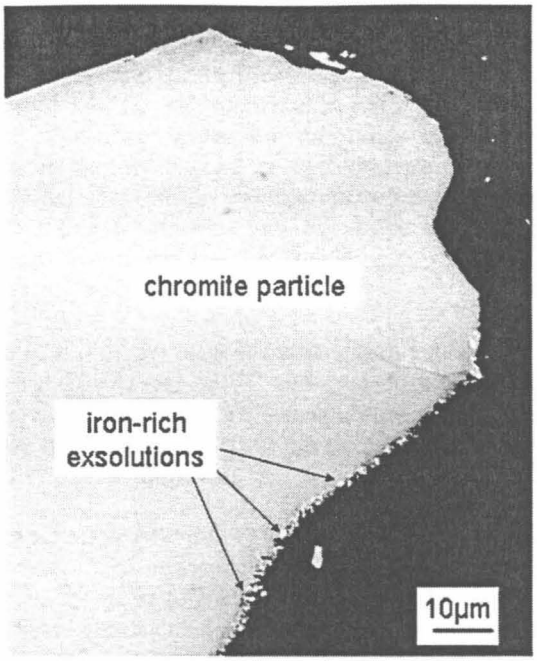


**Figure 4.8: SEM micrograph (back-scattered electron image) of a UG1 chromite particle roasted at 750°C in air for 20 minutes indicating iron rich exsolutions on the particle surface.**

**Table 4.12: Chemical composition (EDX), in mass per cent, of the iron rich exsolution in the UG 1 chromite roasted at 750°C for 20 minutes in air**

| Analysis number | Element mole % | | | | | Element mass % | | | | |
|---|---|---|---|---|---|---|---|---|---|---|
| | Si | Cr | Fe | Mg | Al | Si | Cr | Fe | Mg | Al |
| 1 | 0.2 | 16.9 | 67.3 | 5.1 | 10.5 | 0.1 | 17.4 | 74.4 | 2.5 | 5.6 |
| 2 | 0.9 | 10.1 | 63.3 | 18.2 | 7.6 | 0.6 | 11.1 | 74.7 | 9.3 | 4.3 |
| 3 | 1.3 | 11.7 | 64 | 12.5 | 10.4 | 0.8 | 12.7 | 74.3 | 6.3 | 5.9 |
| 4 | 3 | 16.3 | 57.4 | 14.2 | 9.1 | 1.8 | 17.9 | 67.8 | 7.3 | 5.2 |
| 5 | 7.3 | 12 | 53.9 | 15.9 | 10.9 | 4.6 | 13.8 | 66.6 | 8.6 | 6.5 |
| 6 | 2.1 | 7.4 | 62.8 | 7.5 | 20.2 | 1.3 | 8.3 | 75 | 3.9 | 11.6 |
| 7 | 1.4 | 7.2 | 61.7 | 24.7 | 5 | 0.8 | 8.2 | 75 | 13.1 | 2.9 |
| 8 | 0.7 | 9.7 | 58.8 | 25 | 5.8 | 0.4 | 11.1 | 71.8 | 13.3 | 3.4 |
| 9 | 0.2 | 36.2 | 24.6 | 16 | 23 | 0.2 | 44.1 | 32.1 | 9.1 | 14.5 |
| 10 | 0 | 39 | 26.2 | 13.3 | 21.5 | 0 | 46.2 | 33.2 | 7.4 | 13.2 |
| 11 | 0 | 39.4 | 25.6 | 13.2 | 21.8 | 0 | 46.7 | 32.6 | 7.3 | 13.4 |
| 12 | 0.1 | 39 | 26.4 | 13.1 | 21.4 | 0.1 | 46.1 | 33.5 | 7.2 | 13.1 |
| 13 | 0.3 | 37.8 | 26.3 | 14.1 | 21.5 | 0.2 | 45.1 | 33.6 | 7.8 | 13.3 |
| 14 | 0.3 | 38.8 | 26.1 | 13.4 | 21.3 | 0.2 | 46 | 33.3 | 7.4 | 13.1 |
| 15 | 0 | 38.3 | 27.4 | 13 | 21.4 | 0 | 45.1 | 34.6 | 7.2 | 13.1 |
| 16 | 0.1 | 37.9 | 26.9 | 14 | 21.1 | 0 | 44.9 | 34.2 | 7.8 | 13 |
| **Average** | **1.1** | **24.9** | **43.7** | **14.6** | **15.8** | **0.7** | **29.0** | **52.9** | **7.8** | **9.5** |
| Standard deviation | 1.9 | 14.1 | 18.3 | 5.0 | 6.8 | 1.2 | 17.2 | 20.3 | 2.7 | 4.4 |
| Minimum | 0.0 | 7.2 | 24.6 | 5.1 | 5.0 | 0.0 | 8.2 | 32.1 | 2.5 | 2.9 |
| Maximum | 7.3 | 39.4 | 67.3 | 25.0 | 23.0 | 4.6 | 46.7 | 75.0 | 13.3 | 14.5 |

It is postulated here that these iron rich exsolutions is the cause of the increase in magnetic susceptibility observed in figure 4.6. This mechanism would be similar to that described for ilmenite by Guzman, Taylor and Giroux (1992). It would be valuable to study this mechanism further by subjecting UG 1 chromite to longer residence times (60, 120 and 180 minutes) at 750°C in air, included in the future study.

The effect of variation in temperature on magnetic susceptibility was not as strong for the chromite as for the ilmenite – represented by LSR. The different effects are shown in greater detail in figure 4.9 a) to d). As shown by figure 4.9 a) and b), the ilmenite increased significantly in magnetic susceptibility after roasting at 700°C and 750°C, and significantly more so than the chromite. This is of course favourable for magnetic separation, where the difference in magnetic susceptibility between the ilmenite and the chromite is used to separate the two minerals. Roasting at 750°C is more favourable for magnetic separation than at 700°C, yielding differences in magnetic susceptibility (between ilmenite and chromite) of factors of three and two respectively. For these two temperatures, no significant decrease in magnetic susceptibility of the ilmenite below that of the chromite was observed for the roasting times used in this study.

As illustrated by figure 9 c) and d), the magnetic susceptibility of the ilmenite increased strongly at first (for 5 minutes' roasting) at 800°C and 850°C and then decreased below that of the chromite upon further roasting. The decrease in the magnetic susceptibility of the ilmenite was due to over-roasting. Over-roasting of chromite was only observed in one case, and then it was a weak effect, namely after 40 minutes' roasting at 850°C (see figure 4.6).

The large change in the magnetic susceptibility of the ilmenite for roasting at 850°C for relatively small differences in retention times is an undesired effect: the control of the retention time in the roasting reactor would have to be very precise to ensure separation of ilmenite from chromite. This is unlikely to be practical in industrial-scale reactors. When roasting the LSR under the tested conditions, more than one control strategy could be followed:

- High temperature, short retention time e.g. at 800°C for 5-10 minutes. The risk of over-oxidation would be high and the retention time of material in a reactor should be closely controlled. Equipment suitable for this process would be a batch reactor or a plug flow reactor with a very good control system (Levenspiel 1999)
- Lower temperature, longer retention time e.g. at 750°C for 10-40 minutes or even more. Although the maximum increase in magnetic susceptibility was not reached, a larger range of retention times in the reactor would result in very similar increases in magnetic susceptibility. This strategy would therefore be very suitable for a reactor where material had a retention time distribution, e.g. a continuous stirred tank reactor (CSTR) (Levenspiel 1999).

### 4.2.2 Concluding interpretation

The results in figure 4.2 and figure 4.3 confirm the observations made by Nell & Den Hoed (1997) when investigating the roasting of crude ilmenite: the rate of oxidation is controlled by temperature rather than gas composition.

The results of this study clearly indicate that the hypothesis that the magnetic susceptibility of chromite remains constant during magnetising roasting of an ilmenite concentrate under the oxidising conditions as used before, is not true. A change in the magnetic susceptibility of the UG 1 chromite was observed, but it was not large and it is postulated here that the mechanism for this change is the formation of iron rich exsolutions with a higher magnetic susceptibility than the chromite matrix during oxidative roasting.

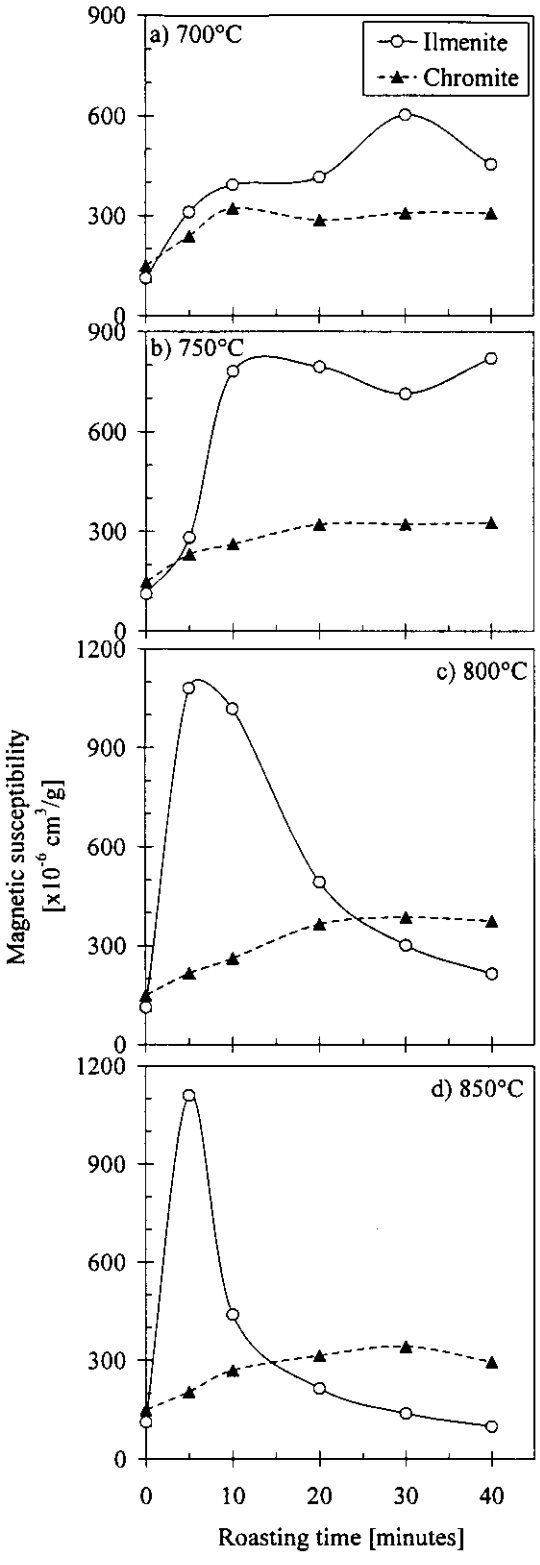


**Figure 4.9: Magnetic susceptibility of LSR and UG1 chromite samples after roasting for different time intervals in air, at different temperatures: a) 700°C, b) 750°C, c) 800°C and d) 850°C.**

Based on the assumptions that the bulk magnetic susceptibility of the LSR samples represents that of the ilmenite in the LSR, and the bulk magnetic susceptibility of UG1 chromite that of the of chromite in the LSR, the results also served to confirm that following observations regarding the conditions required for maximal separation between ilmenite and chromite:

The LSR with a high chromite content should be roasted under oxidising conditions, in a reactor with a well-defined retention time distribution (i.e. a fluidized bed reactor), at a roasting temperature of 750°C (rather than the higher temperature ranges of 800°C and 850°C).

### *4.3 Fractionation of crude ilmenite, LSR and UG 1 chromite before roasting*

#### 4.3.1 Presentation and discussion of results

In figure 4.10a) and 4.11a) separability curves are presented for the $TiO_2$ and $Cr_2O_3$ content of unroasted samples of crude ilmenite and LSR respectively.

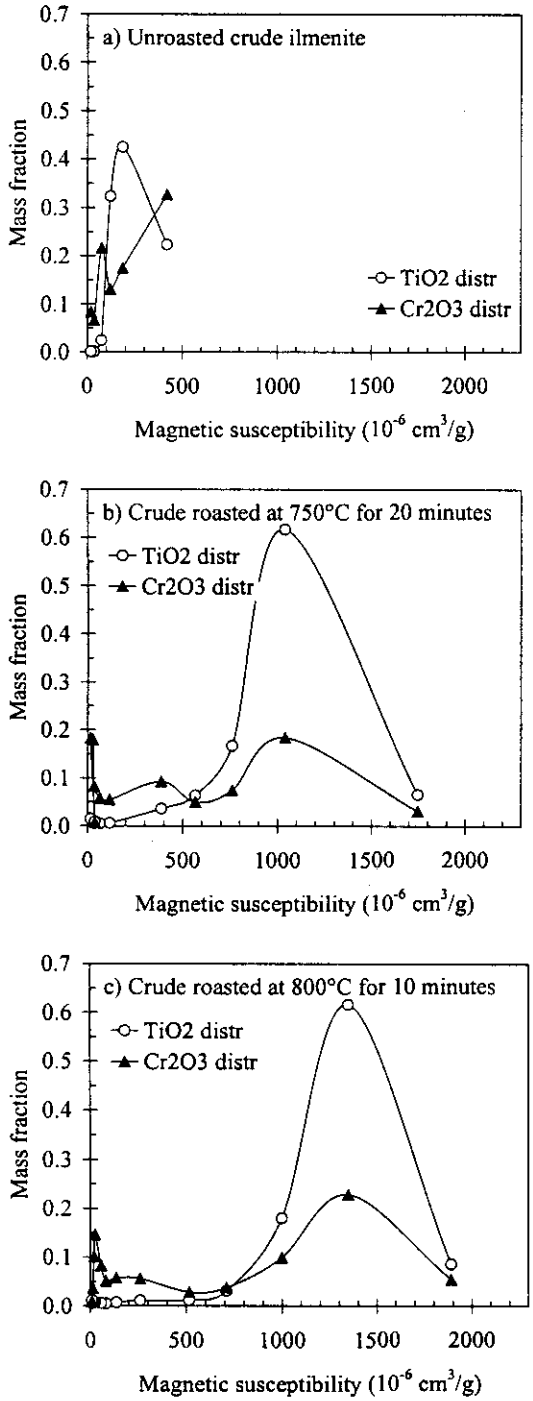


**Figure 4.10: Separability curves indicating the $TiO_2$ and $Cr_2O_3$ distributions in a) unroasted crude ilmenite; b) crude ilmenite roasted at 750°C for 20 minutes in air and c) crude ilmenite roasted at 800°C for 10 minutes in air.**

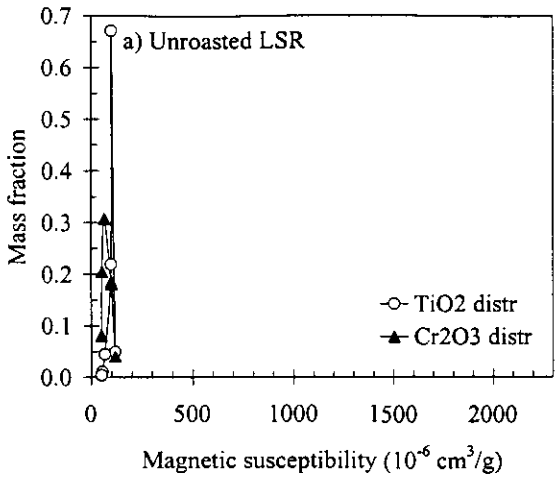


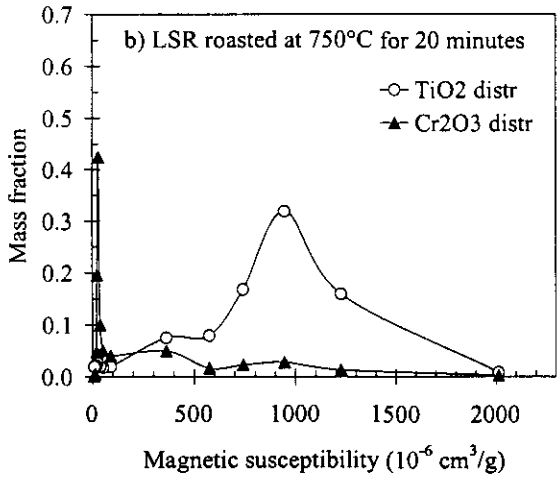


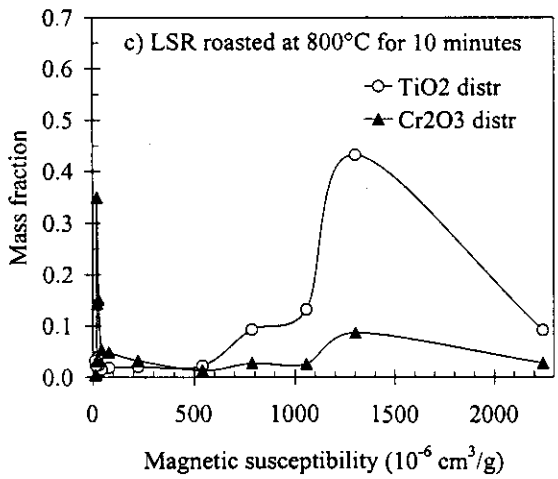


**Figure 4.11: Separability curves indicating the $TiO_2$ and $Cr_2O_3$ distributions in a) unroasted LSR; b) roasted at 750°C for 20 minutes in air and c) LSR roasted at 800°C for 10 minutes in air. The units of measurement for magnetic susceptibility are $cm^3/g$.**

The assumption was made that $TiO_2$ in the chemical analysis of each fraction represented ilmenite only and $Cr_2O_3$ chromite. This was not necessarily true as $TiO_2$ could represent ilmenite, rutile or pseudorutile. The fractionation data utilized to construct these curves are presented in table 4.13 for unroasted LSR and table 4.14 for crude ilmenite.

**Table 4.13: Fractionation results for unroasted LSR – field strength reported in Gauss; mass fraction as per cent; magnetic susceptibility reported as $*10^{-6}$ $cm^3/g$; and chemical components as mass per cent**

| Field strength | Mass fraction | Magnetic susceptibility | $TiO_2$ | $Cr_2O_3$ |
|---|---|---|---|---|
| 1375 | 10.7 | 117 | 19 | 0.20 |
| 2150 | 60.6 | 100 | 45 | 0.16 |
| 2735 | 19.5 | 99 | 46 | 0.51 |
| 3450 | 5.6 | 66 | 33 | 2.96 |
| 4050 | 1.8 | 54 | 25 | 6.14 |
| 4650 | 0.7 | 50 | 25 | 6.20 |

**Table 4.14: Fractionation results for unroasted crude ilmenite – field strength reported in Gauss; mass fraction as per cent; magnetic susceptibility reported as $*10^{-6}$ $cm^3/g$; and chemical components as mass per cent**

| Field Strength | Mass fraction | Magnetic susceptibility | $TiO_2$ | $Cr_2O_3$ |
|---|---|---|---|---|
| 1375 | 23.2 | 418 | 46 | 0.25 |
| 2150 | 42.4 | 184 | 47 | 0.07 |
| 2735 | 30.7 | 120 | 50 | 0.08 |
| 3450 | 3.0 | 74 | 40 | 1.30 |
| 4050 | 0.3 | 36 | 23 | 4.22 |
| 4650 | 0.3 | 19 | 21 | 5.50 |

The $TiO_2$ and $Cr_2O_3$ distributions of unroasted crude ilmenite in figure 4.10a) did not have a fraction of the 'high susceptible rejects' as described by Beukes and Van Niekerk (1999). This implies that the 'crude ilmenite' roasted in the fractionation exercise was more of an 'HSR-stripped crude ilmenite'. The HSR was most probably removed by the LIMS operation during pilot plant trials. The bimodal populations observed by Nell and Den Hoed (1997) for $Cr_2O_3$ were absent from these samples. In the unroasted LSR sample the $TiO_2$ was concentrated in a single population to the higher magnetic susceptible side. $Cr_2O_3$ was distributed over a larger range of magnetic susceptibility (perhaps reflecting the range of compositions shown in figure 4.1).

Representing the same set of data in a different manner recovery data sets were developed for both $TiO_2$ and $Cr_2O_3$ in unroasted crude ilmenite and unroasted LSR. The data for $Cr_2O_3$ are plotted in figure 4.12a) and figure 4.13a). Recall that the $Cr_2O_3$ content must be less than 0.1 per cent to meet the specification.

In figure 4.14 separability curves for ilmenite (represented by LSR), chromite in LSR and UG1 chromite are presented. The data used for these curves are reported in table 4.13 and table 4.15. In these separability curves the mass fraction is plotted as a function of the applied magnetic field strength and not as the inverse of magnetic susceptibility as in previous separability curves. Both the ilmenite curve and the UG 1 chromite curve have tight, single distributions while the chromite in the LSR has a wider distribution, but with a peak at the same field strength as the UG 1 chromite.

**Table 4.15: Fractionation results for unroasted UG 1 chromite – field strength reported in Gauss and mass fraction as per cent**

| Field Strength | Mass fraction |
|---|---|
| 1375 | 0.0 |
| 2150 | 0.1 |
| 2735 | 3.4 |
| 3450 | 96.1 |
| 4050 | 0.4 |

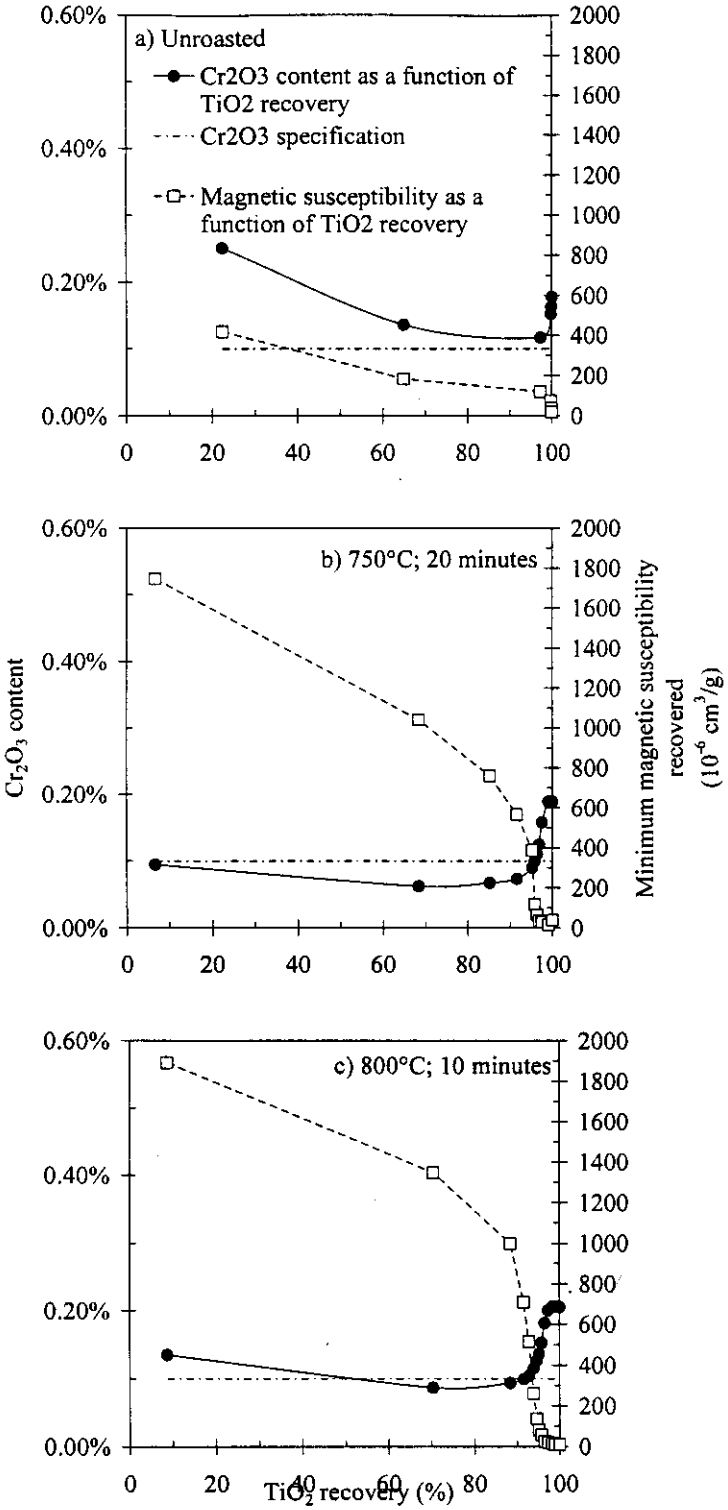


**Figure 4.12: Recovery curves of crude ilmenite indication the $Cr_2O_3$ distribution in a) unroasted crude ilmenite; b) crude ilmenite at 750°C for 20 minutes in air and c) crude ilmenite roasted at 800°C for 10 minutes in air.**

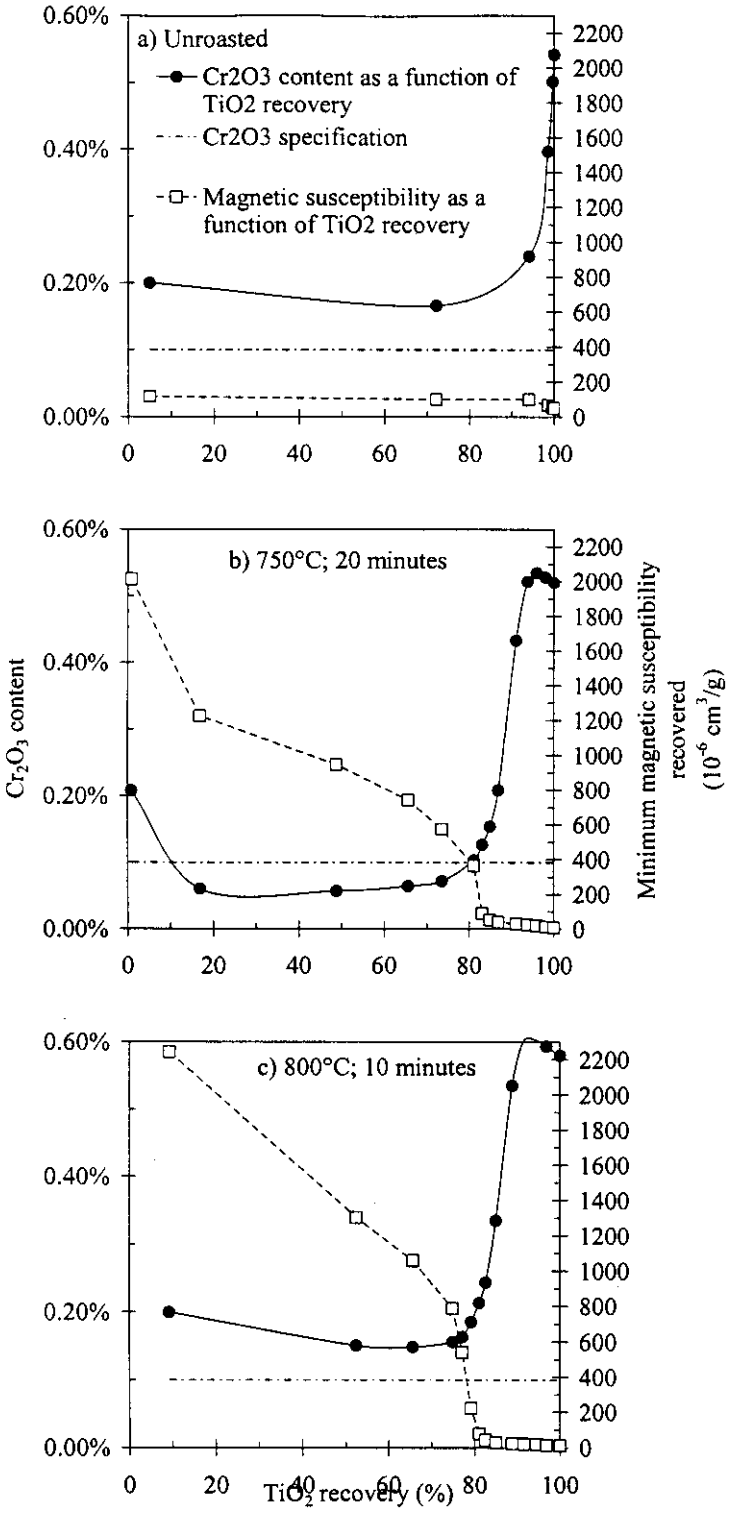


**Figure 4.13: Recovery curves of LSR indication the $Cr_2O_3$ distribution in a) unroasted LSR, b) LSR roasted at 750°C for 20 minutes in air and c) LSR roasted at 800°C for 10 minutes in air.**

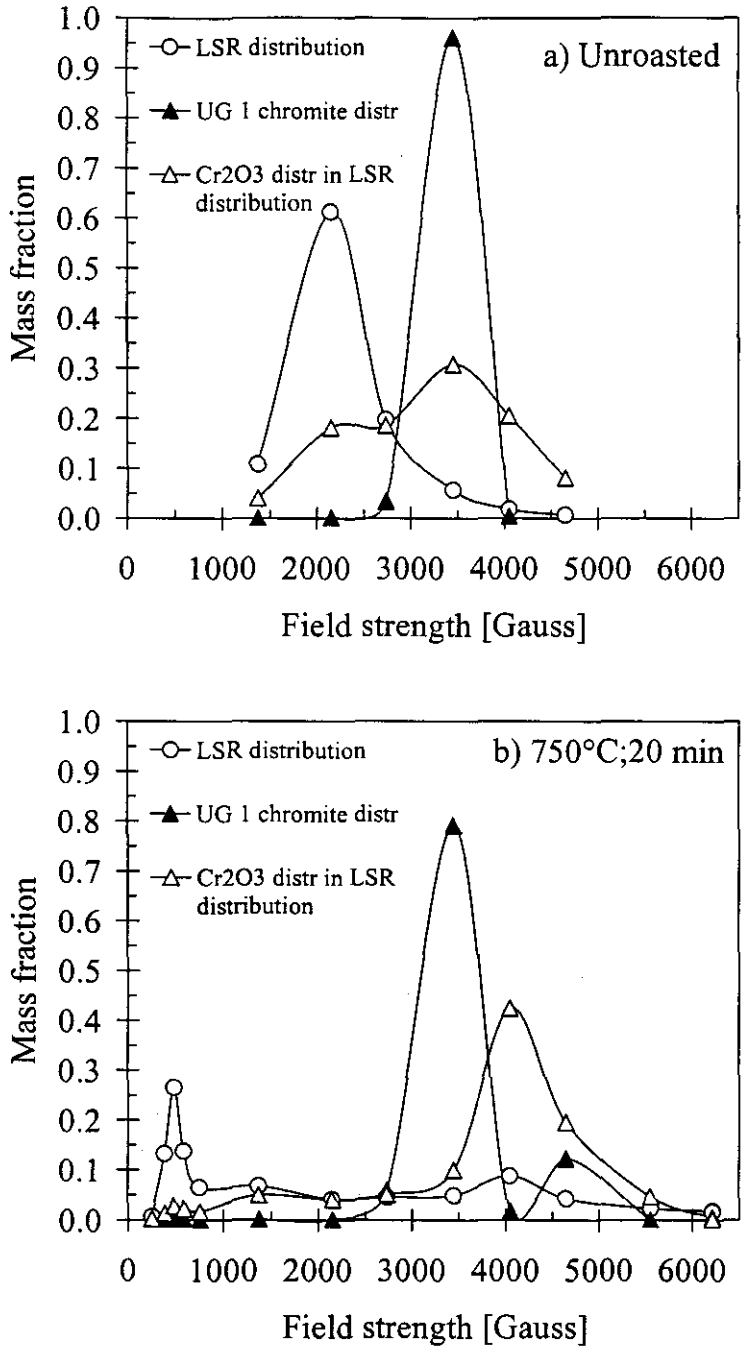


**Figure 4.14: Separability curves indicating the mass distribution of a) unroasted LSR, the chromite in unroasted LSR and unroasted UG1 chromite, and b) LSR, chromite in LSR and UG 1 chromite roasted at 750°C for 20 minutes, when fractionated at various field strengths.**

### 4.3.2 Concluding interpretation

From figure 4.12a) and 4.13a) it is concluded that without roasting a product with acceptably low $Cr_2O_3$ cannot be produced from either crude ilmenite or LSR. The results in figure 4.14 indicate that the UG 1 chromite represented at least part of the chromite in the LSR.

## *4.4 Fractionation of crude ilmenite, LSR and UG 1 chromite after roasting*

### 4.4.1 Presentation and discussion of results

After roasting crude ilmenite at 750°C for 20 minutes in air the $TiO_2$ distribution was concentrated in a single population and the $Cr_2O_3$ distribution was bimodal (see figure 4.10b). Roasting resulted in an increase in the magnetic susceptibility, in the order of $856x10^{-6}$ $cm^3/g$, for the peak in the $TiO_2$ distribution. The values obtained at the bimodal $Cr_2O_3$ peaks were $622x10^{-6}$ $cm^3/g$ and $39x10^{-6}$ $cm^3/g$ respectively. The recovery curve in figure 4.12b) indicates that the percentage $Cr_2O_3$ in the ilmenite was 0.1 per cent or less at titanium recoveries ranging from 7 to 95 per cent. The maximum recovery would be obtained by removing material with a magnetic susceptibility of less than about 400 x $10^{-6}$ $cm^3/g$.

After roasting the crude ilmenite at 800°C for 10 minutes in air (figure 4.10c) the $TiO_2$ distribution was concentrated in a single population and the $Cr_2O_3$ distribution was bimodal as also observed by Nell & Den Hoed (1997). Roasting resulted in a significant increase in the magnetic susceptibility, in the order of $1163x10^{-6}$ $cm^3/g$, for the peak in the $TiO_2$ distribution. A significant increase in magnetic susceptibility of $Cr_2O_3$, similar to the $TiO_2$ peak i.e. in the order of $1163x10^{-6}$ $cm^3/g$, was observed for the peak in the $Cr_2O_3$ distribution to the high susceptible side and a slight decrease of $159x10^{-6}$ $cm^3/g$ for that to the low susceptible side. In figure 4.12c) the per cent $Cr_2O_3$ in ilmenite recovered from HSR stripped crude ilmenite reached values of less than 0.1 per cent at titanium recoveries ranging from 55 per cent to 95 per cent. The maximum recovery would be obtained by removing material with a magnetic susceptibility of less than about 1000 x $10^{-6}$ $cm^3/g$.

The fractionation results for LSR roasted at 750°C for 20 minutes in air in figure 4.11b) were very interesting: both the $TiO_2$ and the $Cr_2O_3$ distributions concentrated in single populations. The peak magnetic susceptibility of the $TiO_2$ increased with $845x10^{-6}$ $cm^3/g$ and that of the $Cr_2O_3$ decreased with $37x10^{-6}$ $cm^3/g$. The result of this 'ideal' magnetic behaviour of the chromite and the ilmenite was the production of ilmenite with 0.1 per cent $Cr_2O_3$ or less at titanium recoveries of 10-80 per cent (figure 4.13b)! The maximum recovery would be obtained by removing material with a magnetic susceptibility of less than about 400 x $10^{-6}$ $cm^3/g$.

After roasting LSR at 800°C for 10 minutes in air (figure 4.11c) the $TiO_2$ distribution was concentrated in a single population, but spread over a wider range of susceptibilities than in the unroasted sample. The $Cr_2O_3$ distribution was bimodal. Roasting resulted in a significant increase in the magnetic susceptibility, in the order of $1200x10^{-6}$ $cm^3/g$, for the peak in the $TiO_2$ distribution. A slight decrease in magnetic susceptibility, in the order or $44x10^{-6}$ $cm^3/g$, was observed for the peak in the $Cr_2O_3$ distribution. In figure 4.13c) the per cent $Cr_2O_3$ in the recovered sample never reached the specification of <0.1 per cent.

The bimodality of the $Cr_2O_3$ distribution when roasting LSR at 800°C for 10 minutes in air could be due to:

- The low concentration of $Cr_2O_3$ in the fractions (i.e. an analytical error);
- Roasting under the specific conditions also increased the magnetic susceptibility of the chromite in the LSR fraction; or
- Different chromites in the LSR (based on chemical composition as in figure 4.1) reacts differently under the roasting conditions.

If either or the last two situations were the case it would be a problem as one would not be able to beneficiate ilmenite from chromite. The recovery curves illustrated the problem of ilmenite beneficiation from chromite in LSR more clearly. This observation gave rise to the part of the test program that tested the hypothesis that the magnetic susceptibility of the chromite did not change during roasting.

In figure 4.14b) separability curves for ilmenite (represented by LSR), chromite in LSR and chromite (represented by UG1 chromite) roasted at 750°C for 20 minutes were constructed. The data used for these curves are listed in table 4.14 and table 4.16. In these separability curves the mass fraction is plotted as a function of the applied magnetic field strength and not as the magnetic susceptibility as in previous separability curves. The UG 1 chromite curve had a bimodal distribution indicating a slight decrease in the magnetic susceptibility of some of the chromite after roasting, but also the presence of a slightly larger fraction at the field strength just lower than the peak value. Presumably the size of the

intervals used in these measurements was too large to detect the changes which resulted in the slight increase in bulk magnetic susceptibility shown in Figure 4.6. Although the chromite in the LSR had a tighter distribution than in the unroasted condition the average magnetic susceptibility of the chromite also appeared to decrease after roasting.

**Table 4.16: Fractionation results for UG 1 chromite roasted at 750°C for 20 minutes – field strength reported in Gauss and mass fraction as per cent**

| Field Strength | Mass fraction |
|---|---|
| 250 | 0.3 |
| 384 | 0.2 |
| 481 | 0.1 |
| 584 | 0.1 |
| 751 | 0.1 |
| 1375 | 0.1 |
| 2150 | 0.1 |
| 2735 | 5.8 |
| 3450 | 79.1 |
| 4050 | 1.7 |
| 4650 | 12.3 |
| 5550 | 0.0 |

### 4.4.2 Concluding interpretation

The results in figures 4.10b) and figure 4.11c) indicated that even if roasting decreased the bulk magnetic susceptibility of chromite in a crude ilmenite concentrate, it increased the magnetic susceptibility of some of the chromite particles, just as it did for ilmenite. In roasted, HSR stripped, crude ilmenite there was sufficient magnetically enhanced ilmenite to dilute the effect of the increase in magnetic susceptibility of chromite. In roasted LSR the ilmenite was insufficient to dilute the chromite. The effect was seen in figure 4.12c) and figure 4.13c) where ilmenite, with less than 0.1 per cent $Cr_2O_3$ could be recovered from crude ilmenite but not from LSR. It was possible to produce a suitable product from LSR, though, (figure 4.13b) within the range of conditions published for crude ilmenite in literature. The hypothesis that it would be possible to produce an ilmenite product suitable for ilmenite smelting by subjecting LSR to roasting and subsequent magnetic separation, at the roasting conditions published for crude ilmenite by Nell and Den Hoed (1997) or Bergeron and Prest (1974) hence survived the experimental tests applied here. Oxidising roasting did affect the magnetic susceptibility of chromite.

In short: The results from the test program were presented, discussed and interpreted. I started the discussion with the results from the feed characterization tests: the chemical analyses, the mineralogical analyses and the magnetic susceptibility. Then the results of the determination of the optimum roast conditions followed. I ended the chapter with the results from the fractionation at optimal roast conditions that was the separability curves for the unroasted and roasted material. In chapter 5 the study will be concluded and recommendations made regarding implementation and future studies.

## *4.5 Appendix 2: Method used to calculate the composition of the chromite from elemental EDX or WDS analysis.*

### 4.5.1 Assumptions

1. All the chromium is trivalent i.e. $Cr^{3+}$;
2. The chromium spinel is stoichiometric i.e. $M_3O_4$;
3. In natural magnesiochromites $Fe^{2+}$ replaces $Mg^{2+}$ to some extent and $Al^{3+}$ and $Fe^{3+}$ replace $Cr^{3+}$ to some extent;
4. The composition of natural magnesiochromites could be simplified to containing MgO, FeO, $Fe_2O_3$, $Cr_2O_3$ and $Al_2O_3$ only.

### 4.5.2 Calculations

#### *4.5.2.1 Calculation 1: The $Fe^{2+}$ and $Fe^{3+}$ content of the mineral*

The data that would be available for the calculation of the $Fe^{2+}$ and $Fe^{3+}$ content of a stoichiometric chromite spinel is as in table 4.17.

**Table 4.17: Data available when calculating the $Fe^{2+}$ and $Fe^{3+}$ content of the chromium spinel from elemental WDS and EDX analyses**

| Element | Assumed valence state | Molar mass | Mole per cent |
|---|---|---|---|
| O | 2- | 16.0 | As received |
| Mg | 2+ | 24.3 | As received |
| $Fe_{total}$ | 2+ and 3+ | 55.9 | As received |
| Al | 3+ | 27.0 | As received |
| Cr | 3+ | 52.0 | As received |

The $Fe^{2+}$ content is calculated according to equation 4.2 and the $Fe^{3+}$ content according to equation 4.3 where $^{m}/_{o}$ means mole per cent.

**Equation 4.2: Calculation of the $Fe^{2+}$ content of a stoichiometric chromite spinel**

$$n^{Fe2+} = \tfrac{1}{3}(n^{Cr3+} + n^{FeTotal} + n^{Al3+} - 2\,n^{Mg2+})$$

**Equation 4.3: Calculation of the $Fe^{3+}$ content of a stoichiometric chromite spinel**

$$^{m}/_{o}Fe^{3+} = {}^{m}/_{o}Fe_{total} - {}^{m}/_{o}Fe^{2+}$$

Equation 4.2 was derived as follows: the mole ratio of $M^{2+}$:O:$M^{3+}$:O in stoichiometric spinel ($M_3O_4$ or $M^{2+}O.M^{3+}{}_2O_3$) is 1:1:2:3. This means that the spinel would contain half a mole of cation in the trivalent state for every mole of cation in the divalent state as in equation 4.4 where *n* is the mole fraction of a cation:

**Equation 4.4: Balance of divalent and trivalent cations in a stoichiometric spinel**

$$n^{2+} = \tfrac{1}{2}n^{3+}$$

The divalent cations in the magnesiochromites are $Fe^{2+}$ and $Mg^{2+}$ and the trivalent cations $Al^{3+}$; $Fe^{3+}$ and $Cr^{3+}$. Incorporating this knowledge in equation 4 leads to equation 4.5:

**Equation 4.5: Incorporating the divalent and trivalent cations for a magnesiochromite in equation 4.4**

$$(n^{Fe2+} + n^{Mg2+}) = \tfrac{1}{2}(n^{Cr3+} + n^{Fe3+} + n^{Al3+})$$

From table 4.17 the results reported in the WDS or EDX analyses are for the total Fe content of the mineral. In the mineral itself the Fe are in both the divalent or trivalent states. This leads to the mass balance in equation 4.6:

**Equation 4.6: Mass balance of iron in the magnesiochromite spinel**

$$n^{FeTotal} = n^{Fe3+} + n^{Fe2+}$$

or

$$n^{Fe3+} = n^{FeTotal} - n^{Fe2+}$$

Equation 4.2 is then derived from equation 4.5 and equation 4.6 as in the series of equations in equation 4.7:

**Equation 4.7: Derivation of equation 4.2 from equation 4.5 and equation 4.6**

$$\begin{aligned}
(n^{Fe2+} + n^{Mg2+}) &= \tfrac{1}{2}(n^{Cr3+} + n^{FeTotal} - n^{Fe2+} + n^{Al3+}) \\
2\ (n^{Fe2+} + n^{Mg2+}) &= (n^{Cr3+} + n^{FeTotal} - n^{Fe2+} + n^{Al3+}) \\
2\,n^{Fe2+} + 2\,n^{Mg2+} + n^{Fe2+} &= n^{Cr3+} + n^{FeTotal} + n^{Al3+} \\
3\,n^{Fe2+} &= n^{Cr3+} + n^{FeTotal} + n^{Al3+} - 2\,n^{Mg2+} \\
n^{Fe2+} &= \tfrac{1}{3}(n^{Cr3+} + n^{FeTotal} + n^{Al3+} - 2\,n^{Mg2+})
\end{aligned}$$

Therefore if the results of equation 4.3 are negative (negative $Fe^{3+}$ content) it would mean that iron are only present in the divalent state in the magnesiochromite spinel.

*4.5.2.2 Calculation 2: The composition of the mineral*

Once the molar per cent $Fe^{2+}$ and $Fe^{3+}$ of the mineral has been determined the composition of the mineral can be derived by firstly calculation the mass and then the mass per cent of each component in the mineral. The equations for these calculations are given in table 4.18 – note the difference in the mass calculations for components in the divalent and trivalent state. For these calculations the information in table as well as the results of equation 4.2 and equation 4.3 is utilized.

**Table 4.18: Equations used to calculate the mass per cent of the components in the chromium spinel from elemental WDS and EDX analyses where $^{m}/_{o}$ means mole per cent and $^{w}/_{o}$ mass per cent.**

| Component | Mass calculations | Mass per cent calculations |
|---|---|---|
| MgO | $MgO_{mass} = {}^{m}/_{o}\ Mg^{2+} \times MgO_{molar\ mass}$ | $^{w}/_{o}\ MgO = MgO_{mass} / total_{mass} \times 100$ |
| FeO | $FeO_{mass} = {}^{m}/_{o}\ Fe^{2+} \times FeO_{molar\ mass}$ | $^{w}/_{o}\ FeO = FeO_{mass} / total_{mass} \times 100$ |
| $Fe_2O_3$ | $Fe_2O_{3\ mass} = {}^{m}/_{o}\ Fe^{3+} \times ½(Fe_2O_{3\ molar\ mass})$ | $^{w}/_{o}\ Fe_2O_3 = Fe_2O_{3\ mass} / total_{mass} \times 100$ |
| $Cr_2O_3$ | $Cr_2O_{3\ mass} = {}^{m}/_{o}\ Cr^{3+} \times ½(Cr_2O_{3\ molar\ mass})$ | $^{w}/_{o}\ Cr_2O_3 = Cr_2O_{3\ mass} / total_{mass} \times 100$ |
| $Al_2O_3$ | $Al_2O_{3\ mass} = {}^{m}/_{o}\ Al^{3+} \times ½(Al_2O_{3\ molar\ mass})$ | $^{w}/_{o}\ Al_2O_3 = Al_2O_{3\ mass} / total_{mass} \times 100$ |
| Total | $Total_{mass} = MgO_{mass} + FeO_{mass} + Fe_2O_{3\ mass} + Cr_2O_{3\ mass} + Al_2O_{3\ mass}$ | |

*4.5.2.3 Calculation 3: The normalized elemental composition of the mineral*

For ease of interpretation and comparison of results the elemental results from the EDX and WDS analysis (in mole per cent) are normalized by dividing the mole per cent of a specific element by the totalized mole per cent of the elements in the analysis. As an example the chrome content of the magnesiochromite is normalized in equation 4.8:

**Equation 4.8: Example of normalized elemental results**

$$^{m}/_{o}\ Cr_{normalised} = {}^{m}/_{o}\ Cr / ({}^{m}/_{o}\ Mg + {}^{m}/_{o}\ Fe_{total} + {}^{m}/_{o}\ Al + {}^{m}/_{o}\ Cr) \times 100$$

# Chapter 5: Conclusions & recommendations

In chapter 4 the results from the test program were presented, discussed and interpreted. In this chapter the study is concluded and recommendations made regarding implementation and future studies. I start this chapter by summarizing the main findings of the study. Then these findings are linked to literature and theory. Gaps, anomalies and deviations in the data are discussed. The chapter is concluded with recommendations for future studies. The order of discussions is:

5.1 Summary of main findings
5.2 Results linked to literature and theory
5.3 Gaps, anomalies and deviations in data
5.4 Recommendations

## 5.1 Summary of main findings

During preparation of the LSR sample from a crude ilmenite concentrate 90 per cent of the chromite and 29 per cent of the ilmenite in the crude ilmenite reported to the LSR fraction. The ilmenite content of LSR at 84.6 per cent was lower than that of crude ilmenite at 90.8 per cent, reflecting a higher content of non-ilmenite related minerals in the LSR (15.4 per cent vs. 9.2 per cent). The chromite content of LSR at 1.1 per cent was double that of crude ilmenite at 0.4 per cent resulting in a $Cr_2O_3$ content of LSR at 0.56 per cent vs. 0.21 per cent in crude ilmenite. I came to the conclusion that it would be more difficult to decrease the $Cr_2O_3$ content of the LSR to less than 0.1 per cent, than for crude ilmenite, given the higher $Cr_2O_3$ content in LSR as well as the lower $TiO_2$ available for dilution of the $Cr_2O_3$.

With the $Fe_2O_3$: FeO mass ratios of both the crude ilmenite and the LSR being less than 1-1.57 (0.44 and 0.74 respectively), I assumed that oxidative roasting will enhance the magnetic susceptibility of the ilmenite in both types of material. No amount of roasting and/or magnetic separation would decrease the content of MgO, MnO and $V_2O_5$ in the final ilmenite product though, because these components are in solid solution in the ilmenite. If the magnetic susceptibility of only the ilmenite in crude ilmenite or LSR could be increased, the content of CaO, $SiO_2$ and $Al_2O_3$ in the final ilmenite product could be decreased by magnetic separation.

When roasting LSR the rate of oxidation – as measured by the rate of increase in magnetic susceptibility - is controlled by temperature rather than the oxygen content of the oxidizing gas atmosphere. As for crude ilmenite an ideal, single roasting condition does not exist for LSR and the appropriate roasting conditions for crude ilmenite are also appropriate to LSR. The study indicated that when roasting LSR two control strategies could be followed: a high temperature (800°C), short retention time (5 to10 minutes) strategy or low temperature (750°C), long retention time (10 to 40 minutes) strategy. When exceeding the maximum retention time limits the magnetic susceptibility of the both the crude ilmenite and the LSR decreased. This decrease was attributed to over-roasting as described by Nell and Den Hoed (1997).

Separability curves for crude ilmenite and LSR samples roasted at 800°C for 10 minutes in air indicated that roasting increased the magnetic susceptibility of both the ilmenite in the concentrate as well as the chromite. In the roasted crude ilmenite sufficient ilmenite was available to dilute the chromite present to less than 0.1 per cent $Cr_2O_3$. (It is worth recalling that the $Cr_2O_3$ content of LSR was much higher than crude ilmenite: 0.6 per cent compared with 0.2 per cent). In LSR insufficient ilmenite was present to dilute the chromite present to less than 0.1 per cent $Cr_2O_3$. Separability curves for crude ilmenite and LSR samples roasted at 750°C for 20 minutes in air indicated that roasting increased the magnetic susceptibility of both the ilmenite in the concentrate as well as the chromite. In both the roasted crude ilmenite and the LSR sufficient ilmenite was available to dilute the chromite present to less than 0.1 per cent $Cr_2O_3$. Therefore the quality and recovery of ilmenite was a function of the rate of enhancement of magnetic susceptibility of ilmenite relative to that of chromite. These results show that it is possible to produce an ilmenite product suitable for ilmenite smelting by subjecting LSR to roasting and subsequent magnetic separation, under the roasting conditions published for crude ilmenite by Nell and Den Hoed (1997) or Bergeron and Prest (1974).

The chromite in the LSR was of the magnesiochromite spinel series. The chromite in the UG1 sample was also of the magnesiochromite spinel series and very close in composition to that of the chromite in LSR – this being the reason for the selection of UG1 chromite for this study. The mass ratio of $Fe_2O_3$:FeO in the chromite from the LSR was 0.5 whilst in the UG 1 chromite it was 0.64. I therefore assumed that should roasting have an impact on the magnetic susceptibility of the UG1 chromite the impact on the chromite in LSR would be more significant that that of the UG1 chromite. When subjecting the UG1 chromite to varying roasting conditions the results indicated that the hypothesis that the magnetic susceptibility of chromite remains constant during magnetizing roasting of an ilmenite concentrate under the oxidising conditions, was not true. Roasting did increase the magnetic susceptibility of the UG1 chromite and iron rich exsolutions was observed on the roasted UG 1 chromite particle surface. I then postulated that these iron rich exsolutions is the cause of the increase in magnetic susceptibility observed in UG 1 chromite.

## 5.2 Results linked to literature and theory

The crude ilmenite used in this study had a composition similar to that of the crude ilmenite described by Nell and Den Hoed (1997). At 90.8 per cent the ilmenite content of the crude ilmenite was similar to the 90.0 per cent reported by Nell and Den Hoed (1997). The $Cr_2O_3$ content of the crude ilmenite used in this study (0.21 per cent) was less than the typical values quoted by Nell and Den Hoed (0.3 per cent). No published data was available on the composition of LSR. The $Fe_2O_3$: FeO ratios of both the crude ilmenite and the LSR, 0.44 and 0.74 respectively, were less than 1-1.57. According to Walpole (1991) this ratio would have been the $Fe_2O_3$: FeO ratio at which the magnetic susceptibility of ilmenite would be at a maximum. It was therefore concluded that to increase this ratio from 0.44-0.77 to 1-1.57 the ilmenite in both the LSR and the crude ilmenite had to be oxidized.

Beukes and Van Niekerk (1999) did not propose roasting conditions for LSR. This study indicates that for beneficiation purposes LSR could be roasted under some of the conditions used for the roasting of crude ilmenite, but that the roasting conditions should be chosen with care. This study confirms observations made by previous investigators on the effect of the roasting atmosphere, temperature range and retention time ranges on the magnetic susceptibility of crude ilmenite (Nell and Den Hoed 1997; Bergeron and Prest 1974). Nell and Den Hoed reported a five– to six fold increase in magnetic susceptibility of crude ilmenite at 750°C in about 30 minutes. Similar results were observed for crude ilmenite roasted at 750°C from 5 to 40 minutes and for LSR from 10 to 40 minutes. At 800°C the results of this study differed from that of Nell and Den Hoed (1997), though. For 30 minutes at 800°C Nell and Den Hoed (1997) reported their optimum increase in magnetic susceptibility, while the results of this investigation indicate that much shorter reaction times (less than 10 minutes) are required at 800°C for both LSR and crude ilmenite. Nell and Den Hoed (1997) stated that the risk of over roasting at 800°C was high and less so at 750°C. This was also observed in this study.

Nell and Den Hoed (1997) reported a 90 per cent recovery when separating material at about 500 x $10^{-6}$ $cm^3/g$ for crude ilmenite roasted at 750°C for 30 minutes. The results of this study indicate the same recovery (90 per cent) for crude ilmenite but with separation at lower magnetic field strengths (about 400 x $10^{-6}$ $cm^3$cc/g). The recovery for LSR is less, at 65 per cent, for separation at 400 x $10^{-6}$ $cm^3/g$, which was expected, given that LSR contained so much more gangue and material other than ilmenite. Nell and Den Hoed (1997) stated that roasting did not increase the magnetic susceptibility of other minerals present in their crude ilmenite concentrate. They stated that there was a tendency for Fe-containing spinels (including chromium) to become less magnetized during roasting under oxidizing conditions. The results in this study indicated that roasting under oxidizing conditions could increase as well as decrease the magnetic susceptibility of chromite in both the crude ilmenite and the LSR concentrate. The rate at which the increase in magnetic susceptibility took place was different for the ilmenite and the chromite – more so at 800°C than at 750°C. At 750°C the risk of over-roasting of ilmenite is lower than at 800°C and the prospect of separation of ilmenite from chromite higher.

## 5.3 Gaps, anomalies and deviations in the data

One might ask the question: How would the results from a small sample of crude ilmenite or LSR prepared on laboratory scale equipment compare to the variation in composition observed in a full scale operation?

Another question that arose was: How would the results from this laboratory scale, batch process investigation compare to that of a full scale continuous process plant where retention time distributions and temperature gradients in the roasting reactor are realities that have to be dealt with?

Utilizing one type of natural chromite, UG1 chromite, to represent another type of natural chromite, chromite in the unroasted LSR, is risky. The first prize would have been to separate chromite from the LSR to utilize in the study. Practical problems render such an approach unfeasible (the chromite content of LSR, expressed as mass percentage of $Cr_2O_3$, is only 0.6 per cent).

## 5.4 Recommendations

1. When characterizing the feed material used for these types of experiments the following analysis methods were most useful:
   - XRF analysis
   - Reflected light microscopy
   - Micro-analysis
   - Particle counting
   - QEM-SEM and QEM-scan
   - Malvern particle size analysis
   - Magnetic susceptibility measurements
2. The following analyses should be used or interpreted with caution:
   - Titration ($Fe^{2+}/Fe^{3+}$ analysis)
3. The following analyses were not useful:
   - XRD
4. Further analyses that would have been useful but were not conducted were:
   - $Fe^{2+}/Fe^{3+}$ content of the unaltered and altered ilmenite in the crude ilmenite and the LSR before and after roasting as well as that of the chromite before and after roasting.
5. The study indicated that when roasting LSR two process control strategies could be followed: a high temperature (800°C), short retention time (5-10 minutes) OR low temperature (750°C), long retention time (10-40 minutes). Care should be taken not to over- or under roast the crude ilmenite or LSR. The process control strategies for crude ilmenite could be similar. From a roaster reactor perspective the same reactor could be used to roast both LSR and crude ilmenite, i.e. the roaster for Process #1 and Process #3 described by Beukes and Van Niekerk could be the same reactor. The plants for Process #1 vs. Process #3 would differ in materials handling and magnetic separation equipment.
6. Determining the impact of different roasting conditions on the rate at which the magnetic susceptibility of chromite increases relative to the rate at which the magnetic susceptibility of ilmenite increases would be useful from an operating perspective. The ideal roasting conditions would be where the magnetic susceptibility of the ilmenite increases at a high rate - where the risk of over-roasting could still be managed - while that of the chromite increase at a very low rate. The process should be terminated at the optimum point for separation.
7. To determine how representative the fractionation test results would be of other roasting and magnetic separation methods, the procedure would have to be repeated on the feed material used for the other methods and the results compared to that of the methods. This would provide a basis for comparison of various test results.
8. When roasting LSR under the tested conditions (kinetic control), more than one control strategy could be followed:
   - High temperature, short retention time i.e. at 800°C for 5-10 minutes. The risk of over oxidation was high and the retention time of material in a reactor should be closely controlled. Equipment suitable for this process would be a batch reactor or a plug flow reactor (PFR) with a very good control system (Levenspiel 1999).
   - Lower temperature, longer retention time i.e. at 750°C for 10-40 minutes or even more. Although the maximum increase in magnetic susceptibility was not reached, a larger range of retention times in the reactor would result in very similar increases in magnetic susceptibility. This strategy was therefore very suitable for a reactor where material has a retention time distribution, i.e. a continuous stirred tank reactor (CSTR) (Levenspiel 1999).
9. As a control strategy on LSR roasting the low temperature (750°C), long retention time (10-40 minutes) approach would be recommended, especially when roasting in a reactor that would have a wide retention time distribution. The retention time distribution of a reactor could be determined

by introducing a tracer material with the feed and sample the product at regular intervals with subsequent analysis of the tracer content in the product. The impact of changes in the feed rate and subsequent increase in hold-up on the retention time distribution of the reactor should be determined as well.

10. These tests indicated that because LSR had much higher chromite contents than crude ilmenite and much less ilmenite to dilute it with, it would be very important to enhance the magnetic susceptibility of all of the ilmenite carefully and to enhance the magnetic properties of any of the chromite as little as possible. It seems that the rate of enhancement of the magnetic susceptibility of chromite is considerably lower than that of ilmenite at lower temperatures.
11. It would be interesting to compare the results of this study to high chromite containing ilmenite concentrates from deposits elsewhere in the world.
12. A study should be conducted on the proposed mechanism for the increase in magnetic susceptibility of the UG1 chromite by subjecting both the UG 1 chromite and the LSR chromite to longer residence ties (i.e. 60, 120 and 180 minutes at 750°C in air). Characterisation of both the roasted and unroasted particles should include SEM optical analysis and EDX and WDS chemical analyses.
13. Could these results be extrapolated to include the behaviour of chromite and ilmenite when roasting the high susceptibility rejects (HSR)?

In short: In chapter 5 the study was concluded and recommendations were made regarding implementation and future studies.

**List of References/Bibliography**

Andres U. 1976. Magnetohydrodynamic and magnetohydrostatic methods of mineral separation. John Wiley & Sons, Chichester, The United Kingdom, pp130-158 and 203-218.

Arvidson BR and Rademeyer L. 1997. Rare-earth magnetic separators for mineral sands applications in Proceedings of Heavy Minerals 1997, edited by RE Robinson, Symposium series S17, pp 129-135 (The South African Institute of Mining and Metallurgy: Johannesburg).

Arvidson BR. 1999. Advances in rare-earth magnetic drum separators for heavy mineral sands processing in Proceedings of Heavy Minerals 1999, edited by RG Stimson, Symposium series S23, pp 121-124 (The South African Institute of Mining and Metallurgy: Johannesburg).

Arvidson BR. 2001. The many uses of rare-earth magnetic separators for heavy mineral sands processing, in Proceedings of Heavy Minerals Conference 2001. Fremantle, 18-19 June 2001, pp 131-136 (The Australasian Institute of Mining and Metallurgy: Victoria).

Balderson, GF. 1999. Flowsheet development options for a greenfield titanium minerals project, in Proceedings of Heavy Minerals 1999, edited by RG Stimson, Symposium series S23, pp 125-136 (The South African Institute of Mining and Metallurgy: Johannesburg).

Banerjee SK. 1991. Magnetic properties of Fe-Ti oxides. Oxide minerals: Petrology and magnetic significance, Reviews in Mineralogy, vol 25 edited by DH Lindley, pp107-128 (Mineralogical Society of America).

Bartkowiak RA. 1985. Electric circuit analysis. John Wiley and Sons, Inc. New York. ISBN 0-471-61632-X. Pp240-241

Bergeron, M and Prest, SF, (to QIT-Fer et Titane Inc.), 1974. Magnetic separation of ilmenite, South African Pat 74/7810.

Beukes, JA and Van Niekerk, C, 1999. Chromite removal from crude ilmenite, in Proceedings of Heavy Minerals 1999, edited by RG Stimson, Symposium series S23, pp 97-100 (The South African Institute of Mining and Metallurgy: Johannesburg).

Borowiec K & Rosenqvist T. 1981. Phase relations and oxidation studies in the system Fe-$Fe_2O_3$-$TiO_2$ at 700-1100°C. Scandanavian Journal of Metallurgy 10, pp217-224.

Bozorth RM et al. 1957. Magnetisation of Ilmenite-Hematite system at low temperatures. Letter to the editor of Physical review, volume 108 number 1, October 1, 1957.

Burton, B. Thermodynamic analysis of the system $Fe_2O_3$-$FeTiO_3$. Physics and Chemistry of Minerals Vol 11. 1984. Pp. 217-224.

Coertze FJ and Coetzee CB. 1992. Chromium. Mineral resources of the Republic of South Africa, edited by CB Coetzee. Fifth edition, fourth impression 1992, p117.

Coetzee CB and De Villiers SB. 1992. Silicon. Mineral resources of the Republic of South Africa, edited by CB Coetzee. Fifth edition, fourth impression 1992, pp203.

Dana J.D. and Dana E.S. 1944. The System of Mineralogy. Seventh edition. John Wiley and Sons, Inc, New York, pp.709-711

Deer WA et al. 1966. An Introduction to the Rock-Forming Minerals. Longmans, Green and Co. Ltd, London, pp. 429.

De Waal, SA and Copelowitz, I. 1972. The Interdependence of the Physical Properties and Chemical Composition of Chrome Spinels from the Bushveld Igneous Complex. Proceedings of 24th IGC, 1972 - section 14, pp171-179.

Dunlop, DJ. 1990. Developments in rock magnetism. Rep. Prog. Phys. 53 (1990) p707-792.

Erasmus, DE. 1997. Dry magnetic and electrostatic beneficiation of a Gravelotte heavy mineral spiral concentrate in Proceedings of Heavy Minerals 1997, edited by RE Robinson, Symposium series S17, pp 125-128 (The South African Institute of Mining and Metallurgy: Johannesburg).

Fisher. JR. 1997. Developments in the $TiO_2$ pigments industry which will drive demand for $TiO_2$ mineral feedstock, in Proceedings of Heavy Minerals 1997, edited by RE Robinson, Symposium series S17, pp 207-217 (The South African Institute of Mining and Metallurgy: Johannesburg).

Gaskell. DR. 1981. Introduction to metallurgical thermodynamics, 2nd edition. Hemisphere Publishing Corporation. New York

Gouws JD and Van Dyk JP. 2001. Ilmenite beneficiation by roasting & magnetic separation, , in Proceedings of Heavy Minerals Conference 2001. Fremantle, 18-19 June 2001, pp 201-208 (The Australasian Institute of Mining and Metallurgy: Victoria).

Grey, IE and Li, C, 2001. Low temperature roasting of Ilmenite – phase chemistry & applications, in Proceedings of Heavy Minerals Conference 2001. Fremantle, 18-19 June 2001, pp 201-208 (The Australasian Institute of Mining and Metallurgy: Victoria).

Gupta SK et al. 1989. Phase relationships in the system $Fe$-$Fe_2O_3$-$TiO_2$ at 700 and 900°C. Canadian Metallurgical Quarterly, vol. 28, No 4, pp331-335.

Guzman, S, Taylor JF & Giroux, JC (to QIT-Fer et Titane Inc.), 1992. Beneficiation of ilmenite. South African Pat 924151.

Hammerbeck, ECI. 1992a. Copper. Mineral resources of the Republic of South Africa, edited by CB Coetzee. Fifth edition, fourth impression 1992, p125.

Hammerbeck, ECI. 1992b. Titanium. Mineral resources of the Republic of South Africa, edited by CB Coetzee. Fifth edition, fourth impression 1992, pp221-226.

Hayes, PC. 1993. Process principles in minerals and materials production. Hayes publishing co. Sherwood, Queensland, Australia.

Hopstock DM. 1975. Fundamental aspects of design and performance of low-intensity dry magnetic separators. Transactions of the Society of Mining Engineers, AIME, September 1975 pp 222-227.

Ishikawa Y and Akimoto S. 1957a. Effect of heat treatments on the magnetic properties of the $FeTiO_3$-$Fe_2O_3$ solid solution series. Journal of the Physical Society of Japan vol 12 page 834-835.

Ishikawa Y and Akimoto S. 1957b. Magnetic properties of the $FeTiO_3$-Fe2O3 solid solution series. Journal of the Physical Society of Japan vol 12 page 834-835.

Jones R & Meihack W. 1988-1994. THERMO v2.09. Copyright 1988-94

Kelly EG and Spottiswood DJ. 1995. Introduction to mineral processing. Published by the Australian Mineral Foundation. ISBN 0-471-03379-0, pp 46-61 and pp 274-290.

Lätti, AD. 1997. The application of QEM*SEM to the Quelimane heavy mineral deposit, Mozambique, in Proceedings of Heavy Minerals 1997, edited by RE Robinson, Symposium series S17, pp 197-201 (The South African Institute of Mining and Metallurgy: Johannesburg).

Levenspiel, O. 1999. Chemical reaction engineering 3rd edition. Published by John Wiley and Sons. ISBN 0-471-25424-X.

McPherson, RD. 1982. Mineral processing at Richards Bay Minerals. Proceedings, 12th CMMI Congress. H.W. Glen (ed.) Johannesburg, SAIMM. pp. 835-839

Merritt, RR and Cranswick, LMD. 1994. The origin of magnetic susceptibility in roasted ilmenite, in Proceedings of The 6th AusIMM Extractive Metallurgy Conference Proceedings. Brisbane, 3-6 July 1994, pp 171-180 (The Australasian Institute of Mining and Metallurgy: Victoria).

Nell, J, 2001. Personal communication. March.

Nell, J, 1999. An overview of the phase-chemistry involved in the production of high-titanium slag from ilmenite feedstock, in Proceedings of Heavy Minerals 1999, edited by RG Stimson, Symposium series S23, pp 137-145 (The South African Institute of Mining and Metallurgy: Johannesburg).

Nell, J and Den Hoed, P, 1997. Separation of chromium oxides from ilmenite by roasting and increasing the magnetic susceptibility of $Fe_2O_3$-$FeTiO_3$ (ilmenite) solid solutions, in Proceedings of Heavy Minerals 1997, edited by RE Robinson, Symposium series S17, pp 75-78 (The South African Institute of Mining and Metallurgy: Johannesburg).

Nord GL et al. 1989. Order-disorder transition-induced twin domains and magnetic properties in ilmenite-hematite. American Mineralogist, vol 74 p 160-176.

O'Reilly W and Banerjee SK. 1966. Oxidation of titanomagnetites and self-reversal. Nature July 2, 1966 vol 211 pp26-28.

O'Reilly W and Banerjee SK. 1967. The mechanism of oxidation in titanomagnetites: a magnetic study. p29-37

Pistorius, PC. 1999. Limits on energy and reductant inputs in the control of ilmenite smelters, in Proceedings of Heavy Minerals 1999, edited by RG Stimson, Symposium series S23, pp 183-188 (The South African Institute of Mining and Metallurgy: Johannesburg).

Porter M.E. 1988. Competitive Strategy. Harvard Business School Video

Putnis, A. Introduction to mineral sciences. Cambridge University Press, London. 1992.

Readman PW and O'Reilly W. 1972. Magnetic properties of oxidized (cation-deficient) titanomagnetites (Fe, Ti, □)$_3O_4$ Journal of geomagnetism and geoelectricity vol 24 pp 69-90.

Reaveley BJ and Scanlon TJ. 2001. Murray Basin ilmenite - realizing the value, in Proceedings of Heavy Minerals Conference 2001. Fremantle, 18-19 June 2001, pp 201-208 (The Australasian Institute of Mining and Metallurgy: Victoria).

Schwerer FC and Gundaker W. 1975. Magnetic properties of natural chromites: mechanical and thermal effects. Society of Mining Engineers AIME Transactions vol 258, June 1975. Pp 88-94

Sears FW, Zemansky MA and Young HD. 1987. University Physics, 7th edition. Published by the Addison-Wesley Publishing Company – World series edition ISBN 0-201-06694-7, p714-730

Smith WF. 1990. Principles of materials science and engineering. 2nd edition. McGraw-Hill publishing company, New York ISBN 0-07-100936-1. pp78-81; 571-577; 635-648

Strauss. L. 1990. Inleidende fisika. Published by the author and distributed by Van Schaik, Pretoria. ISBN 0-86979-282-2, pp 264

Svoboda J. 1987. Magnetic methods for the treatment of minerals. Elsevier Science Publishers, Amsterdam, The Netherlands, ISBN 0-444-41804-0, pp1-55 and 222-235.

Ulmer GC. 1970. Chromite spinels. High temperature oxides Part 1. Edited by AM Alper. Academic Press, New York. Pp 251-314

Van der Westhuisen, WG. 2001. Pilot plant work as an aid to process flow line development and process choices, in Proceedings of Heavy Minerals Conference 2001. Fremantle, 18-19 June 2001, pp 101-106 (The Australasian Institute of Mining and Metallurgy: Victoria).

Van Dyk J.P. 1999. Process development for the production of beneficiated titania slag. Thesis for Philosophiae Doctor, 5 November 1999. University of Pretoria, RSA.

Vegter, N et al, 1997. Evaluation of processes to upgrade South African titaniferous materials to synthetic rutile, in Proceedings of Heavy Minerals 1999, edited by RG Stimson, Symposium series S23, pp 159-165 (The South African Institute of Mining and Metallurgy: Johannesburg).

Von Backström JW. 1992. Thorium. Mineral resources of the Republic of South Africa, edited by CB Coetzee. Fifth edition, fourth impression 1992, pp209-212.

Walpole, EA (to Austpac Gold NL), 1991. Improved process for separating ilmenite, South African Pat 916845.

Westcot M.F and Parry LG. 1968. Magnetic properties of some beach sand ilmenite particles. Journal of Geophysical Research vol 73 no 4 pp. 1269-1277.

Wills, B.A. 1992. Mineral Processing Technology. 4th edition. Permagon Press, Oxford, England. Pp 700, 715.